A STUDY OF THE PROPAGATION OF ACOUSTIC WAVES
AND INSTABILITIES IN INHOMOGENEOUS MEDIA

by

GEORGE C. MALING, JR.

A.B., Bowdoin College
(1954)

S.B., S.M., E.E., Massachusetts Institute of Technology
(1954, 1958)

SUBMITTED IN PARTIAL FULFILLMENT
OF THE REQUIREMENT FOR THE
DEGREE OF DOCTOR OF
PHILOSOPHY

at the

MASSACHUSETTS INSTITUTE OF TECHNOLOGY

January, 1963

Signature of Author. . . . .
Department of Physics, January 7, 1963

Certified by . . . .
Thesis Supervisor

Accepted by. . . . .
Chairman, Departmental Committee
on Graduate Students

*Physics
Thesis
1963*

A STUDY OF THE PROPAGATION OF ACOUSTIC WAVES

AND INSTABILITIES IN INHOMOGENEOUS MEDIA

by

GEORGE C. MALING, JR.

A.B., Bowdoin College
(1954)

S.B., S.M., E.E., Massachusetts Institute of Technology
(1954, 1958)

SUBMITTED IN PARTIAL FULFILLMENT
OF THE REQUIREMENT FOR THE
DEGREE OF DOCTOR OF
PHILOSOPHY

at the

MASSACHUSETTS INSTITUTE OF TECHNOLOGY

January, 1963

Signature of Author . . . .
Department of Physics, January 7, 1963

Certified by . . . .
Thesis Supervisor

Accepted by . . . .
Chairman, Departmental Committee
on Graduate Students

A Study of the Propagation of Acoustic Waves

and Instabilities in Inhomogeneous Media

by

George C. Maling, Jr.

Submitted to the Department of Physics on January 7, 1963 in partial fulfillment of the requirement for the degree of Doctor of Philosophy.

ABSTRACT

The influence of turbulence, external forces, and a heat source on the propagation and stability of an acoustic wave has been studied. The general theory of sound propagation in a turbulent medium has been used to study the statistics of a sound field above a plane boundary. The analysis has been compared with experimental data obtained in the laboratory and in the field.

In order to study the propagation of finite amplitude waves in a stratified medium, it is necessary to modify the classical theory of large amplitude propagation. This modification has been made, and the results are applied to a specific problem, the propagation of an N-wave in a gas stratified by the gravitational force.

The acoustic instability known as the Rijke phenomenon has been treated as a scattering problem, and a characteristic equation has been derived that defines the stability limits of the oscillation. Some experimental results have also been obtained, and are compared with the analysis.

Thesis Supervisor: Uno Ingard

Title: Associate Professor of Physics

ACKNOWLEDGEMENT

TABLE OF CONTENTS

FIGURE CAPTIONS FOR CHAPTER TWO

FIGURE CAPTIONS FOR CHAPTER THREE

FIGURE CAPTIONS FOR CHAPTER FOUR

Chapter 1. Introduction

1. Statement of the Problem

In the continuum description, the motion of fluids is governed by a set of non-linear partial differential equations, and therefore it has always been necessary to attempt to find approximate solutions to the equations. These attempts make up a body of literature to which workers in acoustics have contributed a great deal. A comparatively recent viewpoint is that not only external source terms are thought of as producing a disturbance that can propagate, but also that the non-linear terms may, under certain circumstances, be considered to be source terms, and by using this notion, problems such as the generation and scattering of sound by sound have been explored. Although the general form of all of the source terms has been recognized, there are many specific problems that remain to be worked out before our understanding is complete.

It has been found that the fluctuation in the amplitude of a sound wave measured in the field is frequently much larger than one would predict using the theory of sound propagation in an unbounded turbulent medium. In an effort to understand this difference we have considered the influence of a plane boundary on the statistics of the sound field. Measurements have been made both in the field and in the

laboratory, and have been compared with an analysis that includes amplitude and phase fluctuations in the sound field. Reasonably good agreement between the two has been obtained, as is shown in Chapter 2.

Another problem that has not yet been completely worked out is the motion of a steep-fronted wave in a stratified medium. The classical theory of propagation of finite amplitude waves has been modified and applied to the propagation of a wave in a medium stratified by the gravitational force. Although some of the results can be obtained by accounting for the wave energy lost by dissipation in the shock front, the analysis presented here is more general and can be used to study many features of the motion that cannot be studied by using an energy approach.

A third problem that has not yet been completely understood is an acoustic instability caused by a heat source. An oscillation, first observed by Rijke, is produced by the presence of a heated grid in the lower half of a vertical tube, and has been studied by a number of workers. In this thesis, the problem is treated in terms of the scattering of sound by a heat source. It is found that many of the features of the oscillation can be rather easily understood when examined from this point of view. The analysis is compared with experimental results obtained by the author and by other workers.

Before proceeding with a detailed treatment of each problem, it will be convenient to present a very brief

summary of the equations of motion, and to point out the specific source terms to be included in the analysis.

2. The Equations of Motion

The equations that provide a continuum description of the motion of fluids, the equations of conservation of fluid mass, momentum, and energy, may be most conveniently written in terms of an Eulerian description of the motion. That is, the field variables are taken to be functions of two independent variables, the position x and time t. If we allow for the fact that an external source may inject mass into the fluid, that external forces may act on the fluid, on that external energy sources are present, then the conservation laws may be written in the following[1, 2] form:

$$\frac{\partial \rho}{\partial t} + \frac{\partial}{\partial x_i} (\rho v_i) = Q \tag{1-1}$$

$$\frac{\partial}{\partial t}(\rho v_i) + \frac{\partial t_{ij}}{\partial x_j} = F_i + Q v_i \tag{1-2}$$

$$\frac{\partial h}{\partial t} + \frac{\partial I_i}{\partial x_i} = W \tag{1-3}$$

A repeated index indicates a summation from 1 to 3. In these equations is the fluid density, v_i is the ith component of the velocity, and t_{ij} represents the stress in the fluid, $t_{ij} = p\delta_{ij} - D_{ij} + v_i v_j$. D_{ij} is the viscous stress tensor and p is the pressure in the fluid. In the energy equation (1-3) h is the energy density of the fluid, $v^2/2 + \rho e$ and I_i is the ith component of the energy flow vector. All of

the terms on the right hand side of the above equations represent source terms. Q is the rate at which mass is introduced per unit volume into the fluid, and the term Qv_i represents a change in momentum per unit volume due to convection. F_i represents the external force acting per unit volume, and W represents energy sources. These equations plus the equation of state are sufficient to describe the motion of the fluid.

We next derive a wave equation by taking $\partial/\partial t$ of Eq. (1-1) and $\partial/\partial x_i$ of Eq. (1-2) and subtracting the two resulting equations. We obtain

$$\frac{\partial^2 \rho}{\partial t^2} - \frac{\partial^2 p}{\partial x_i^2} = + \frac{\partial Q}{\partial t} - \frac{F_i}{x_i} - \frac{\partial}{\partial x_i}(Qv_i) + \frac{\partial^2}{\partial x_i \partial x_j}(\rho v_i v_j) - \frac{\partial^2 D_{ij}}{\partial x_i \partial x_j}$$

(1-4)

We may now add $(^1/c^2)\, \partial^2 p/\partial t^2$ to both sides and obtain a wave equation for p in the following form:

$$\frac{\partial^2 p}{\partial x_i^2} - \frac{1}{c^2}\frac{\partial^2 p}{\partial t^2} = \frac{\partial F_i}{\partial x_i} - \frac{\partial Q}{\partial t} + \frac{\partial}{\partial x_i}(Qv_i) - \frac{\partial^2}{\partial x_i \partial x_j}(\rho v_i v_j) + \frac{\partial^2 D_{ij}}{\partial x_i \partial x_j} - $$
$$- \frac{\partial^2}{\partial t^2}(\rho - p/c^2) \quad (1-5)$$

c is a constant which will turn out to be the adiabadic speed of sound, $(\partial p/\partial \rho)_s$. Note that we have not up to now made any approximations to the conservation laws, and therefore this equation may be taken as the starting point for a solution to all problems that involve a continuum description of the motion of fluids. The analysis and experiments in the following chapters were performed in order to learn more

about some of these source terms, and include both linear
and non-linear problems. In the following sections of this
introduction we will discuss the source terms that are of
importance in the problems that we wish to study in the
following chapters.

3. Influence of Turbulence on the Sound Field Over a Plane Boundary

The influence of turbulence on the sound propagated in
an unbounded medium has been presented in the recent books
by Chernov[3] and Tatarski,[4] and in the recent article by
Morse and Ingard.[1] The important source term to be con-
sidered is the term $\partial^2/\partial x_i \partial x_j$ $(\rho v_i v_j)$ in Eq. (1-5). If we
assume that the acoustic velocity field is represented by a
plane harmonic wave of wave number k_o, then we may separate
the above term into $\partial^2/\partial x_i \partial x_j$ $(\rho(V_i V_j + V_i u_j + V_j u_i + u_i u_j))$
where V_i represents the turbulent velocity field. If we
neglect the term responsible for the generation of sound by
turbulence[5, 6] $(V_i V_j)$ and the term responsible for the
scattering of sound by sound $(u_i u_j)$, then the part of the
remaining cross-terms linear in the acoustic variable are
$\partial^2/\partial x_i \partial x_j$ $(\rho_o(V_i u_j + V_j u_i))$, and are the important source
terms. If the quantity added to both sides of Eq. (1-4) is
taken to be $(1/c_o^2) \partial^2 p/\partial t^2$ where c_o is the speed of the
acoustic wave in the absence of turbulence, then the acoustic
variables in the last term of Eq. (1-5) cancel out for
isentropic flow, and the wave equation for the sound pressure
(p) may eventually be written:

$$\frac{\partial^2 p}{\partial x_i^2} + k_o^2\, p = -\,\frac{2Vx}{C_o}\, k_o^2\, p \qquad\qquad (1\text{-}6)$$

where the term on the right is obtained from the source term by using the linear form of the equation of continuity and the relation $p = c_o^2 \delta$, where δ is the density perturbation in the fluid. Using this approximation, the variance of the amplitude and phase fluctuations of the acoustic wave may be found. In Chapter 2 we have included a boundary in the medium, and have studied both the changes in the RMS level and the fluctuations that occur because of the interference between the direct wave from the source and the wave reflected from the boundary.

4. Propagation of Waves of Finite Amplitude in Inhomogeneous Media

It is necessary to retain more terms in Chapter 3 where the propagation of finite amplitude waves is studied. The medium is assumed to be stratified by the presence of a body force that also produces an entropy gradient. Thus, both the first and last terms will have to be retained, the latter because the difference between p/c^2 and ρ is not only caused by heat conduction, but also because there is a convection of entropy by the particle velocity in the wave. In the dissipationless approximation, the change in entropy of a fluid element is zero only when a Lagrangian description of the motion is used. In the Eulerian description that we have adopted, the entropy at a point in space can vary (even in the linear approximation) and so these convection terms as well as the loss terms will have to be retained. We will

also have to keep a portion of the fourth term to account
for progressive distortion in the wave. These facts lead to
a modification of the classical theory of Riemann[7] and
Stokes[8] that can be applied to the propagation of finite
amplitude waves in inhomogeneous media. Since any pertur-
bation, no matter how small, eventually leads to a double-
valued field variable in the lossless approximation, we will
have to include dissipative effects in order to obtain valid
results. In the approximation used in Chapter 3, the loss
terms are included in a somewhat different manner. Since we
do not consider the growth of an initial small disturbance
into a steep-fronted (shock) wave, but rather the propagation
of an already formed shock in an inhomogeneous medium, the
approximation is made that all of the dissipation occurs in
the steep front because the field variables have large
gradients in this region. Application of the conservation
laws across the shock front leads to the Rankine[9]-Hugoniot[10]
shock relations, and when these relations are used with the
loss-free equations, a relation may be found that describes
the decay of pressure at the shock front with distance. Such
an analysis has been performed by Dumond, Cohen, Panofsky and
Deeds[11] for an N-wave in a homogeneous medium, and our
results will reduce to results obtained by those workers in
the limit $F_i \rightarrow 0$. For this particular problem, it is best to
identify the source terms that are important using Eq. (1-5),
but in order to perform the analysis it is more convenient to
use the equations of motion directly as will be shown in
Chapter 3.

Even if the non-linear effects are neglected, calculation
of the propagation constant for a plane harmonic wave in a
medium stratified by the gravitational force leads to an
attenuation or amplification of the sound pressure (p)
consistent with conservation of energy, $p^2/2\rho_e c_e$ = constant.
In addition to the change in amplitude, the imaginary part
of the propagation constant decreases with decreasing
frequency until the density fluctuations are balanced out
by the entropy fluctuations, and then no pressure wave is
propagated. The former effect is shown to occur for finite
amplitude waves as well, but is modified by dissipation in
the steep front. The additional factors that have to be
included to obtain the latter effect are also pointed out.

5. The Scattering of Sound by a Heat Source

The last term in Eq. (1-4) is important when the
generation or scattering of sound by heat is being considered.
The portion of the last term linear in the acoustic variables
for a homogeneous medium is $\partial^2/\partial t^2 (\delta - p/c^2)$ which, using
the equation of state $p = p(\rho,s)$ may be written $(1/c^2 T)$
$(\partial p/\partial s)_\rho (\partial q/\partial t)$ where q is the rate at which heat is added
per unit mass to the fluid. For an ideal gas, the source
term is $(\gamma-1)(1/c^2)(\partial q/\partial t)$. When the heat added is influ-
enced by a velocity perturbation in the fluid, the acoustic
variables may, under certain conditions, grow with time.
The particular problem worked out in Chapter 4 is the Rijke
phenomenon, the oscillation caused by the presence of a heated
grid in the lower half of a tube open at both ends. Up to

now, the problem has been attacked by using the source-free wave equation and requiring that the acoustic variables satisfy the appropriate boundary conditions on either side of the heater as well as the conservation laws across the heater. Such an approach leads to a rather complicated characteristic equation that must be solved either by machine computation or by a perturbation expansion around approximate values of the eigenvalues. These complications are avoided when one views the phenomenon as a one-dimensional scattering problem. If the source term is treated as a spacial δ-function whose magnitude depends on the value of the particle velocity at some point, then the pressure perturbation can be expanded into an infinite series of orthonormal functions that satisfy the appropriate boundary conditions. When the actual eigenvalue for the tube is sufficiently close to an eigenvalue of one of the modes, then only one term in the sum will be important. A characteristic equation is obtained after the acoustic variable is eliminated by means of a self-consistent requirement on the particle velocity, and the stability limits of the system can be found immediately. After the relation between the acoustic particle velocity and the fluctuating component of the heat added is discussed, the results are compared with some experimental data, and good agreement between the two is found for some features of the oscillation.

Having presented a very brief outline of some of the terms in the wave equation to be considered, we now proceed

directly to a discussion of each of the three problems.
Additional introductory material is presented at the
beginning of each chapter.

REFERENCES FOR CHAPTER ONE

1. Morse, P.M. and Ingard, U., Linear Acoustic Theory, Handbuch der Physik, Springer-Verlag (1961)

2. Ingard, U., Notes for Physics 8.461, Massachusetts Institute of Technology, Fall 1962

3. Chernov, L.A., Wave Propagation in a Random Medium, McGraw-Hill (1960)

4. Tatarski, V.I., Wave Propagation in a Turbulent Medium, McGraw-Hill (1961)

5. Lighthill, M.J., Proc. Roy. Soc. (London) A, 211, 564 (1952)

6. Lighthill, M.J., Proc. Roy. Soc. (London) A, 222, 1 (1954)

7. Riemann, B., Göttingen Abh., 8, 43 (1859)

8. Stokes, G.G., Phil. Mag., 33, 349 (1848)

9. Rankine, W., Phil. Trans. Roy. Soc., 160, 277 (1870)

10. Hugoniot, A., J. Éc. Polyt. (Paris), 58, 1 (1889)

11. Dumond, J.M., Cohen, E.R., Panofsky, W.H., and Deeds, E., J. Acoust. Soc. Am., 18, 97 (1946)

12. Rijke, P.L., Phil. Mag., 17, 419 (1859)

Chapter 2. The Influence of a Boundary on the Propagation
of Sound through Atmospheric Turbulence

1. Introduction

The general aspects of sound propagation in a turbulent
medium have been discussed in several basic papers by
Obhukov,[1] Krasilnikov,[2] Chernov,[3] Lighthill,[4]
Batchelor,[5] Kraichnan,[6] Mintzer[7,8] and others as
well as in the recent books by Chernov[9] and Tatarski[10]
in which extensive lists of references are given. One
aspect of the problem that has not yet received a great
deal of attention is the influence of the turbulence on
the propagation of sound in the presence of a boundary.
Even if the turbulence is so weak that it has practically
no influence on the sound field in free space, the influ-
ence on the sound field can be large when a boundary is
present because the field above the boundary is critically
dependent upon the phase relationship between the direct
and reflected waves. Clearly in the regions where the
interference between these two waves is normally destruc-
tive, small fluctuations in the phase difference can
cause large fluctuations in the amplitude of the sound
field. In addition the rms sound pressure level must be
greater in the minima of the sound field. At large

distances from the source, the well-known mirror effect
which normally makes the sound pressure decrease as the
inverse square of the distance from the source will be
eliminated because the direct and reflected waves become
uncorrelated in phase. In the sections to follow we will
present a detailed analysis of the sound field above a
plane boundary. In section 3 some experimental results
obtained in the laboratory will be presented. In sec-
tions 4 and 5 calculations of the statistics of the sound
field have been made, and these calculations are compared
with some experimental data in section 7.

2.   Calculation of the rms Sound Field

In this section we shall consider the field from a
harmonic monopole point source located a distance h above
a plane boundary. The geometry is illustrated in
Figure 2-1. The boundary is specified acoustically by a
known normal admittance $\beta/\rho c$ (the ratio of the normal
particle velocity to the sound pressure) which we assume
to be real. Since the source will generally be several
wavelengths above the boundary, we may neglect the fact
that the wave front is spherical and use the plane wave
reflection coefficient $R = (\cos \theta - \beta)/(\cos \theta + \beta)$ to
obtain the image source strength. For the moment we
shall call the amplitude of the image A_r and write the
sound pressure at the point P

SOURCE

x

h

$\rho c \, \mathcal{S} = p/u$

BOUNDARY

r
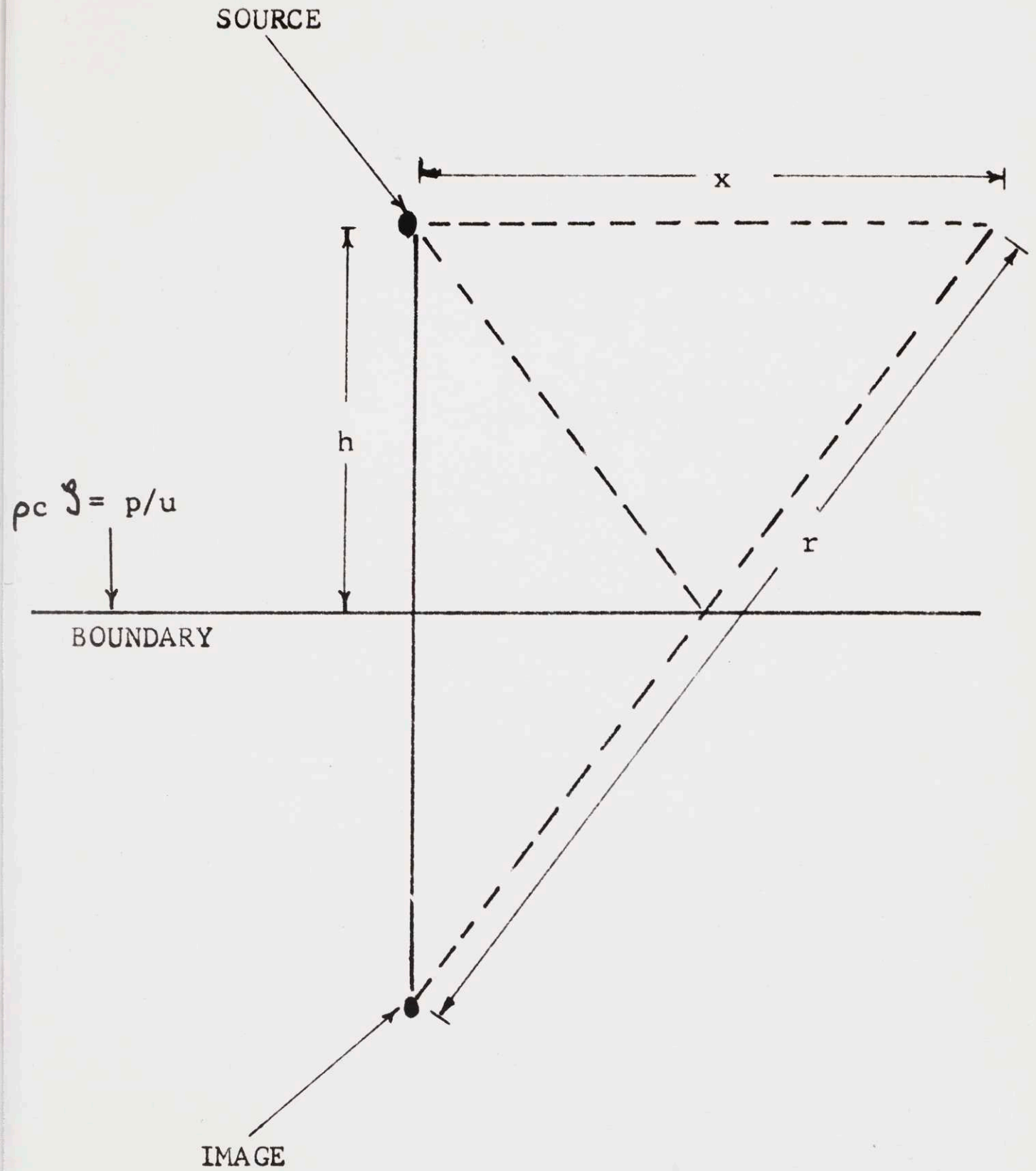
IMAGE

FIGURE 2-1

$$p = \frac{A_d}{x} e^{i(k_d x - \omega t)} + \frac{A_r}{r} e^{i(k_r r - \omega t)} \qquad (2\text{-}1)$$

where A_d is the amplitude of the wave from the source, x
is the distance from the source, r is the distance from
the image, ω is the frequency of the emitted sound, and
k_d and k_r are the wave numbers of the direct and reflected
waves respectively. A_d, A_r, k_d, and k_r are not constants
but fluctuate about some mean value because of the turbu-
lence. We shall define $A_d = 1 + a_d$ and $A_r = R(1 + a_r)$
where $\langle a_d \rangle = \langle a_r \rangle = 0$ (the $\langle \ \rangle$ indicates an average over
a long period of time which we shall later assume to be
identical to a statistical average). The fluctuating
phase difference, δ, may be included by taking $k_d x =$
$k_o x + \delta_d$ and $k_r r = k_o r + \delta_r$ where $\langle \delta_d \rangle = \langle \delta_r \rangle = 0$. k_o
is the wave number in the absence of turbulence, ω/c_o.
In order to find the fluctuating parts of the amplitude
and phase, we assume that the fluctuating part of the
velocity of the medium may be replaced by a randomly
varying index of refraction $n = 1 + \mu$ where $\mu \ll 1$.

An approximate solution to the wave equation
$\Box^2 p = -2k_o^2 \mu p$ may be obtained by using the method of
lateral diffusion. A concise account of the method may
be found in a recent article by Morse and Ingard,[11] or
in reference (9). If it is assumed that the spacial
correlation of the turbulence is of the form $\langle \mu_1 \mu_2 \rangle =$
$\mu_o^2 \exp(-\xi^2/L)$ where L is a measure of the scale of the

turbulence, then it can be shown that for deep penetration into the medium ($x \gg \sqrt{L\lambda}$) the variance of the amplitude and phase fluctuations is given by[11]

$$\langle \delta_d \rangle = \frac{1}{2}\sqrt{\pi}\, k_o^2 (xL)\mu_o^2 \qquad (2\text{-}2a)$$

$$\langle (\ln(1 + a_d))^2 \rangle = \frac{1}{2}\sqrt{\pi}\, k_o^2 (xL)\mu_o^2 \qquad (2\text{-}2b)$$

In the analysis to follow, we shall assume that $\langle \delta_d^2 \rangle = \langle \delta_r^2 \rangle$ and $\langle a_d^2 \rangle = \langle a_r^2 \rangle$ because the path difference between the direct and reflected waves is small for most problems of interest. It can also be shown[9] that for $x \gg \sqrt{L\lambda}$ the phase and amplitude fluctuations are uncorrelated, and this result will make possible considerable simplification of the analysis. One last fact must be pointed out before proceeding with the analysis. It has been found experimentally that the fluctuations of the sound pressure amplitude have a time scale which is much longer than the period of the acoustic wave. Under these conditions it is meaningful to speak of a time-dependent mean square pressure which will be denoted by $\overline{p^2}$. The averaging time for obtaining this pressure is long compared to the period of the acoustic wave but short compared to a characteristic period of the random amplitude and phase fluctuations of the wave. We may therefore calculate $\overline{p^2}$ from Eq. (2-1). The result is

$$\overline{p^2} = \frac{1}{x^2}\left(A_d^2 + A_r^2\left(\frac{x^2}{r^2}\right) + 2A_dA_r\frac{x}{r}\cos(k_o(r-x)+\delta)\right) \quad (2\text{-}3)$$

where δ is the relative phase shift between the direct and reflected waves, $\delta_d - \delta_r$. What is needed first is $\overline{p^2}$ averaged over a time long compared to the period of the fluctuations. We shall denote this average by $\langle \overline{p^2} \rangle$. If we use the fact that the amplitude and phase fluctuations are uncorrelated, $\langle \overline{p^2} \rangle$ may be written

$$\langle \overline{p^2} \rangle = \frac{1}{x^2}\left(1 + \langle a_d^2\rangle + R^2\frac{x^2}{r^2}(1 + \langle a_r^2\rangle + 2R\frac{x}{r}\langle\cos(\beta_o+\delta)\rangle\right)$$

$$(2\text{-}4)$$

where $\beta_o = k_o(r-x)$. If we now take $\langle a_d^2\rangle = \langle a_r^2\rangle = \langle a^2\rangle$, Eq. (2-4) may be put in the following form:

$$\langle \overline{p^2} \rangle = \frac{2R}{xr}\left[\frac{a^2}{2R}(\frac{r}{x}+R^2\frac{x}{r}) + \frac{r}{2xR}(1-R\frac{x}{r})^2 + \langle 1 + \cos(\beta_o+\delta)\rangle\right]$$

$$(2\text{-}5)$$

In this form, the effect of the turbulence can easily be seen. For $R = 1$ (rigid boundary) and no turbulence ($a^2 = \delta = 0$), the term $(1 - Rx/r)$ is small and so when $\beta_o = \pi$ (destructive interference) the mean-square pressure is very small. If, however, the turbulence is included, these minima are raised considerably by the first and last terms in Eq. (2-5). At large distances from the source, $\langle 1 + \cos(\beta_o+\delta)\rangle \longrightarrow 2$ for $\delta = 0$ since $\beta_o \longrightarrow 0$. In the presence of turbulence, large fluctuations in δ at large distances make $\langle\cos\delta\rangle = 0$ and so $\langle 1 + \cos(\beta_o+\delta)\rangle \longrightarrow 1$.

The mean level is therefore lowered by the turbulence and it will be seen later that the inclusion of $\langle a^2 \rangle$ in the analysis will not change these conclusions very much.

In order to see more clearly the effect of the turbulence, Eq. (2-5) has been plotted in Figure 2-2, using the following parameters: $\mu_o = 0.005$, $h = 6$ ft, $L = 3$ ft, $\beta = 0$. Note that $\langle \delta^2 \rangle = \langle (\delta_d - \delta_r)^2 \rangle = 2\langle \delta_d^2 \rangle$ if we take $\langle \delta_d^2 \rangle = \langle \delta_r^2 \rangle$. In these sample calculations we have used the approximation $\langle \cos \delta \rangle = \cos \sqrt{\langle \delta^2 \rangle}$ for $\langle \delta^2 \rangle$ less than 1 and $\langle \cos \delta \rangle = 0$ for $\langle \delta^2 \rangle$ greater than π. The former is actually valid only when $\langle \delta^2 \rangle << 1$ but these approximations are sufficient to illustrate the effect of turbulence on the pressure field. For $\beta \neq 0$ it is clear from the definition of R that $R \longrightarrow -1$ as x becomes large. In the absence of turbulence $\langle 1 + \cos \beta_o \rangle \longrightarrow 2 - k_o^2/2(r - x)^2 \doteq 2 - (k_o^2/2)(2h^2/x)^2$ and so $\langle \overline{p^2} \rangle \sim 1/x^2 r^2$ for large values of x (and r). In the presence of turbulence, however, $\langle 1 + \cos(\beta_o + \delta) \rangle \longrightarrow 1$ for large x and $\langle \overline{p^2} \rangle \sim 1/x^2$. Thus the "mirror effect" is eliminated by the turbulence. These results are illustrated in Figure 2-3, which has been calculated using the same approximations as were used above except that β has now been assumed to be 0.05. The large interference minima are of course almost completely eliminated even in the absence of turbulence because of the difference in amplitude between the direct and reflected waves.
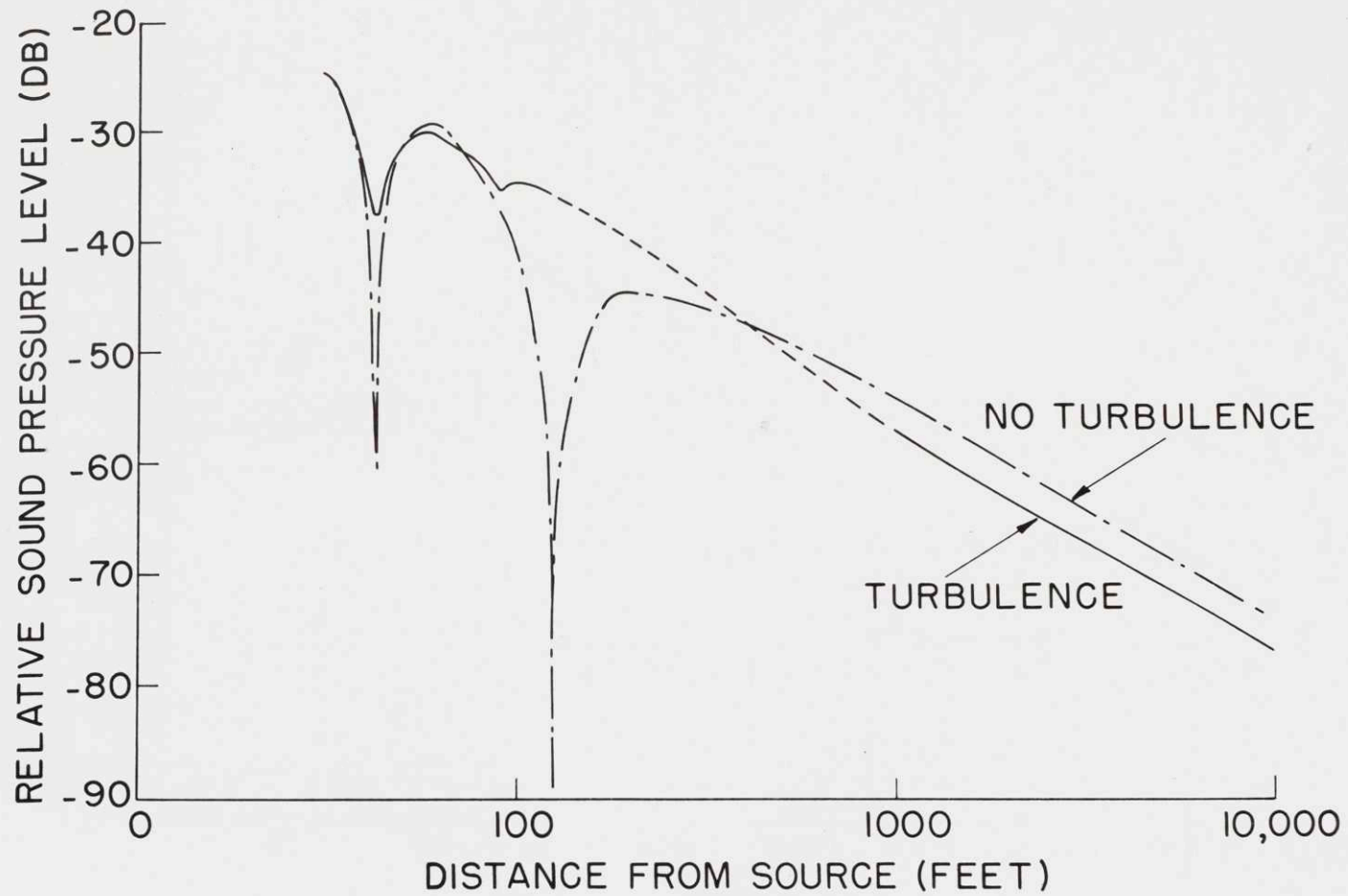
FIGURE 2-2
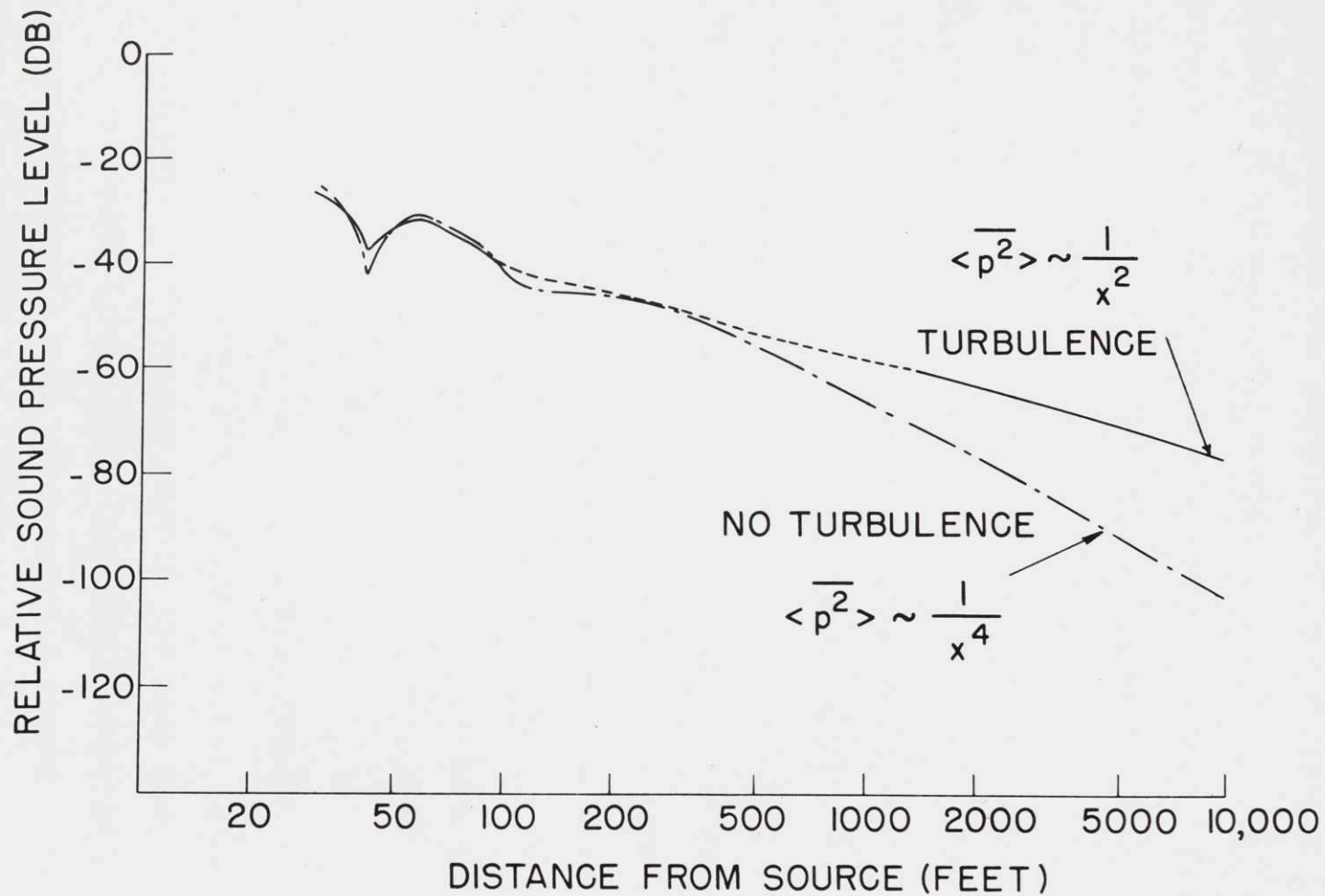
FIGURE 2-3

3.   Preliminary Analysis of Fluctuations

The variance of the amplitude fluctuations for a wave propagating in an unbounded medium is known (see Eq. (2-21)) to increase monotonically with distance from the source. Data obtained from field measurements, however, have shown that the fluctuations are frequently much larger than those to be expected assuming that the variance can be calculated from Eq. (2-2), and they do not always increase with distance. Some field data obtained by Ingard[12] are illustrated in Figure 2-4. The source and receiver were located approximately 6 ft above ground which consisted of sand with sparse grass about 12-15 in. high. The fluctuations are the peak-to-peak values of the fluctuating envelope of the pure tone as measured on a Bruel and Kjaer graphic level recorder. Since the exact shape of the boundary is unknown we shall not attempt to obtain these results by calculation, but will assume that the boundary can be specified by a known normal admittance, and compare the calculations with experimental results obtained using a plane boundary. In this preliminary analysis we shall neglect the amplitude fluctuations in the wave and assume that only the phase fluctuations need to be considered. Since the experimental data previously available refer only to the fluctuation amplitude read by eye from a logarithmic sound level recorder, it is of interest to try and obtain some systematic method of comparing theory and

PEAK-TO-PEAK FLUCTUATION
PURE TONE TRANSMISSION
IN THE WIND DIRECTION

Wind Velocity: ≈ 3 m/sec.

Ipswich Beach, Aug. 1, 1953

O 5000 cps
× 2900 cps
△ 1700 cps
● 1200 cps
+ 500 cps
▽ 200 cps

DISTANCE IN FEET
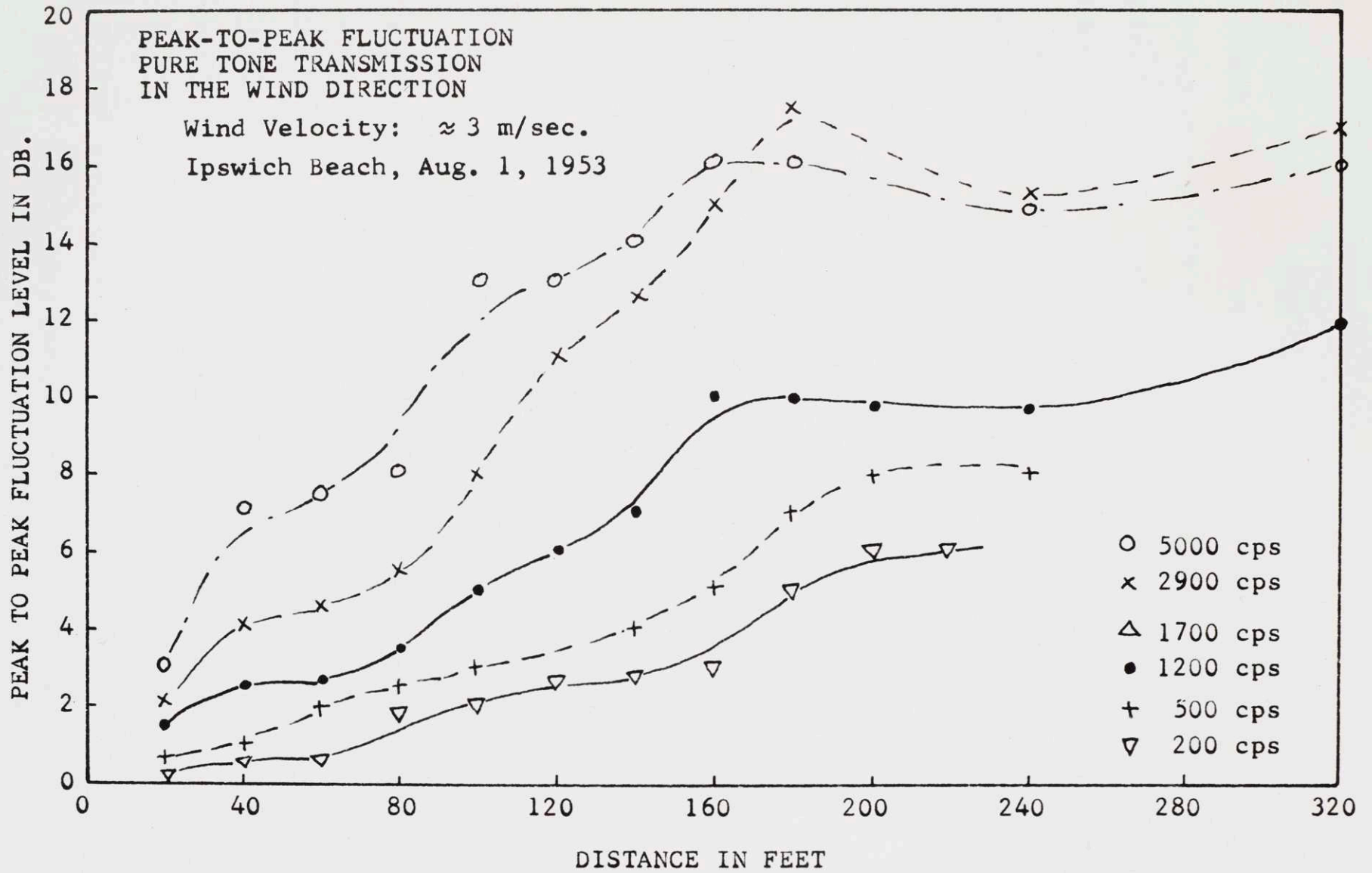
FIGURE 2-4

experiment. Although the method to be developed in this section should be regarded as only a rough approximation, it has been possible to use it to obtain reasonable agreement with some experimental data taken in the anechoic chamber at M.I.T.

We regard $\overline{p^2}$ given in Eq. (2-3) as a slowly varying random function of time because of the random variations in δ. We shall neglect the amplitude fluctuations and so take $A_d = 1$ and $A_r = R$. Then Eq. (2-3) may be written

$$\overline{p^2} = \frac{2R}{xr}\left\{\frac{r}{2xR}\left(1 - R\,\frac{x}{r}\right)^2 + 1 + \cos(\beta_o + \delta)\right\} \qquad (2-6)$$

We note that $\overline{p^2}$ is limited to the region between $\overline{p^2_{max}}$ and $\overline{p^2_{min}}$ determined by the values $+1$ and -1 of $\cos(\beta_o + \delta)$. If, however, the fluctuations in δ are small the probability that these maximum and minimum values will occur will be very small, and it seems reasonable to assume that the experimental data on fluctuations do not represent $10 \log(\overline{p^2_{max}}/\overline{p^2_{min}})$. Instead, we shall assume that $10 \log(\overline{p^2_1}/\overline{p^2_2})$ is more representative, where $\overline{p^2_1}$ and $\overline{p^2_2}$ are defined by allowing $\overline{p^2}$ to be larger than $\overline{p^2_1}$ for 10 percent of the time and less than $\overline{p^2_2}$ for 10 percent of the time. Although this definition is arbitrary, it at least gives a consistent procedure for calculating the fluctuations and can therefore be used to illustrate the shape of the curves of fluctuation level vs distance. In performing the computations, it has been assumed that δ can be represented by a

normal distribution $P(\delta) = (1/\sqrt{2\pi}\sigma)\exp(-\delta^2/2\sigma^2)$ where $\sigma^2 = \langle\delta^2\rangle$.

In general it is necessary to construct a distribution function for $\overline{p^2}$ using the entire expression given in Eq. (2-6), but for R near 1 and x $\gg$ h, the first term may be neglected provided that $\beta_0 \neq \pi$. Under these conditions, the fluctuation in sound pressure (in dB) may be written

$$L = 10 \, \log(\overline{p_1^2}/\overline{p_2^2})$$

$$= 10 \, \log \frac{(1 + \cos(\beta_0 + \delta))_1}{(1 + \cos(\beta_0 + \delta))_2} \qquad (2\text{-}7)$$

This level may now be calculated as a function of $\langle\delta^2\rangle$ (which in turn is a function of x since $\langle\delta^2\rangle = 2\langle\delta_r^2\rangle$) by using the criterion outlined above. The results of such calculations are shown in Figure 2-5. For $\beta_0 = \pi$, the minimum level is determined by the first term in Eq. (2-6) and must therefore be included in the calculations at the interference points. This procedure has been followed in the calculations of a curve for comparison with some experimental data obtained in the M.I.T. anechoic chamber. As pointed out earlier, the normal impedance of the surface has a considerable influence on the magnitude of the fluctuations observed, and for most outdoor experiments this impedance is not known. In the model experiments described below, the boundary impedance was well defined and so we shall consider only these experiments in this section.
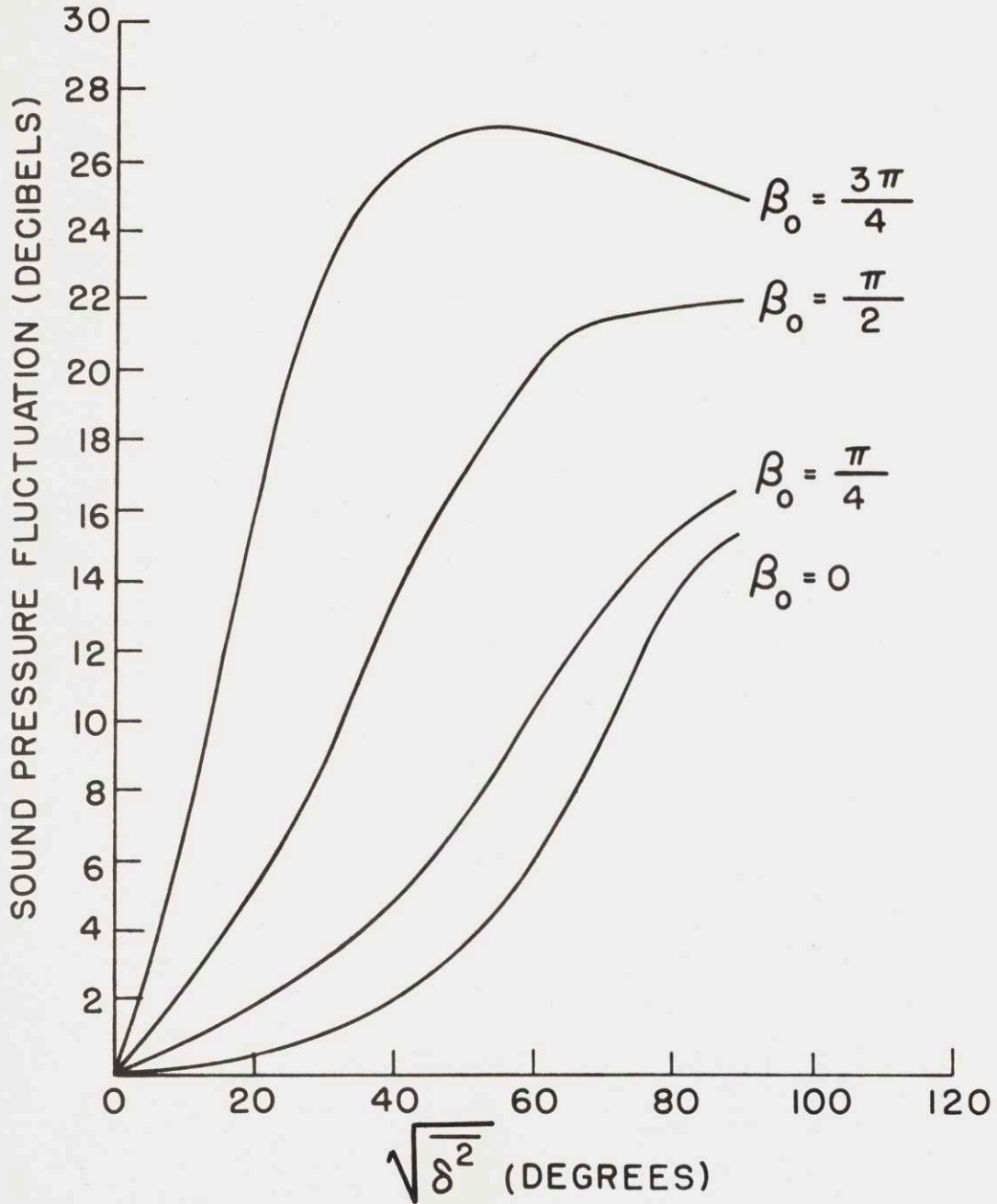
FIGURE 2-5

The sound pressure level was measured as a function of
distance from a 5000 cps source located above a floor made
up of 1 in. thick plywood sheets above which a turbulent
air stream was produced by a number of propeller fans.
The reflection coefficient of the boundary was estimated
from the measured values of the sound pressure level in
the minima of the pressure pattern above the boundary.
In Figures 2-6 and 2-7 the long time average sound pres-
sure level is plotted as a function of distance from the
source together with the corresponding calculated curves
(with a rigid plane assumed). The main effect of the
turbulence is to raise the rms level in the minima of the
pressure pattern. It is important to note that the micro-
phone position was not changed when the difference in level
between propagation in turbulent air and quiescent air was
being measured. Thus the increase measured is a conse-
quence of the turbulent state of the air, and not a small
difference in the microphone position. More satisfying
data will be presented in section 6. The average fluctua-
tion of the sound pressure level was also measured and the
results are shown in Figure 2-8. The theoretical curve
calculated from Eqs. (2-6) and (2-7) can be obtained once
we assume a value of $\mu_o^2 L$. We select a value of $\mu_o^2 L$ to
produce the best fit with the experimental data, and with
a value of $u_o^2 L = 6.5 \times 10^{-6}$ in. we obtain the calculated
curves shown in Figure 2-8. It can be seen that fair
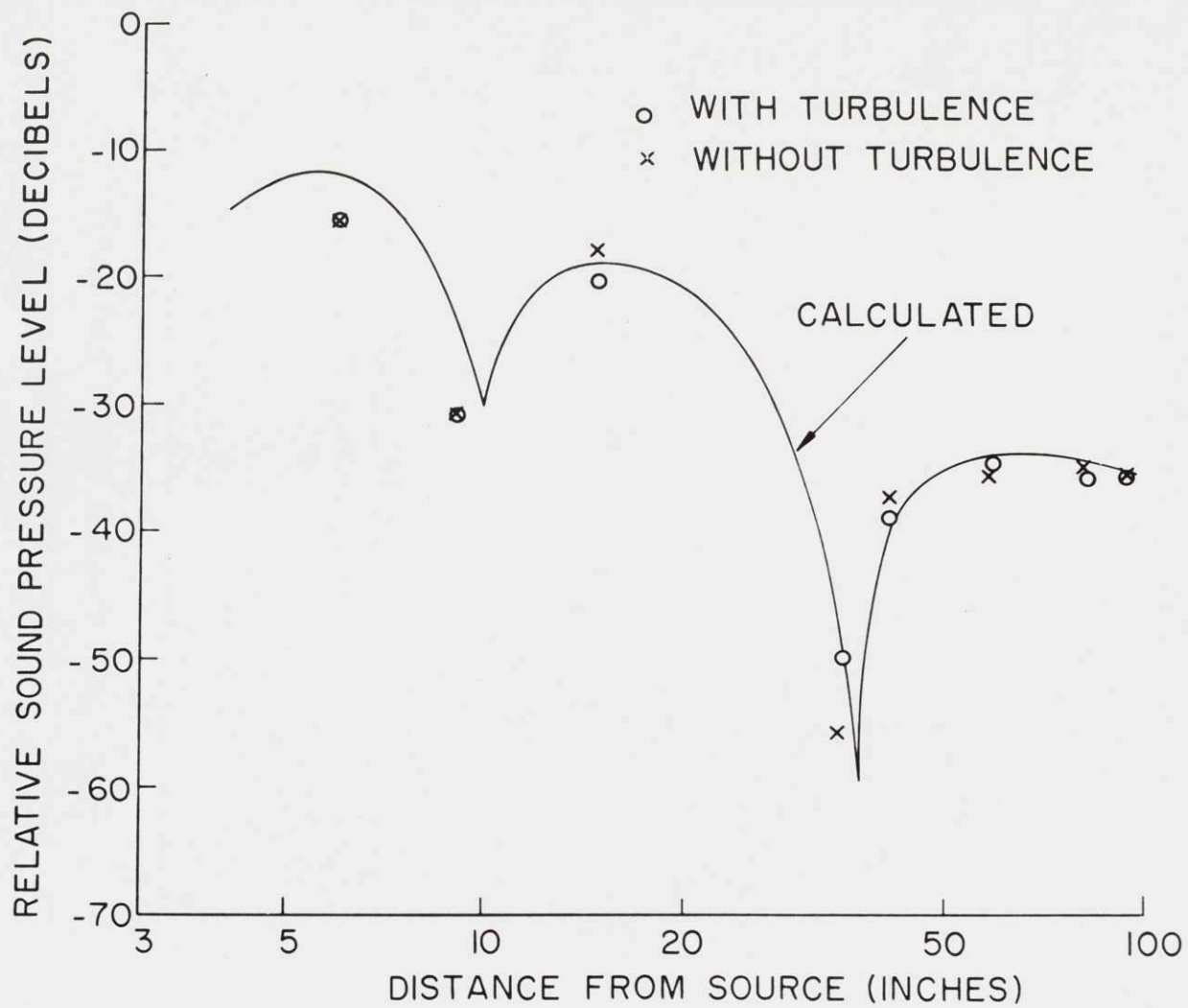
FIGURE 2-6
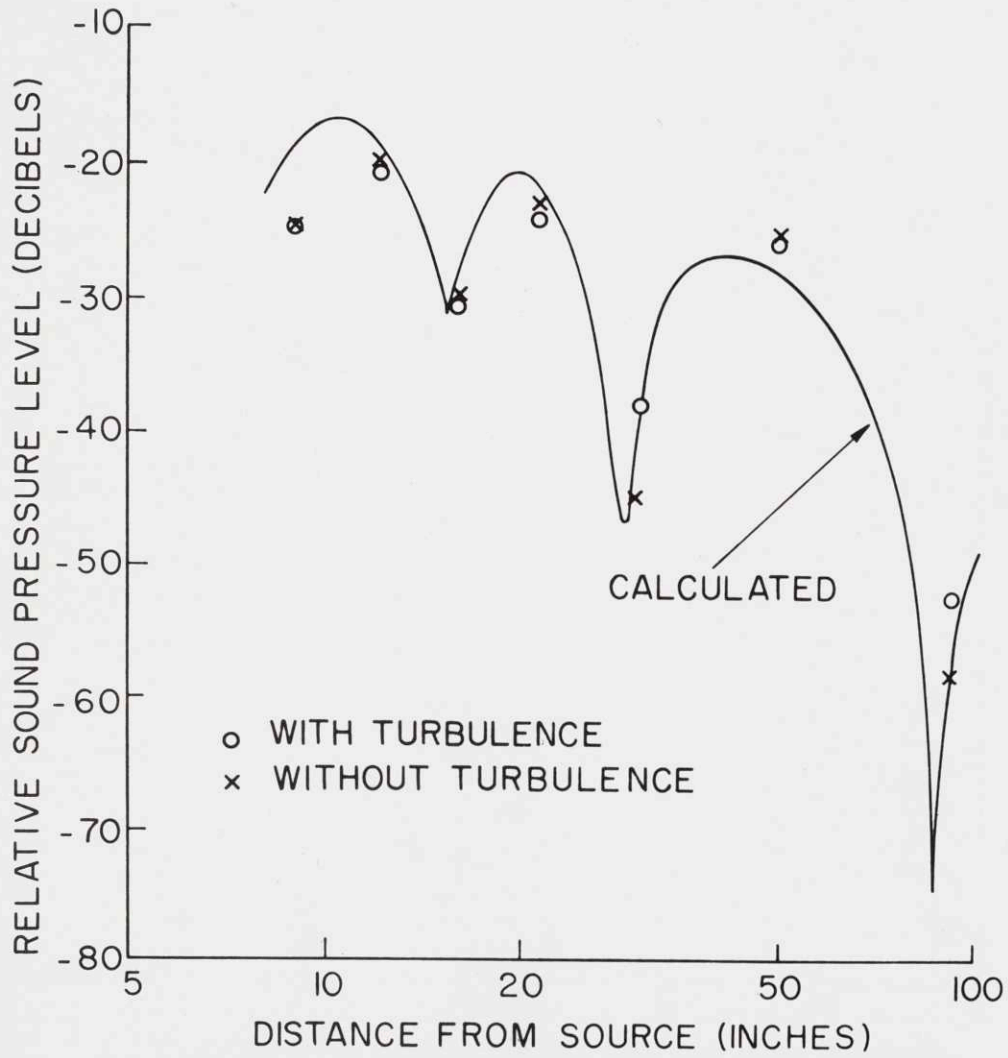
FIGURE 2-7
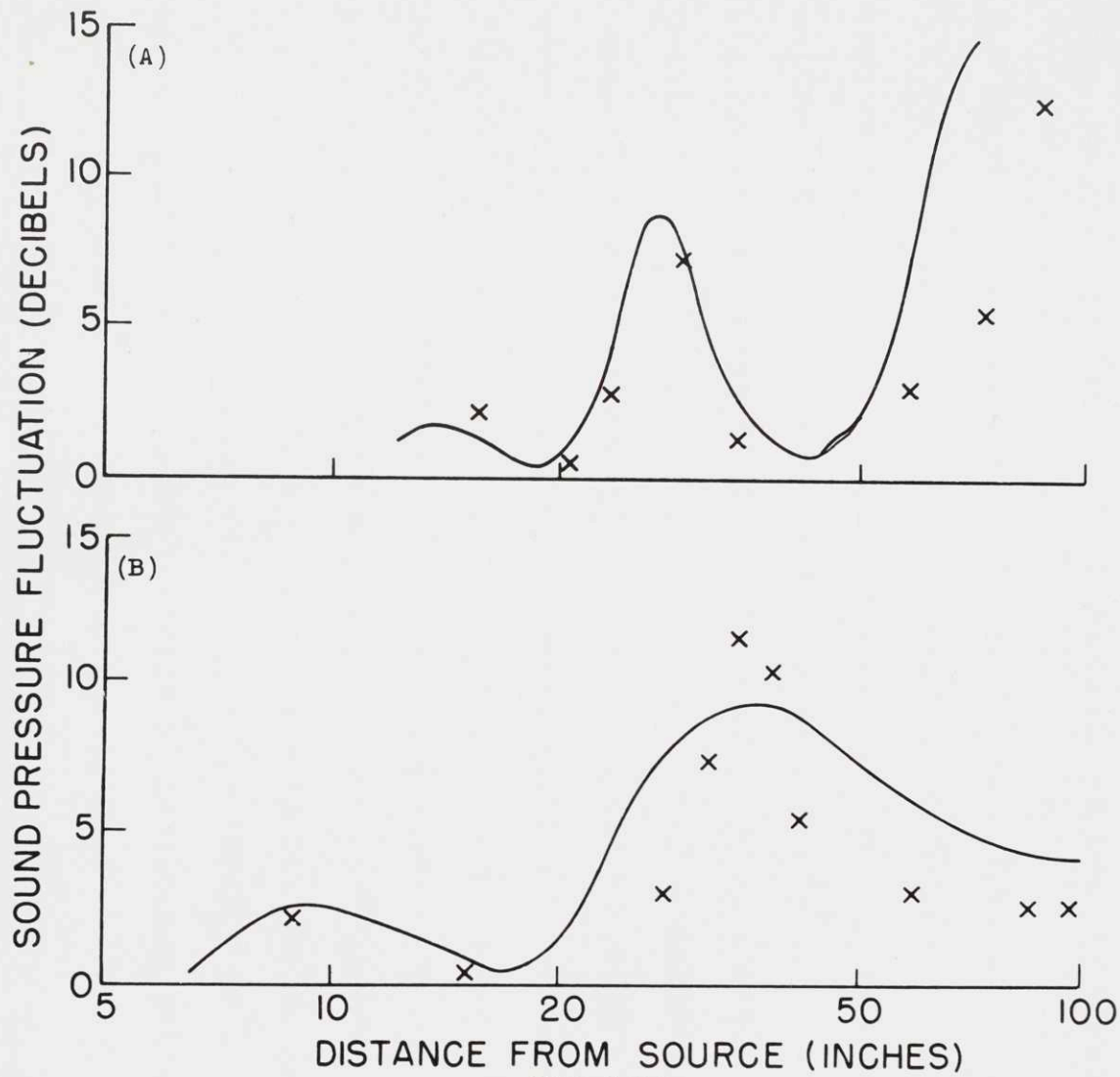
FIGURE 2-8

agreement is obtained, but in a more detailed analysis one should compare the statistics of the fluctuations with the calculated statistics. In addition, amplitude fluctuations as well as phase fluctuations must be included in the analysis. We shall present such an analysis in the next section.

4. Statistical Analysis of the Mean Square Pressure Field

We obtained in section 2 an expression for the long time average of $\overline{p^2}$ (see Eq. (2-5)) and some of the differences between the results obtained in a quiescent and turbulent atmosphere were pointed out. The results were, however, obtained by assuming that $\cos \delta = 1 - \delta^2/2$ for small δ and therefore that the mean value of $\cos \delta$, $\langle \cos \delta \rangle$ could be expressed in terms of the variance of δ ($\langle \cos \delta \rangle = \cos \sqrt{\langle \delta^2 \rangle}$). Clearly, for large values of δ it is necessary to have all of the higher moments of δ in order to obtain $\cos \delta$ and this would require one to assume a form for the higher spacial correlations in the turbulent velocity field. For the purpose of this study, we shall assume that δ is a normally distributed random function with standard deviation σ. σ is to be obtained from Eq. (2-2b).

$$\sigma^2 = \langle \delta^2 \rangle = \langle (\delta_r - \delta_d)^2 \rangle = \sqrt{\pi}(k_o x)(k_o L)\mu_o^2 \qquad (2-8)$$

The amplitude fluctuations are also assumed to be normally distributed with standard deviation $\sqrt{\langle a^2 \rangle}$. With these assumptions, the only details to be worked out to obtain

the mean square pressure are to calculate $\langle 1 + \cos(\beta_0 + \delta)\rangle$ in Eq. (2-5) using $P(\delta) = (1/\sqrt{2\pi}\sigma)\exp(-\delta^2/2\sigma^2)$ and to calculate $\langle a^2\rangle$ when $\langle(\ln(1 + a))^2\rangle$ is given by Eq. (2-2b). The former is calculated simply by taking

$$\langle 1 + \cos(\beta_0 + \delta)\rangle = \frac{1}{\sqrt{2\pi}\sigma} \int_{-\infty}^{\infty} (1 + \cos(\beta_0 + \delta))e^{-\delta^2/2\sigma^2} d\delta \quad (2-9)$$

The result can be easily shown to be

$$\langle 1 + \cos(\beta_0 + \delta)\rangle = 1 + \cos\beta_0 e^{-\sigma^2/2} \quad (2-10)$$

Plots of the left-hand side of this equation vs σ for several values of β_0 are presented in Figures 2-9 and 2-10. These plots will facilitate the calculation of theoretical curves for comparison with some experimental data to be presented in the next section. In order to obtain $\langle a^2\rangle$ from $\langle(\ln(1 + a))\rangle$, one simply expands the logarithm in powers of a, and then uses the fact that a is normally distributed to replace all of the higher moments by powers of the second moment. Thus $\langle a^4\rangle = 3\langle a^2\rangle^2$, $\langle a^6\rangle = 5\langle a^2\rangle^3$, etc. This has been done keeping terms up to $\langle a^6\rangle$, and the resulting curve is shown in Figure 2-11. The convergence is fairly good up to $\langle a^2\rangle = 0.5$ which is adequate for our purposes since it corresponds to $\langle(\ln(1 + a))^2\rangle = 2.19$. This curve will also be useful for the calculation of theoretical mean pressure levels.

Before continuing with an analysis of the fluctuations, let us summarize the results of this section. It has been
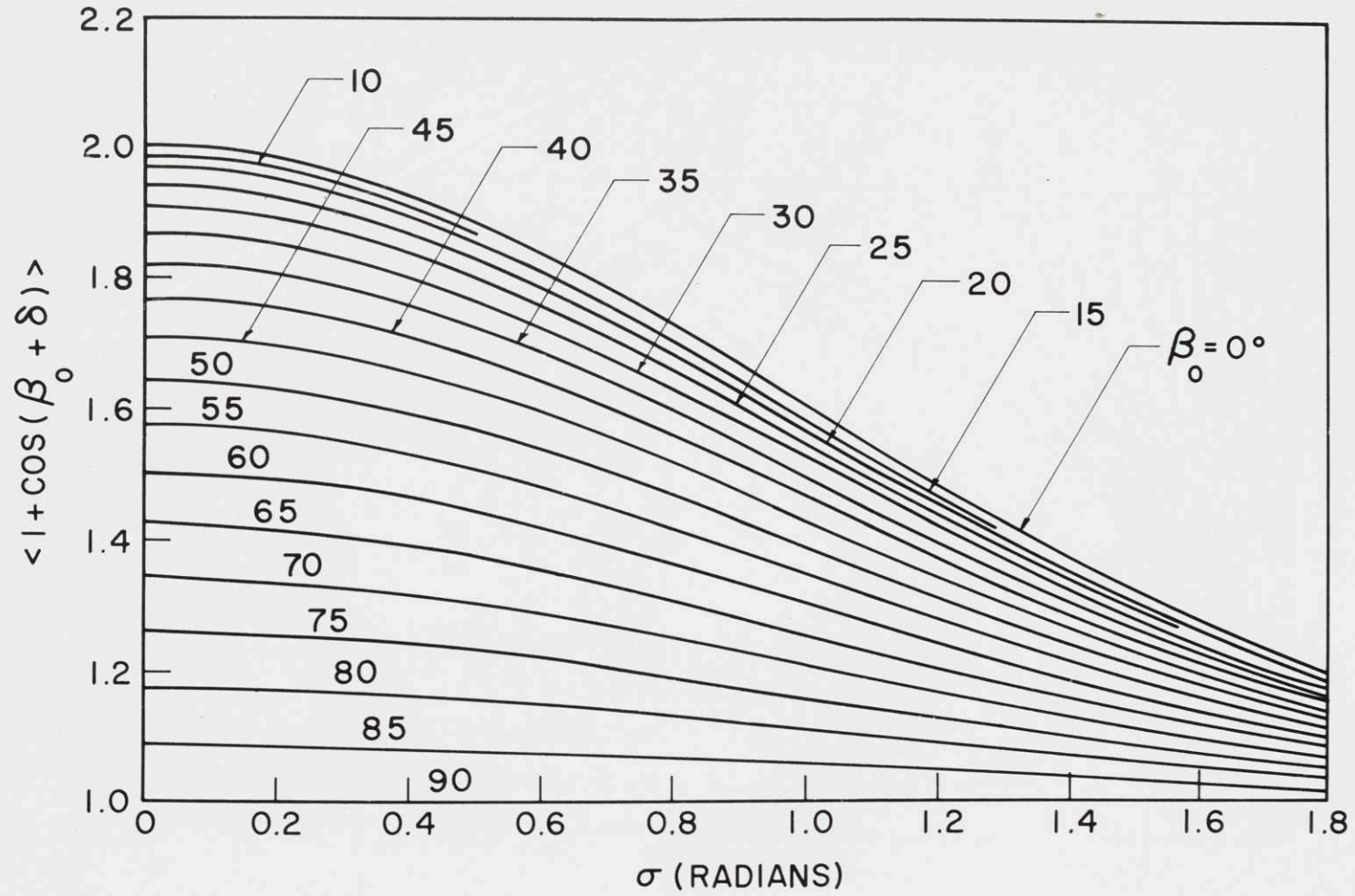
FIGURE 2-9
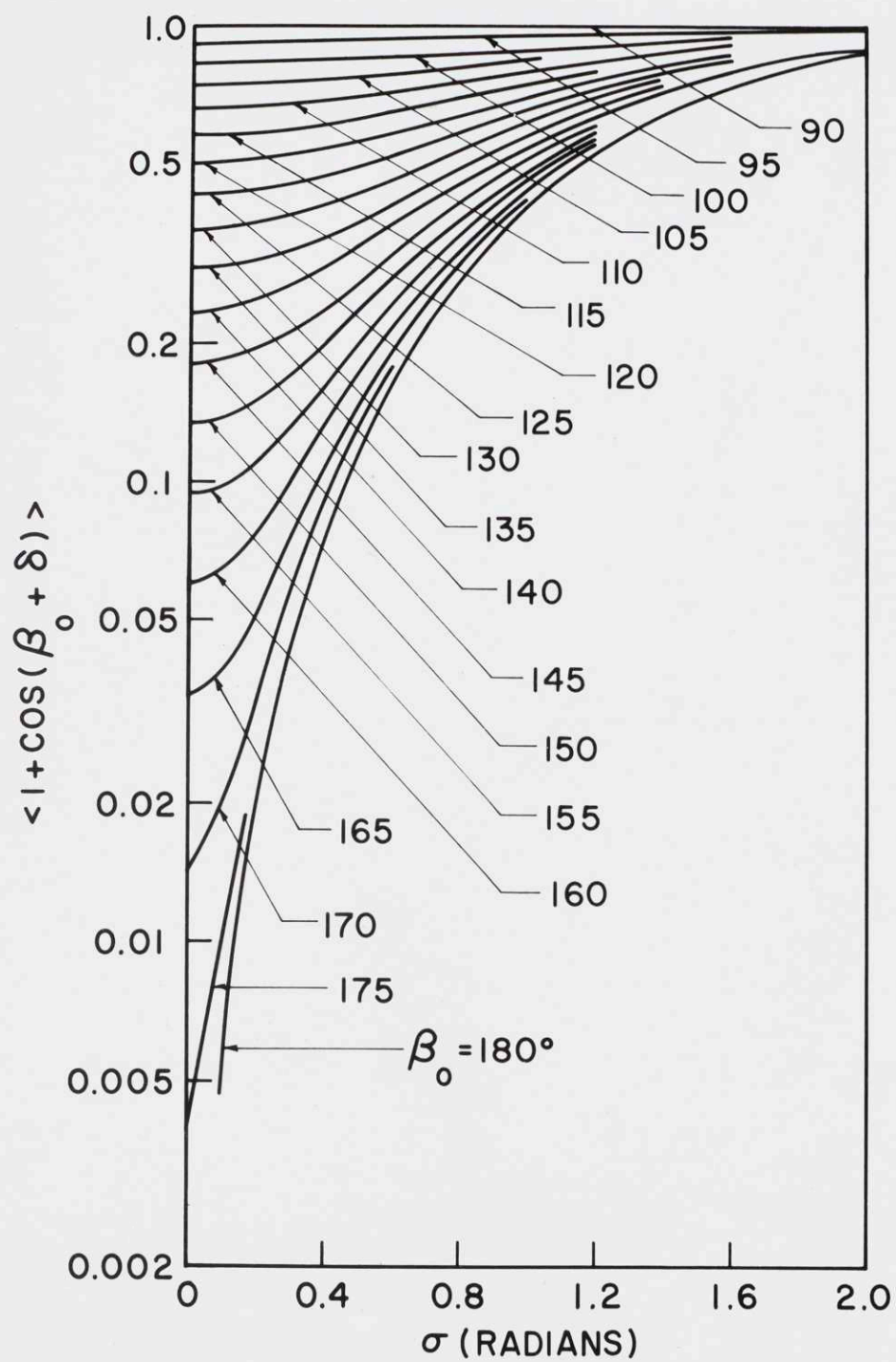
FIGURE 2-10
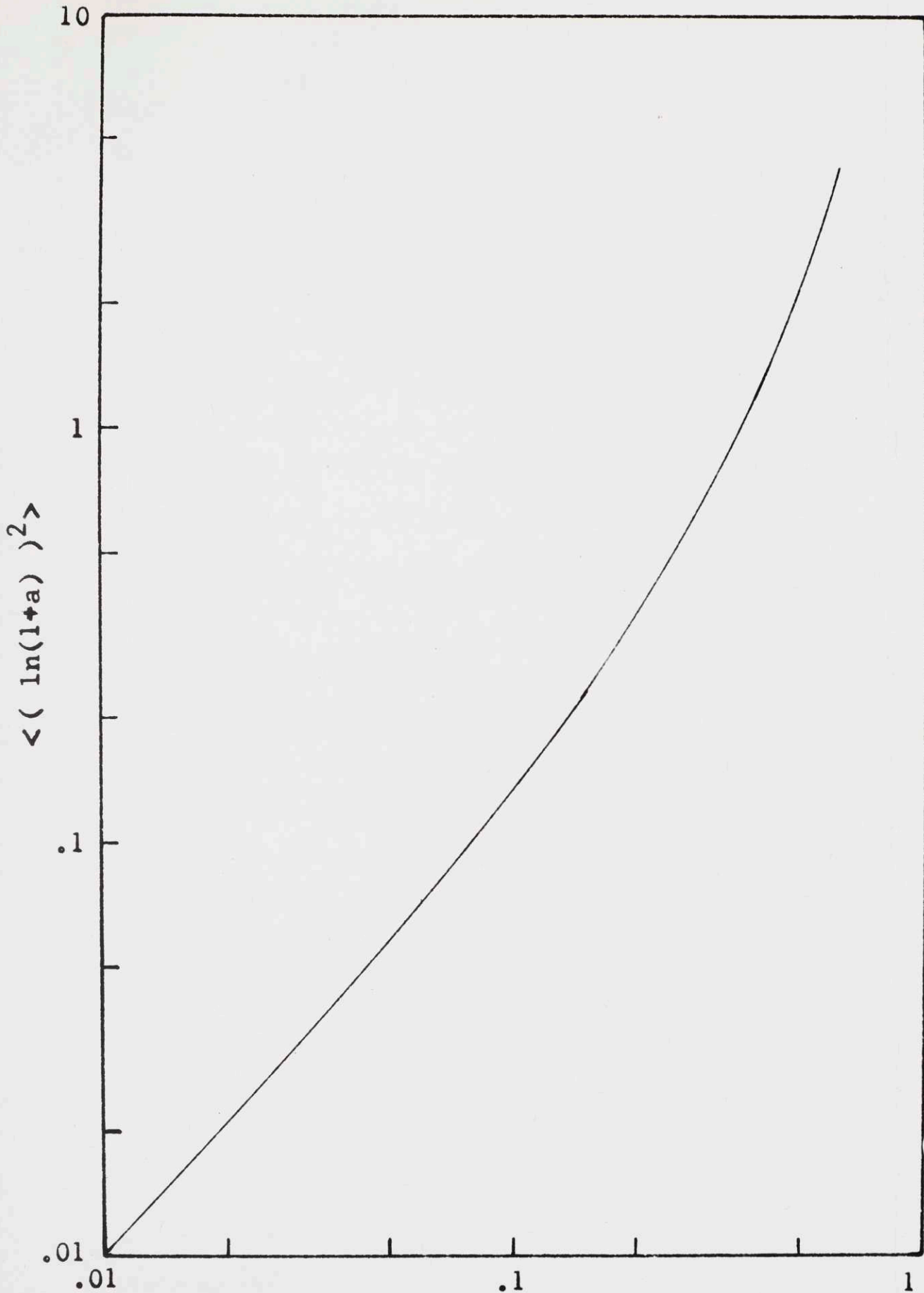
FIGURE 2-11

shown that $\langle \overline{p^2} \rangle$ may be calculated using the following equation

$$\langle \overline{p^2} \rangle = \frac{2R}{xr}\left\{\frac{\langle a^2 \rangle}{2R}\left(\frac{r}{x} + R\,\frac{x}{r}\right) + \frac{r}{2xR}\left(1 - R\,\frac{x}{r}\right)^2 + \left(1 + \cos\,\beta_o e^{-\sigma^2/2}\right)\right\}$$

$$(2\text{-}11)$$

where $\langle a^2 \rangle$ is obtained from

$$\langle (\ln(1 + a))^2 \rangle = \frac{\sqrt{\pi}}{2}(k_o x)(k_o L)\mu_o^2 \qquad (2\text{-}12)$$

and the plot of $\langle a^2 \rangle$ vs $\langle (\ln(1 + a)^2 \rangle$ presented in Figure 2-11. σ is given by

$$\sigma^2 = \langle \delta^2 \rangle = \sqrt{\pi}(k_o x)(k_o L)\mu_o^2 \qquad (2\text{-}13)$$

5. Statistical Analysis of the Fluctuations

Having obtained the rms pressure as a function of distance from the source, it is relatively easy to obtain an approximate expression for the variance of the fluctuations by doing integrals similar to that in Eq. (2-9). One can of course calculate either the statistics of the "instantaneous rms" pressure defined in section 2 or calculate the statistics of the "instantaneous mean square pressure" $\overline{p^2}$. We shall choose the latter because it is much easier to calculate and therefore define the variance v by

$$v = \langle (\overline{p^2} - \langle \overline{p^2} \rangle)^2 \rangle \qquad (2\text{-}14)$$

We start with Eq. (2-3) and take $A_d = 1 + a_d$, $A_r = 1 + a_r$. Since A_d and A_r appear as squared terms in Eq. (2-3),

terms such as a_d^4, a_r^4, etc. will appear when Eq. (2-3) is put into Eq. (2-14). The higher order products must be written in terms of second order moments when $\langle (\overline{p^2})^2 \rangle$ is calculated. Equation (2-11) is used for $\langle \overline{p^2} \rangle$ and $\langle \overline{p^2} \rangle^2$. We shall work out an expression for $\sqrt{v}/m$ assuming that the boundary is rigid (R = 1) and assuming that the cross-correlations between amplitude and phase can be neglected as well as the cross-correlation between the amplitude and phase along the direct and reflected path. The substitution is simple but algebraically tedious, and the integrals are of the same type evaluated in Eq. (2-9). The result is:

$$v = \left(\frac{2}{rx}\right)^2 (1 + 2\langle a^2 \rangle)\Big\{(1 - e^{-\sigma^2})(1 - e^{-\sigma^2} \cos 2\beta_o)$$

$$+ 2\langle a^2 \rangle (1 + \cos \beta_o e^{-\sigma^2/2})\Big\} \qquad (2-15)$$

We shall compare the ratio $\sqrt{v}/\langle \overline{p^2} \rangle$ with experimental data, and so the factor $2R/xr$ in Eq. (2-11) and the factor $(2/rx)^2$ in Eq. (2-15) may be dropped. For convenience in calculation, the term inside the square brackets in Eq. (2-15) has been calculated as a function of σ for several values of β_o. The results are shown in Figure 2-12. These results will be used in the next section where the calculation is compared with some experimental results.

6. Experimental Results

After the experiments described in section 3 were completed, it was realized that more detailed experimental
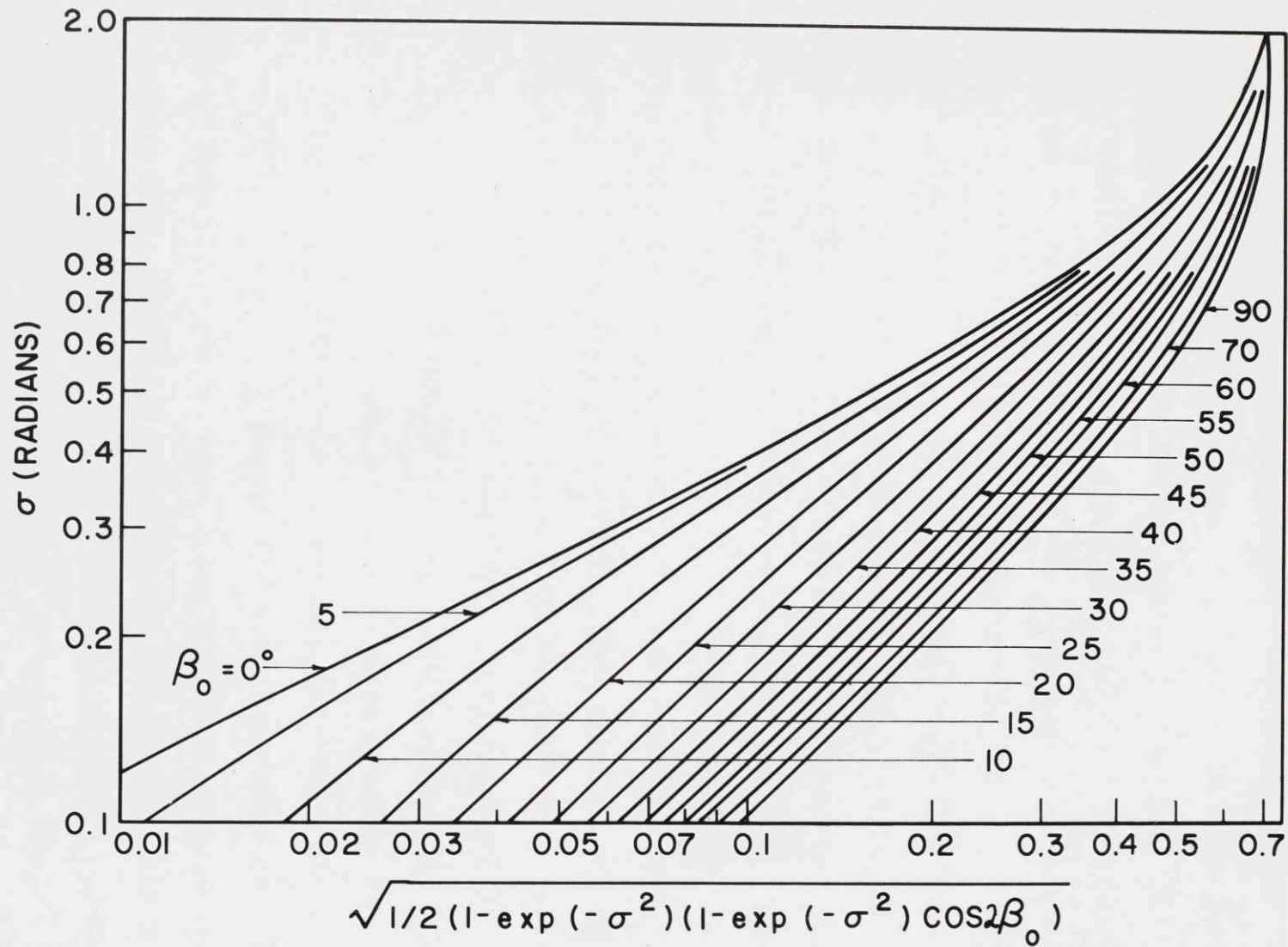
FIGURE 2-12

data would be desirable from which it would be possible
to obtain more information about the statistics of the
fluctuations and the rms value. The data to be described
in this section were obtained in the parking lot of the
M.I.T. Lincoln Laboratory. The rigid plane surface and
large size made this area ideal for studying fluctuations
outdoors relatively far away from reflecting objects. The
necessary equipment was obtained and set up on three suc-
cessive Sundays during March and April, 1962. A small
loudspeaker driver, oscillator and amplifier were used as
a source, and the received signal was recorded on an Ampex
tape recorder for analysis in the laboratory. The source
height chosen was four feet so that measurements could be
made both inside and outside of the interference zone for
the three frequencies used. The data obtained were later
played back through a Bruel and Kjaer level recorder with
a writing speed high enough to follow the envelope of the
received signal. The data were analyzed by reading the
level from the recorder tape at regular intervals along
the record. Two to four points per second were taken off
the tape depending on the time scale of the fluctuations.
From these data, the mean square sound pressure and vari-
ance of the mean square pressure were calculated. Approxi-
mately 16,000 data points were used in computing the
results to be presented. We shall choose a value of $\mu_o^2 L$
to give the best fit with the measured rms value of the

pressure at the last interference point at 500 cps. This
value was then used to calculate the mean pressure curves
for the other two frequencies and the curves of $\sqrt{v}/m$ for
all three frequencies. The value of $\mu_o^2 L$ equal to
2.62×10^{-5} ft. corresponds to $\langle \delta^2 \rangle = 0.0625$ radians^2 at
500 cps and 28.5 ft. At this point $\langle a^2 \rangle$ is 0.0312 and it
can be seen by using Eq. (2-11) that for $R = 1$ and $x/r =$
$(1 - 2h^2/xr)$ the middle term in the parentheses can be
neglected and the first and last terms contribute equally
to the mean-square pressure. For larger distances, the
term involving σ changes much more rapidly than the term
involving $\langle a^2 \rangle$ and so the amplitude fluctuations become of
relatively less importance. A comparison of all the
experimental and calculated data on mean values is pre-
sented in Figures 2-13, 2-14, and 2-15. It is felt that
the agreement here is reasonably good considering that the
data were obtained on three different days. The mean wind
speed during all of these measurements was relatively con-
stant at approximately 750 fpm.

The data on fluctuations are presented in Figure 2-16.
Two sets of calculated curves are shown because the frac-
tional variance was first calculated assuming that the
fluctuations in amplitude of the direct and reflected waves
could be neglected, and the sharply peaked curves were
obtained. The assumption of no amplitude fluctuations in
the direct and reflected waves leads to larger fluctuations
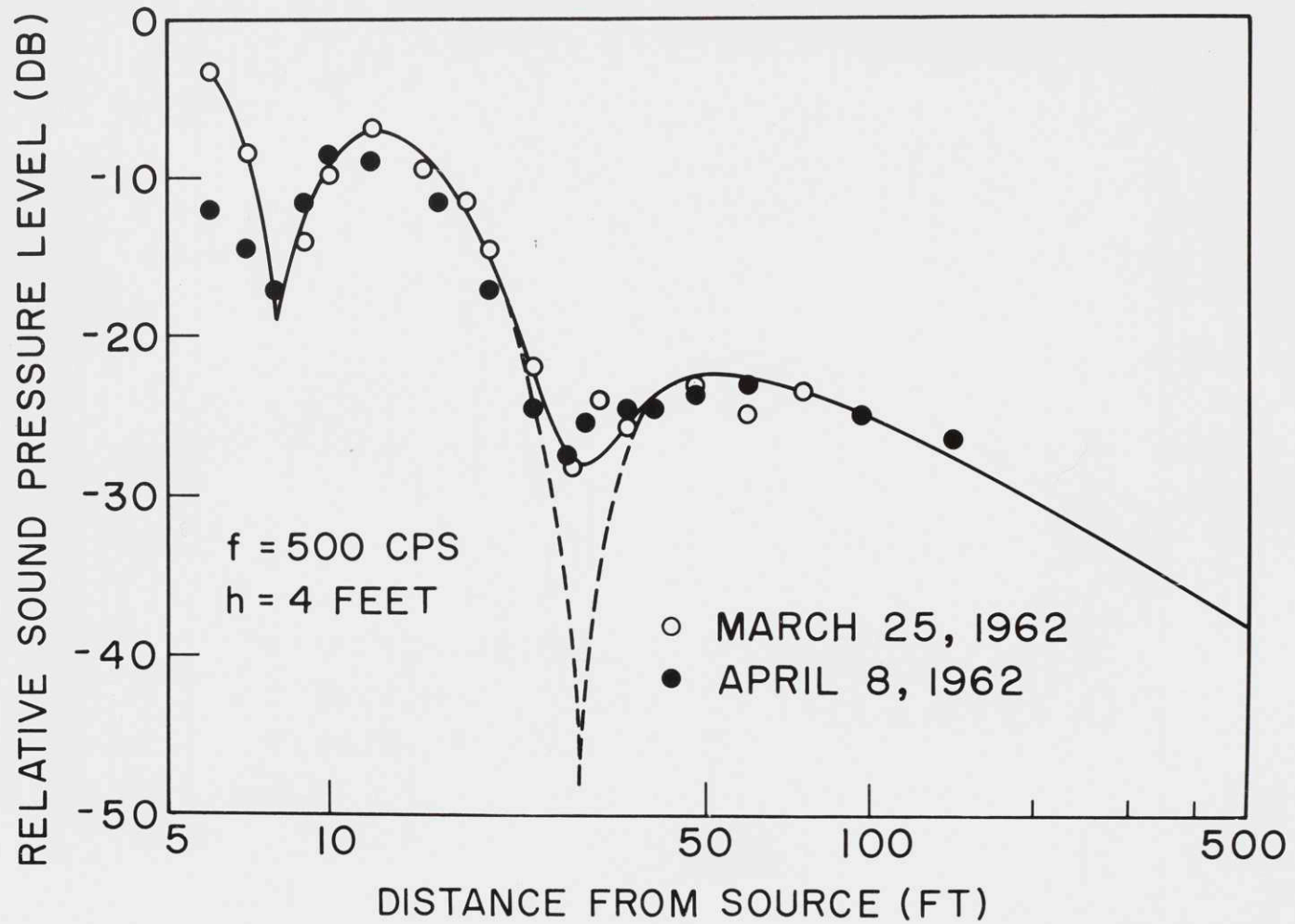
FIGURE 2-13
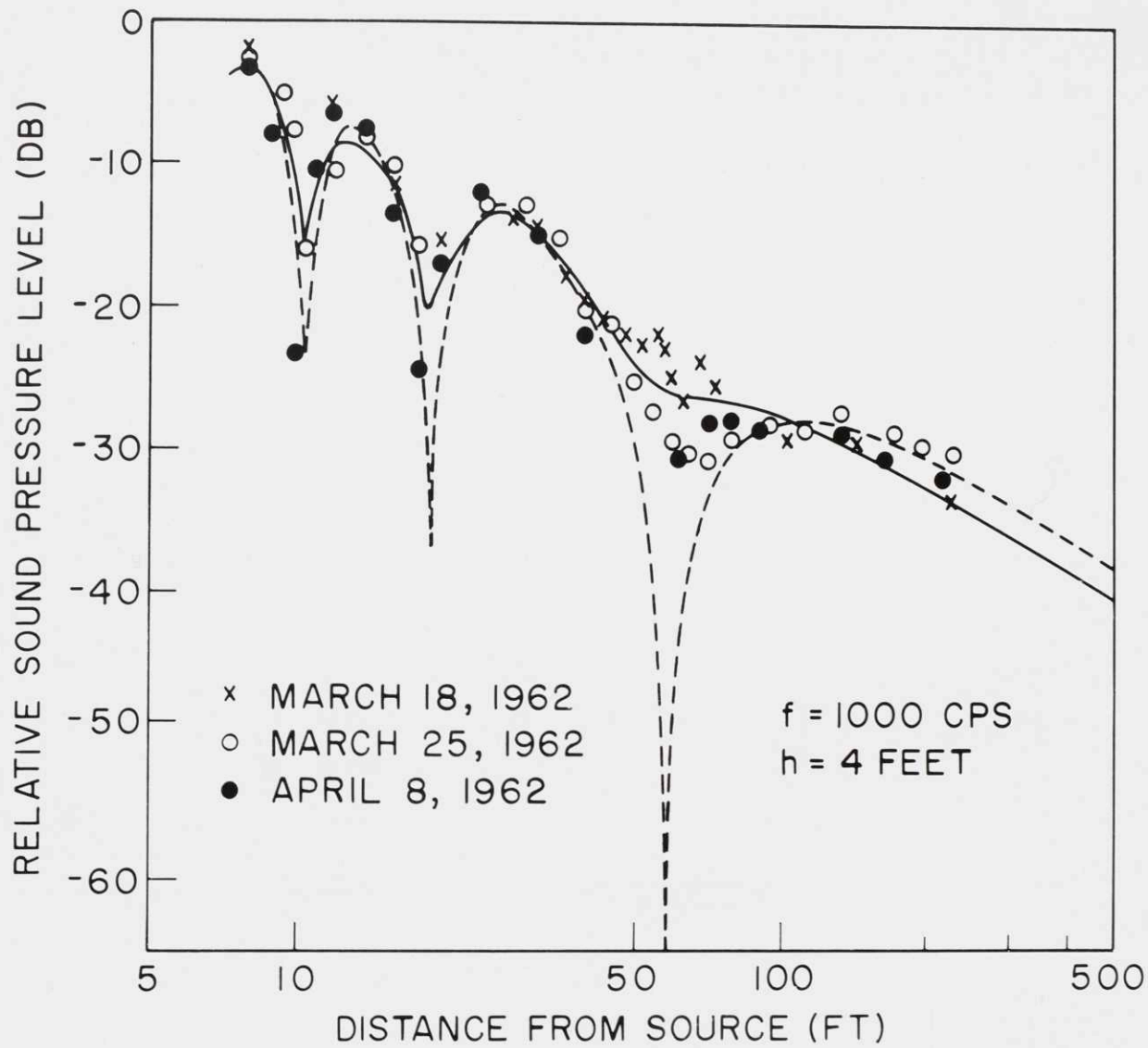
FIGURE 2-14
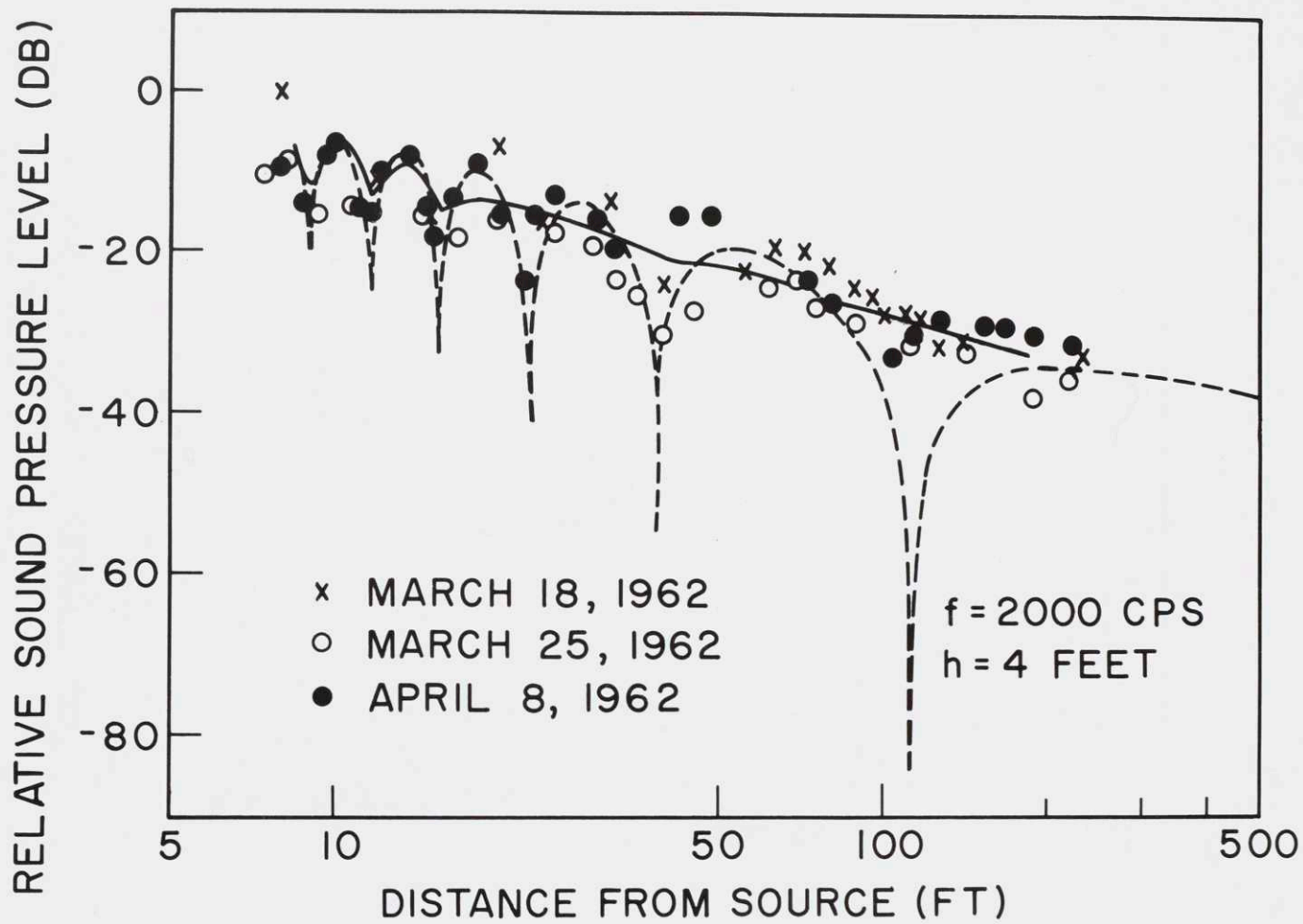
FIGURE 2-15
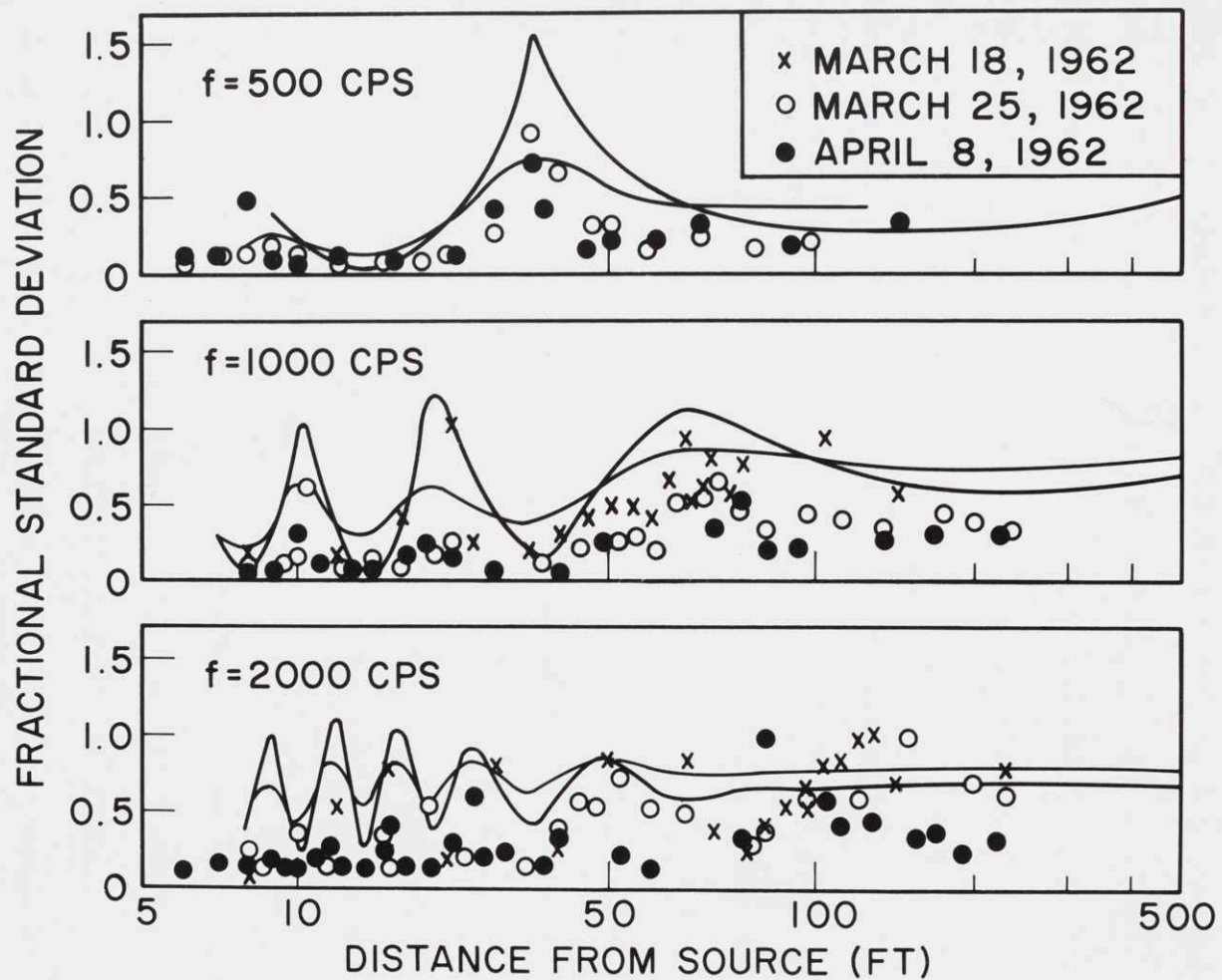
FIGURE 2-16

in the sum at the interference points because the
probability of having a high degree of cancellation (and
thus a large fluctuation) between the waves must be
related to the joint probability of finding the amplitudes
nearly equal and the phases different by nearly 180°.
When the amplitudes are assumed to be equal, cancellation
is more probable, and hence the fluctuations are larger.
These observations are borne out by the calculated curves.
Although the agreement between theory and experiment is
good at the lower frequencies, the calculated values are
generally too high at the higher frequencies. The shape
of the curves is generally correct, that is, the fluctua-
tions are larger in the minima of the mean pressure pattern
and smaller in the maxima, but the fluctuations tend to be
too small at all distances, especially near the source at
2000 cps. It can easily be shown, however, that at least
in the interference minima the fractional standard devia-
tion is sensitive to the relation between the square of
the second moment and the fourth moment. Thus one might
be able to get better agreement with the experimental data
by assuming a different probability distribution.

Finally, it should be noted that in this statistical
analysis it is still possible to estimate the average
fluctuations to be expected when one calculates a frac-
tional standard deviation. The data on fluctuations taken
from the Bruel and Kjaer tapes have been used in the

following manner. The upper and lower 10 percent of the
amplitude distribution curve has been neglected in obtain-
ing a fluctuation level L which can be plotted against the
calculated fractional standard deviation of the same curve.
The results, presented in Figure 2-17, show that the
fluctuation level can be reasonably well estimated from
the fractional standard deviation.

FIGURE 2-17

54
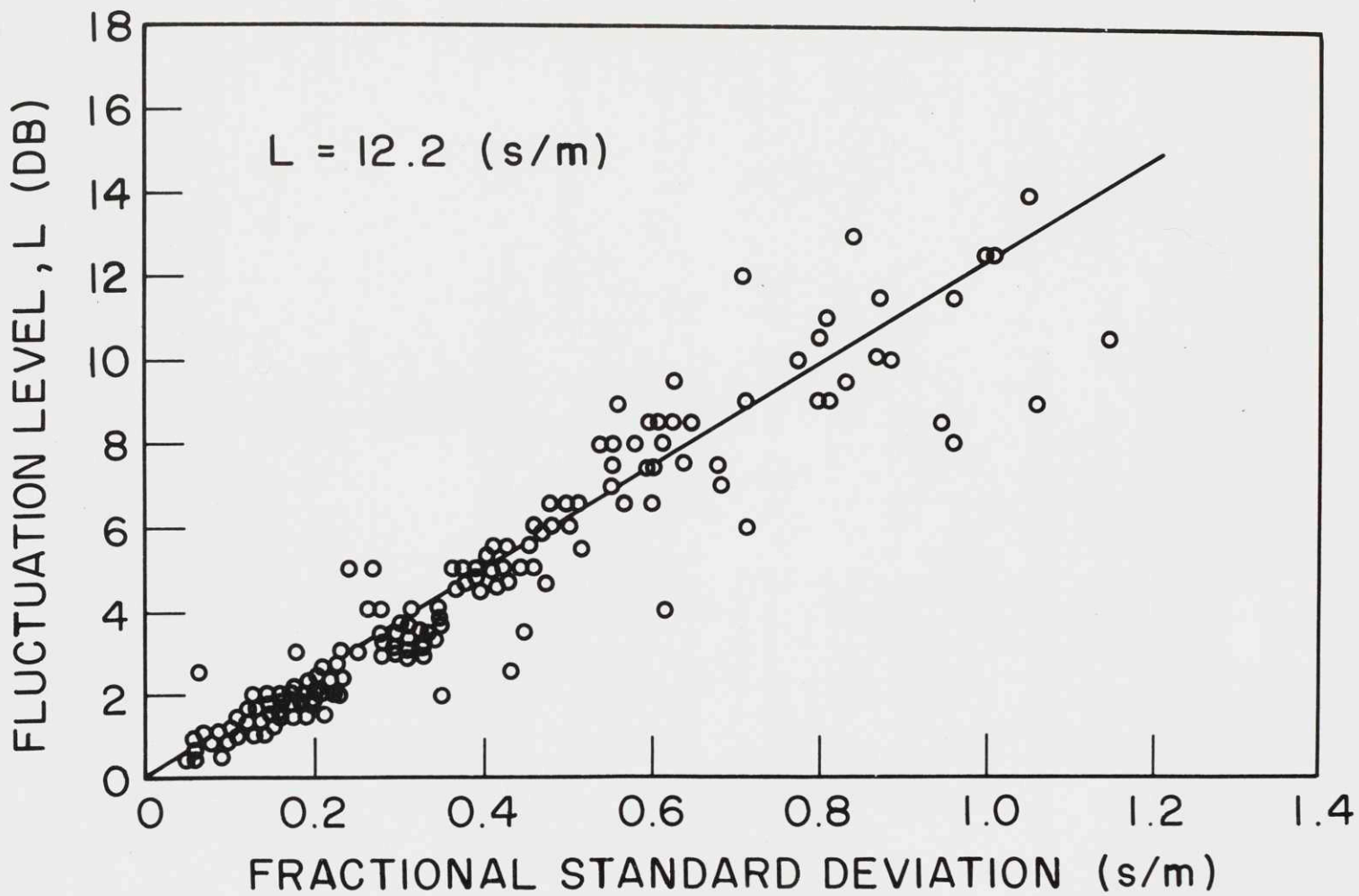
REFERENCES FOR CHAPTER TWO

1.   Obukhov, A.M., Dokl. Acad. Nauk., USSR, 30, 611 (1941)

2.   Krasilnikov, V.A., Dokl. Akad. Nauk., USSR, 58, 1353 (1957)

3.   Chernov, L.A., Dokl. Akad. Nauk., USSR, 98, 953 (1954)

4.   Lighthill, M.J., Proc. Cambridge Phil. Soc., 49, 531 (1952)

5.   Batchelor, G.K., Homogeneous Turbulence, Cambridge
     University Press (1953)

6.   Kraichman, R.H., J. Acoust. Soc. Am., 29, 65 (1957)

7.   Minzer, D., J. Acoust. Soc. Am., 25, 922 (1953)

8.   Minzer, D., J. Acoust. Soc. Am., 25, 1107 (1953)

9.   Chernov, L.A., Wave Propagation in a Random Medium,
     McGraw-Hill (1960)

10. Tatarski, V.I., Wave Propagation in a Turbulent Medium,
     McGraw-Hill (1961)

11. Morse, P.M. and Ingard, K.U., Linear Acoustic Theory,
     Handbuch der Physik, XI/1 Springer-Verlag (1961)

12. Ingard, K.U., Field Studies of Sound Propagation over
     Ground, M.I.T. Acoustics Laboratory (1954)

Chapter 3. The Propagation of Waves of Finite Amplitude
              in a Stratified Medium

1.   Introduction

Because the equations that govern fluid motion are
nonlinear, the progress that has been made towards find-
ing solutions of the exact equations of motion (including
terms arising from loss mechanisms in the fluid) has
necessarily been made slowly. Much of the work of
Lighthill,[1] Fay,[2] Fubini[3] and others has been
thoroughly reviewed in a report by Blackstock.[4] The
above workers have all found approximate solutions to
the equations that describe large-amplitude wave propaga-
tion in a viscous heat-conducting fluid.

On the other hand, it is appropriate in many cases
to examine the motion of a wave that consists of an already
formed shock front followed by a decay in pressure that is
governed by the loss-free nonlinear equations of motion.
The classical Rankine[5]-Hugoniot[6] shock relations may
be used to describe the change in pressure, density and
velocity across the shock front, whereas the motion behind
the shock is governed by the exact loss-free equations of
motion. In homogeneous media, the classical formulation
of Riemann[7] and Stokes[8] may be used, but for

inhomogeneous media that formulation must be modified as shown in the next section. We shall work out the general theory only for a very special case, namely that of weak "N-waves" (see Figure 3-3) in an inhomogeneous medium. The results of this analysis may be compared to an approximate method developed by Whitham[9] for propagation of shock waves in an inhomogeneous medium, and it will be shown that the present method yields a somewhat better approximation, at least for weak shock waves. For simplicity we shall limit ourselves to a one-dimensional treatment.

2.   The Exact Non-Dissipative Equations of Motion

In this section we shall formulate the exact equations of motion in an inhomogeneous medium in a form similar to the classical equations for a homogeneous medium. The essential difference, in addition to the body force, is that in our treatment the entropy of the fluid will be considered to be a point function of space in the absence of any fluid motion. Thus, although the equations are loss-free in the sense that in the presence of motion the entropy of a fluid particle is constant, the motion cannot be considered to be isentropic if an Eulerian description of the motion is used. When one looks at a fixed point in the fluid, entropy changes of the order of $\zeta (\partial s_e/\partial x)$ are to be expected where ζ is the particle displacement in a Lagrangian description and $\partial s_e/\partial x$ is the mean entropy

gradient in the fluid. We shall include an external force per unit volume (F) in the analysis, but neglect any external sources of mass.

The exact one-dimensional equations of continuity and conservation of momentum are:

$$\frac{\partial \rho}{\partial t} + u\,\frac{\partial \rho}{\partial x} + \rho\,\frac{\partial \rho}{\partial x} = 0 \qquad (3\text{-}1)$$

$$\frac{\partial u}{\partial t} + u\,\frac{\partial u}{\partial x} + \frac{1}{\rho}\,\frac{\partial p}{\partial x} = \frac{F}{\rho} \qquad (3\text{-}2)$$

The condition that the entropy of a fluid particle is constant is expressed simply by:

$$\frac{\partial s}{\partial t} + u\,\frac{\partial s}{\partial x} = 0 \qquad (3\text{-}3)$$

The classical method of treating these equations for homogeneous media is to take $u = u(\rho)$ and $p = p(\rho)$ (equation of state) since s is supposed to be a constant. In the analysis to follow, s is included as a variable and p rather than ρ is chosen as the second independent variable. The reason for this choice will become apparent as we proceed. We therefore take $u = u(p,s)$ and use the equation of state in the form $p = p(\rho,s)$. We may then write

$$\frac{\partial p}{\partial t} = \left(\frac{\partial p}{\partial \rho}\right)_{s}\frac{\partial \rho}{\partial t} + \left(\frac{\partial p}{\partial s}\right)_{\rho}\frac{\partial s}{\partial t} \qquad (3\text{-}4)$$

$$\frac{\partial p}{\partial x} = \left(\frac{\partial p}{\partial \rho}\right)_{s}\frac{\partial \rho}{\partial x} + \left(\frac{\partial p}{\partial s}\right)_{\rho}\frac{\partial s}{\partial x} \qquad (3\text{-}5)$$

If Eq. (3-5) is multiplied by u and added to Eq. (3-4) we obtain, with $(\partial p/\partial \rho)_s$ the adiabatic speed of sound (c^2),

$$\frac{\partial p}{\partial t} + u \frac{\partial p}{\partial x} = c^2 \left(\frac{\partial \rho}{\partial t} + u \frac{\partial \rho}{\partial x} \right) \tag{3-6}$$

This well-known[9] form of the adiabatic condition will also prove to be useful in the analysis.

We next use $u = u(p,s)$ and $u = u(\rho,s)$ to obtain

$$\frac{\partial u}{\partial t} + u \frac{\partial u}{\partial x} = \left(\frac{\partial u}{\partial p} \right)_s \left(\frac{\partial p}{\partial t} + u \frac{\partial p}{\partial x} \right) \tag{3-7a}$$

and

$$\frac{\partial u}{\partial t} + u \frac{\partial u}{\partial x} = \left(\frac{\partial u}{\partial \rho} \right)_s \left(\frac{\partial \rho}{\partial t} + u \frac{\partial \rho}{\partial x} \right) \tag{3-7b}$$

using relations similar to Eqs. (3-4) and (3-5). The equation of continuity (Eq. (3-1)) may now be written in terms of $dp/dt = \partial p/\partial t + u(\partial p/\partial x)$ by using Eq. (3-6). Thus, Eq. (3-1) becomes

$$\frac{1}{c^2} \left(\frac{\partial p}{\partial t} + u \frac{\partial p}{\partial x} \right) = - \rho \frac{\partial u}{\partial x} \tag{3-8}$$

which can be written as

$$\frac{\partial u}{\partial t} + u \frac{\partial u}{\partial x} = - \rho c^2 \left(\frac{\partial u}{\partial p} \right)_s \frac{\partial u}{\partial x} \tag{3-9}$$

by using Eq. (3-7a).

It is now obvious that if Eqs. (3-9) and (3-2) are both satisfied we must have

$$\frac{\partial p}{\partial x} - \rho^2 c^2 \left(\frac{\partial u}{\partial p}\right)_s \frac{\partial u}{\partial x} = F \qquad (3\text{-}10)$$

When $\partial u/\partial x$ is written in terms of $\partial p/\partial x$ and $\partial s/\partial x$,
Eq. (3-10) may be written

$$\left(1 - \rho^2 c^2 \left(\frac{\partial u}{\partial p}\right)_s^2\right)\frac{\partial p}{\partial x} - \rho^2 c^2 \left(\frac{\partial u}{\partial p}\right)_s \left(\frac{\partial u}{\partial s}\right)_p \frac{\partial s}{\partial x} = F \qquad (3\text{-}11)$$

This result will be important in our analysis. It can be
easily seen that it is analogous to the Riemann Condition
for fluid motion in a homogeneous medium, for if s = con-
stant, the above relation reduces to

$$\left(\frac{\partial u}{\partial p}\right)_s = \pm \frac{1}{\rho c}$$

and since u and p are now functions of density alone, we
may write

$$\left(\frac{du}{d\rho}\right) = \left(\frac{du}{dp}\right)\left(\frac{dp}{d\rho}\right) = \pm \frac{c}{\rho} \qquad (3\text{-}12)$$

which is the Riemann Condition. Equation (3-11) may be
further simplified by using the chain relation well known
in thermodynamics. If s and u are considered to be inde-
pendent variables, we have

$$\left(\frac{\partial u}{\partial s}\right)_p = - \left(\frac{\partial u}{\partial p}\right)_s \left(\frac{\partial p}{\partial s}\right)_u \qquad (3\text{-}13)$$

and consequently Eq. (3-11) may be written

$$\left(1 - \rho^2 c^2 \left(\frac{\partial u}{\partial p}\right)_s^2\right)\frac{\partial p}{\partial x} + \rho^2 c^2 \left(\frac{\partial u}{\partial p}\right)_s^2 \left(\frac{\partial p}{\partial s}\right)_u \frac{\partial s}{\partial x} = F \qquad (3\text{-}14a)$$

or

$$1 - \rho^2 c^2 \left(\frac{\partial u}{\partial p}\right)_s^2 = \frac{F - \left(\frac{\partial p}{\partial s}\right)_u \frac{\partial s}{\partial x}}{\frac{\partial p}{\partial x} - \left(\frac{\partial p}{\partial s}\right)_u \frac{\partial s}{\partial x}} \qquad (3\text{-}14b)$$

We shall use all of these results in the analysis to follow. Next, let us obtain three equations of motion in the form

$$\frac{\partial \textcircled{H}}{\partial t} + (u + c\, \Psi)\frac{\partial \textcircled{H}}{\partial x} = \chi F \qquad (3\text{-}15)$$

where $\textcircled{H}$ is either p, ρ, or u. For $\textcircled{H} = u$ we simply rearrange Eq.

$$\frac{\partial u}{\partial t} + \left(u + c\left\{\rho c\left(\frac{\partial u}{\partial p}\right)_s\right\}\right)\frac{\partial u}{\partial x} = 0 \qquad (3\text{-}16)$$

The equation for p is obtained by using Eq. (3-7) to eliminate $\partial u/\partial t + u(\partial u/\partial x)$ from Eq. (3-2). The result is

$$\frac{\partial p}{\partial t} + \left(u + c\left\{\frac{1}{\rho c\left(\frac{\partial u}{\partial p}\right)_s}\right\}\right)\frac{\partial p}{\partial x} = \frac{F}{\rho\left(\frac{\partial u}{\partial p}\right)_s} \qquad (3\text{-}17)$$

A great deal of manipulation is required to obtain a similar equation for $\textcircled{H} = \rho$. The method to be followed is first to eliminate $\partial u/\partial t + u(\partial u/\partial x)$ from the momentum equation by using Eqs. (3-6) and (3-7). Next $\partial p/\partial x$ is written in terms of $\partial \rho/\partial x$ by using Eq. (3-14) and

$\partial p/\partial x = (\partial p/\partial \rho)_s (\partial \rho/\partial x) + (\partial p/\partial s)_\rho (\partial s/\partial x)$. Finally, Eq. (3-14) is used to eliminate $\partial s/\partial x$ with the result that

$$\frac{\partial \rho}{\partial t} + (u + c\,\Psi)\frac{\partial \rho}{\partial x} = \chi F \qquad (3\text{-}18)$$

where

$$\Psi = \frac{\Lambda}{\rho c \left(\frac{\partial u}{\partial p}\right)_s}$$

$$\chi = \frac{1}{\rho c^2 \left(\frac{\partial u}{\partial p}\right)_s}\left(1 - \frac{\left(\frac{\partial p}{\partial s}\right)_\rho}{\rho^2 c^2 \left(\frac{\partial u}{\partial p}\right)_s \left(\frac{\partial p}{\partial s}\right)_u}\right)$$

and

$$\frac{1}{\Lambda} = 1 + \frac{\left(\frac{\partial p}{\partial s}\right)_\rho \left(1 - \rho^2 c^2 \left(\frac{\partial u}{\partial p}\right)_s^2\right)}{\rho^2 c^2 \left(\frac{\partial u}{\partial p}\right)_s \left(\frac{\partial p}{\partial s}\right)_u}$$

Equations (3-16), (3-17) and (3-18) all reduce to

$$\frac{\partial \mathcal{H}}{\partial t} + (u \pm c)\frac{\partial \mathcal{H}}{\partial x} = 0 \qquad (3\text{-}19)$$

for F and $\partial s/\partial x = 0$ because, from Eq. (3-14), we have $(\partial u/\partial p)_s = \pm \frac{1}{\rho c}$. $\mathcal{H}$ represents either p, ρ, or u. The well-known[10] solution

$$\mathcal{H} = \mathcal{H}(x - (u \pm c)t) \qquad (3\text{-}20)$$

describes the propagation of pressure, density or particle velocity in a homogeneous medium. The quantity $\mathcal{H}$ is

constant along lines of slope dx/dt = u $\pm$ c in the x-t
plane, and these lines are the well-known C^+ and C^- char-
acteristics respectively. The Riemann Condition may be
written in the form

$$1 + \frac{\rho}{c}\left(\frac{du}{d\rho}\right) = 0 \quad \text{on } C^+ \tag{3-21a}$$

$$1 - \frac{\rho}{c}\left(\frac{du}{d\rho}\right) = 0 \quad \text{on } C^- \tag{3-21b}$$

or, after integration,

$$u + \int \frac{c}{\rho} \, d\rho = \text{constant} \equiv 2r \quad \text{on } C^+ \tag{3-22a}$$

$$u - \int \frac{c}{\rho} \, d\rho = \text{constant} \equiv 2s \quad \text{on } C^- \tag{3-22b}$$

r and s are the well-known <u>Riemann Invariants</u>, and are
constant along the C^+ and C^- characteristics respectively.
The condition that waves travel only in the positive
x-direction is that s be a constant everywhere (s_o) for
then u = u(r) and u = constant along r = constant. Thus
p and ρ are also constant on C^+. For waves travelling in
the negative x-direction, it is obvious that r must be a
constant everywhere. Thus, if either the + or - sign in
Eq. (3-19) is chosen ⊕ may be taken to be a constant
along C^+ or C^- respectively, but the general solution to
the problem is that r and s are constants along C^+ and C^-
respectively. It does not appear to be possible to find
such simple relations for inhomogeneous media because two

independent variables are involved. We shall, however, obtain approximate relations that can be used to describe propagation in inhomogeneous media.

Before proceeding with a discussion of the Rankine-Hugoniot shock relations, let us write the equations of motion in characteristic form.[11] Equations (3-1), (3-2) and (3-6) may be written in the following form:

$$\frac{\partial p}{\partial t} + (u \pm c)\frac{\partial p}{\partial x} \pm \rho c\left(\frac{\partial u}{\partial t} + (u \pm c)\frac{\partial u}{\partial x}\right) - cF = 0 \qquad (3\text{-}23)$$

$$\frac{\partial p}{\partial t} + u\frac{\partial p}{\partial x} - c^2\left(\frac{\partial \rho}{\partial t} + u\frac{\partial \rho}{\partial x}\right) = 0 \qquad (3\text{-}24)$$

The equations have been put into the above form because we may now write total differential relations along the C^+ and C^- characteristics. We obviously have

$$dp + \rho c\,du - \frac{cF}{u+c}\,dx = 0 \text{ on } C^+,\ \frac{dx}{dt} = u + c \qquad (3\text{-}25a)$$

$$dp - \rho c\,du - \frac{cF}{u+c}\,dx = 0 \text{ on } C^-,\ \frac{dx}{dt} = u - c \qquad (3\text{-}25b)$$

$$dp - c^2 d\rho = 0 \text{ on } P,\ \frac{dx}{dt} = u \qquad (3\text{-}25c)$$

This form of the equations of motion will be useful when we compare our results with those obtained by other investigators.

3. The Rankine-Hugoniot Shock Relations

In order to derive the classical Rankine-Hugoniot shock relations we assume that there is a very thin

region in the fluid within which the pressure, density and particle velocity change very rapidly. Such a region (shock) is illustrated in Figure 3-1. We shall assume that the shock is moving with velocity U relative to the fluid (at rest) in region A. The equations of conservation of mass, momentum and energy may be put into the following form:[12]

$$\rho_e U = \rho_1 (U - u_1)$$

$$p_1 - p_e = \rho_e U u_1$$

$$p_1 u_1 = \rho_e U (\frac{1}{2} u_1^2 + E_1 - E_e)$$

where U is the velocity of the shock wave, and the subscripts e and 1 refer to quantities ahead of and behind the shock wave respectively. If it is assumed that the fluid is an ideal gas ($p = (\gamma - 1)\rho E$) the above relations may, after considerable manipulation, be put into the form of the Rankine-Hugoniot shock relations:

$$p_1 = \rho_e c_e^2 (\frac{2}{\gamma + 1} M^2 - \frac{\gamma - 1}{\gamma(\gamma + 1)}) \text{ or } \mathcal{S} \equiv \frac{p_1 - p_e}{p_e} = \frac{2\gamma}{\gamma + 1}(M^2 - 1)$$

$$(3\text{-}26a)$$

$$\rho_1 = \rho_e \frac{(\gamma + 1)M^2}{(\gamma - 1)M^2 + 2} \qquad \text{or } \frac{\delta}{\rho_e} = \frac{\rho_1 - \rho_e}{\rho_e} = \frac{M^2 - 1}{\frac{\gamma - 1}{2} M^2 + 1}$$

$$(3\text{-}26b)$$

$$u_1 = c_e \frac{2}{\gamma + 1}(M - \frac{1}{M}) \qquad\qquad\qquad (3\text{-}26c)$$

$$p_1 \,,\, \rho_1 \,,\, u_1$$

$$\underline{B} \qquad\qquad \longrightarrow U \qquad\qquad \underline{A}$$

$$p_e \,,\, \rho_e \,,\, u_e = 0$$

$$x = 0$$
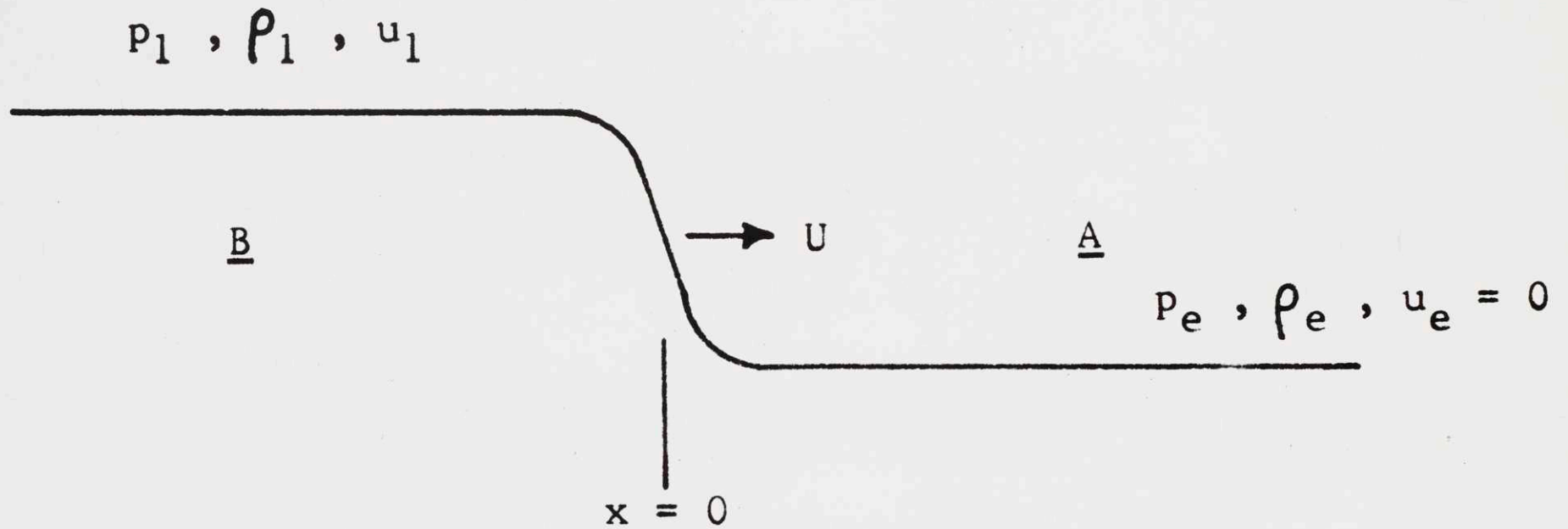
FIGURE 3-1

For weak shock waves, M may be taken to be $1 + \Delta$ where $\Delta \ll 1$ and so the above relations reduce to

$$u_1 = \frac{4\Delta}{\gamma + 1} c_e \tag{3-27a}$$

$$\zeta = \frac{4\gamma\Delta}{\gamma + 1} \tag{3-27b}$$

$$\frac{\delta}{\rho_e} = \frac{4\Delta}{\gamma + 1} \tag{3-27c}$$

For strong shock waves ($M \gg 1$) Eqs. (3-26a, b, c) obviously reduce to

$$p_1 = \frac{2\gamma}{\gamma + 1} \rho_e U^2 \tag{3-28a}$$

$$\rho_1 = \frac{\gamma + 1}{\gamma - 1} \rho_e \tag{3-28b}$$

$$u_1 = \frac{2}{\gamma + 1} U \tag{3-28c}$$

We shall need both of these limits in the analysis to follow.

4. Whitham's Rule

Before continuing we shall present a simple rule due to Whitham[11] that can be used to predict (approximately) the motion of a shock wave in an inhomogeneous medium. The rule is to apply the differential relation (Eq. (3-25a)) that holds along the C^+ characteristic to p_1, ρ_1, and u_1 directly behind the shock wave. Thus, by using Eqs. (3-28a, b, c) in Eq. (3-25a) it can easily be shown[11] that $U \sim \rho_e^{-\beta}$ where $\beta = (2 + \sqrt{2\gamma/(\gamma + 1)}) = 0.215$ for $\gamma = 1.4$.

For an isothermal atmosphere $p_e \sim \rho_e$ and for a strong shock $p_1 \sim \rho_0 U^2$. Thus, the pressure ratio across the shock is:

$$\frac{p_1 - p_e}{p_e} = \varsigma \doteq \frac{p_1}{p_e} \sim p_e^{-2\beta} \sim p_e^{-0.43} \qquad (3-29)$$

The rule does not seem to have been applied to weak shock waves, but the necessary relations can be easily manipulated. Let us consider an isothermal atmosphere under the influence of a gravitational force $F = -\rho g$. For weak shock waves, the speed of sound behind the shock is

$$c = \sqrt{\frac{\gamma p}{\rho}} \doteq c_e (1 + 2 \frac{\gamma - 1}{\gamma + 1} \Delta) \qquad (3-30)$$

and the use of the weak shock relations in Eq. (3-25a) leads to

$$\frac{1}{p_e} \frac{dp_e}{dx} + \frac{2}{\Delta} \frac{d}{dx}(1 + \Delta) = 0 \qquad (3-31)$$

after the equilibrium condition $\partial p_e / \partial x = - \rho_e g$ is used. Thus, for small Δ, $\Delta \sim p_e^{-0.5}$ and since $\varsigma \sim \Delta$, we have simply that

$$\varsigma \sim (p_e)^{-0.5} \qquad (3-32)$$

We recall from our discussion of the small-signal case that the sound pressure p was proportional to $\rho_e^{0.5}$ and hence $\varsigma = p/p_e \sim (p_e)^{-0.5}$. This result can be obtained immediately if it is assumed that the acoustic wave does not lose any energy as it propagates.

5.   Equation Governing the Decay of Pressure at the

     Shock Front

In this section we shall formulate the law that
governs the pressure rise across a shock front as a func-
tion of distance. The pressure decay behind the shock
front is assumed to obey the loss-free equations of motion.
The method used to obtain the equation is extremely simple.
We first separate the pressure, density, and entropy into
time-independent and time-dependent parts:

$$p(x,t) = p_e(x) + p_d(x,t) \qquad (3\text{-}33a)$$

$$\rho(x,t) = \rho_e(x) + \delta(x,t) \qquad (3\text{-}33b)$$

$$s(x,t) = s_e(x) + \sigma(x,t) \qquad (3\text{-}33c)$$

The flow field u is assumed to have no time-independent
part. We draw in the x-t plane a line that represents
the motion of the shock front $(dx/dt)_U$ and a line along
which p_d = constant, $(dx/dt)_{p_d}$ = const.· We shall find
the slope of this line for homogeneous and inhomogeneous
media in the sections to follow. The geometry is illus-
trated in Figure 3-2. The pressure, p_d, at O (p_O) and
A (p_A) is found from the pressure at t = 0. After the
shock front has moved a distance dx, the pressure (p_d) at
B is the same as the pressure at A by construction. Thus,
with $p_A = p_O + (\partial p_d/\partial x)dx'$, we have
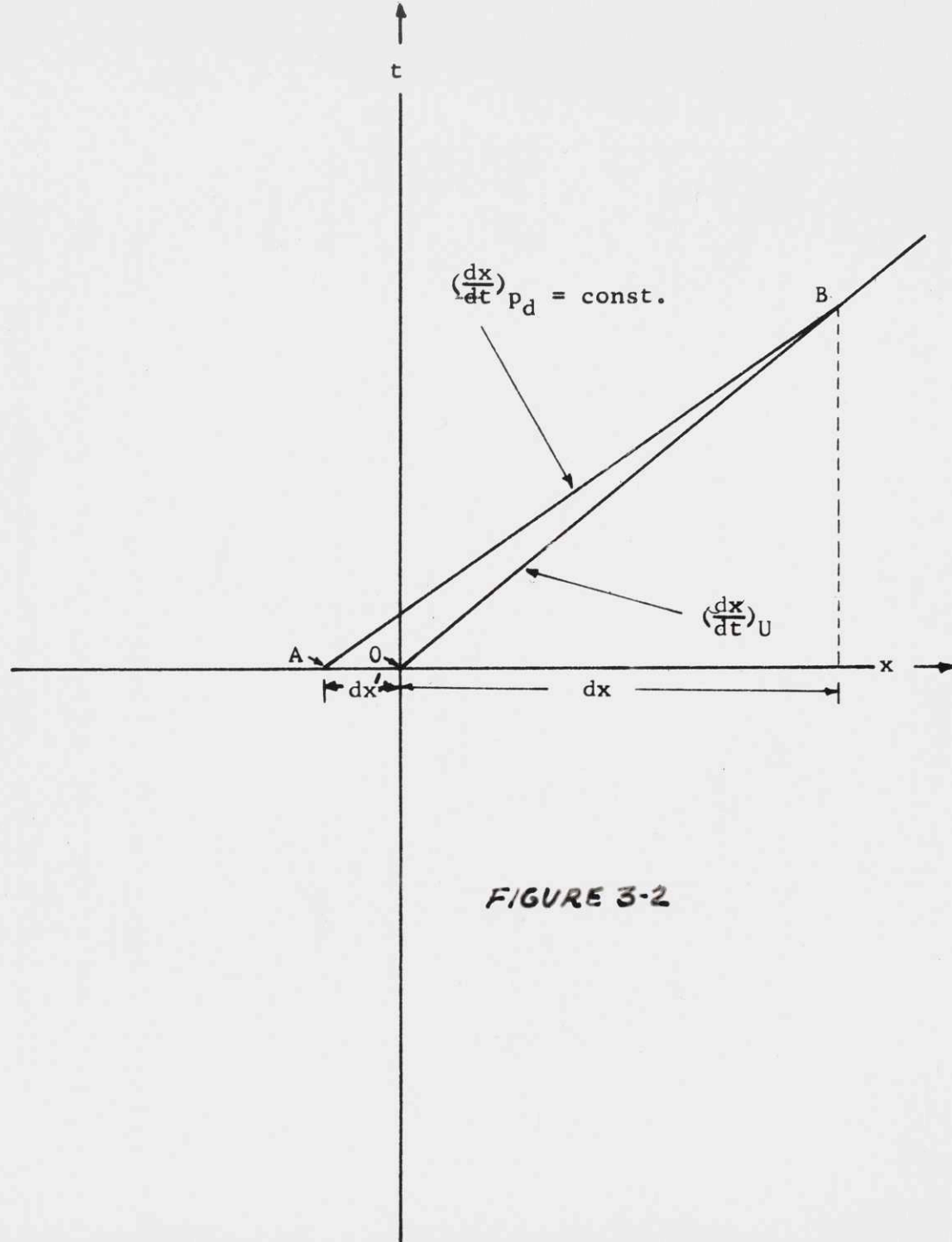
FIGURE 3-2

$$\frac{dp_d}{dx} = \frac{p_O - p_A}{dx} = - \frac{\partial p_d}{\partial x} \frac{dx'}{dx}$$

where $\partial p_d / \partial x \equiv (\partial p_d / \partial x)_{t=o}$. This expression may be written

$$\frac{dp_d}{dx} = - \frac{\partial p_d}{\partial x} \left\{ \frac{\left(\frac{dx}{dt}\right)_{p_d = const.}}{\left(\frac{dx}{dt}\right)_U} - 1 \right\} \qquad (3-34)$$

What is wanted, of course, is not dp_d/dx at the shock front, but $d\varsigma/dx$ where $\varsigma = (p - p_e)/p_e = p_d/p_e$. Making this substitution, we have

$$\frac{d\varsigma}{dx} = - \frac{1}{p_e} \frac{\partial p_d}{\partial x} \left\{ \frac{\left(\frac{dx}{dt}\right)_{p_d = const.}}{\left(\frac{dx}{dt}\right)_U} - 1 \right\} - \frac{\varsigma}{p_e} \frac{dp_e}{dx} \qquad (3-35)$$

This is the final equation for ς. In order to evaluate this we will need $(\partial p_d / \partial x)$ and $(dx/dt)_{p_d = const.}$ which both depend on the initial pressure wave. We shall work out two examples in the next two sections.

6. Application to Weak "N-waves" in a Homogeneous Medium

Before working out the equation derived in the last chapter for an inhomogeneous medium, let us first obtain the decay of ς with distance in a homogeneous medium. We shall adopt as the initial pressure signature the "N-wave" model illustrated in Figure 3-3. The pressure ratio ς is assumed to be much less than 1. We assume that p_e and c_e
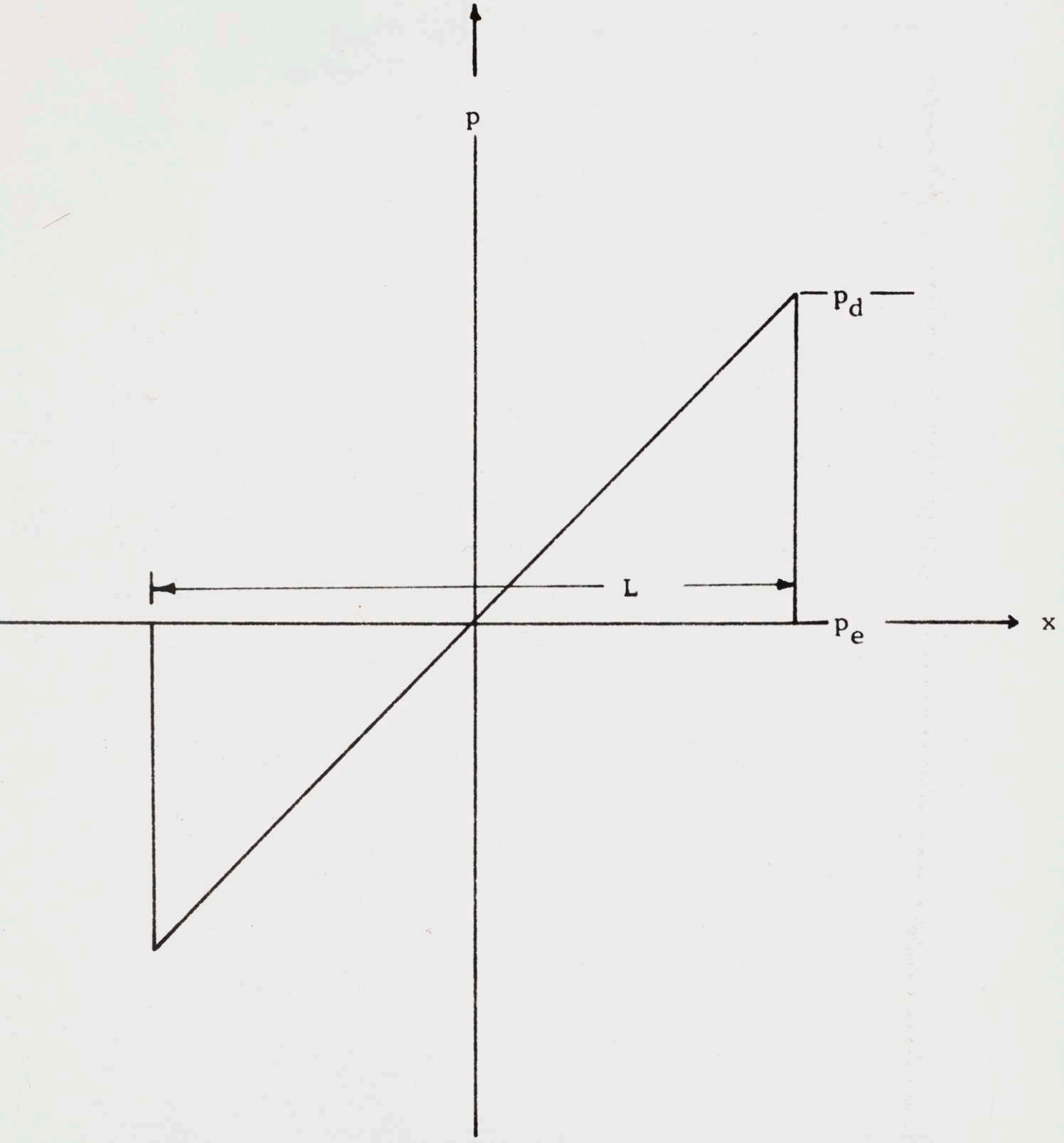
FIGURE 3-3

are constant, and since there are no external forces, $(dx/dt)_{p_d}$ = const. = $c_e(1 + 2\Delta)$ from Eq. (3-19) and the weak shock relations. Also, $(dx/dt)_U = c_e(1 + \Delta)$. Then Eq. (3-33) becomes

$$\frac{d\mathcal{S}}{dx} = -\frac{1}{p_e}\frac{\partial p_d}{\partial x}\left(\frac{1 + 2\Delta}{1 + \Delta} - 1\right) \doteq \frac{\Delta}{p_e}\frac{\partial p_d}{\partial x} \qquad (3-36)$$

$$= -\frac{2\mathcal{S}\Delta}{L}$$

since for this model $\partial p_d/\partial x = 2\mathcal{S}\,p_e/L$. The length of the wave cannot, however, be assumed to be constant because the center of the wave moves with the small-signal speed of sound (c_e), whereas the shock front moves with velocity $U = c_e(1 + \Delta)$. Therefore, the change in length with distance is simply

$$\frac{dL}{dx} = 2\Delta \qquad (3-37)$$

Equations (3-36) and (3-37) were first obtained by Dumond et al.[13] Equation (3-36) was, however, obtained by a somewhat different method. These two equations do not seem to have been solved by these workers in the form given below. By using Eq. (3-27b), Eqs. (3-36) and (3-37) may be written

$$\frac{d\mathcal{S}}{dx} = -\frac{\gamma + 1}{2\gamma L}\mathcal{S}^2 \qquad (3-38a)$$

$$\frac{dL}{dx} = \frac{\gamma + 1}{2\gamma}\mathcal{S} \qquad (3-38b)$$

After elimination of ζ , the equation for L is

$$\frac{d^2 L}{dx^2} + \frac{1}{L}\left(\frac{dL}{dx}\right)^2 = 0 \tag{3-39}$$

For $L = L_o$ and $\zeta = \zeta_o$ at $x = 0$ the solution is

$$L = \left(\frac{\gamma + 1}{\gamma}\right)^{1/2} (L_o \zeta_o)^{1/2} \left(\frac{L_o}{\zeta_o}\frac{\gamma}{\gamma + 1} + x\right)^{1/2} \tag{3-40}$$

and

$$\zeta = \left(\frac{\gamma}{\gamma + 1}\right)^{1/2} (L_o \zeta_o)^{1/2} \left(\frac{L_o}{\zeta_o}\frac{\gamma}{\gamma + 1} + x\right)^{-1/2} \tag{3-41}$$

as can be verified by direct differentiation. Thus, for $x \gg L_o/\zeta_o$, $\zeta \sim x^{-0.5}$. The method therefore predicts a slow decrease of pressure ratio with distance. As an example, L and ζ have been calculated assuming that $L = 30$ meters and $\zeta_o = 0.1$ at $x = 0$. The results are shown in Figures 3-4 and 3-5. If Eq. (3-41) is used to expand $1/\zeta$ about $x = 0$, it can easily be seen that

$$\frac{1}{\zeta} = \frac{1}{\zeta_o} + \frac{\gamma + 1}{2\gamma}\frac{x}{L_o} \tag{3-42}$$

This result is in agreement with the approximate analyses of Fay[14] and Rudnick[15] for the attenuation of repeated shock waves (of wavelength L_o) with distance. At large distances, however, our result predicts that $\zeta \sim x^{-0.5}$ whereas the above analyses predict $\zeta \sim x^{-1}$. The reason for the difference is, of course, that for an N-wave L must be
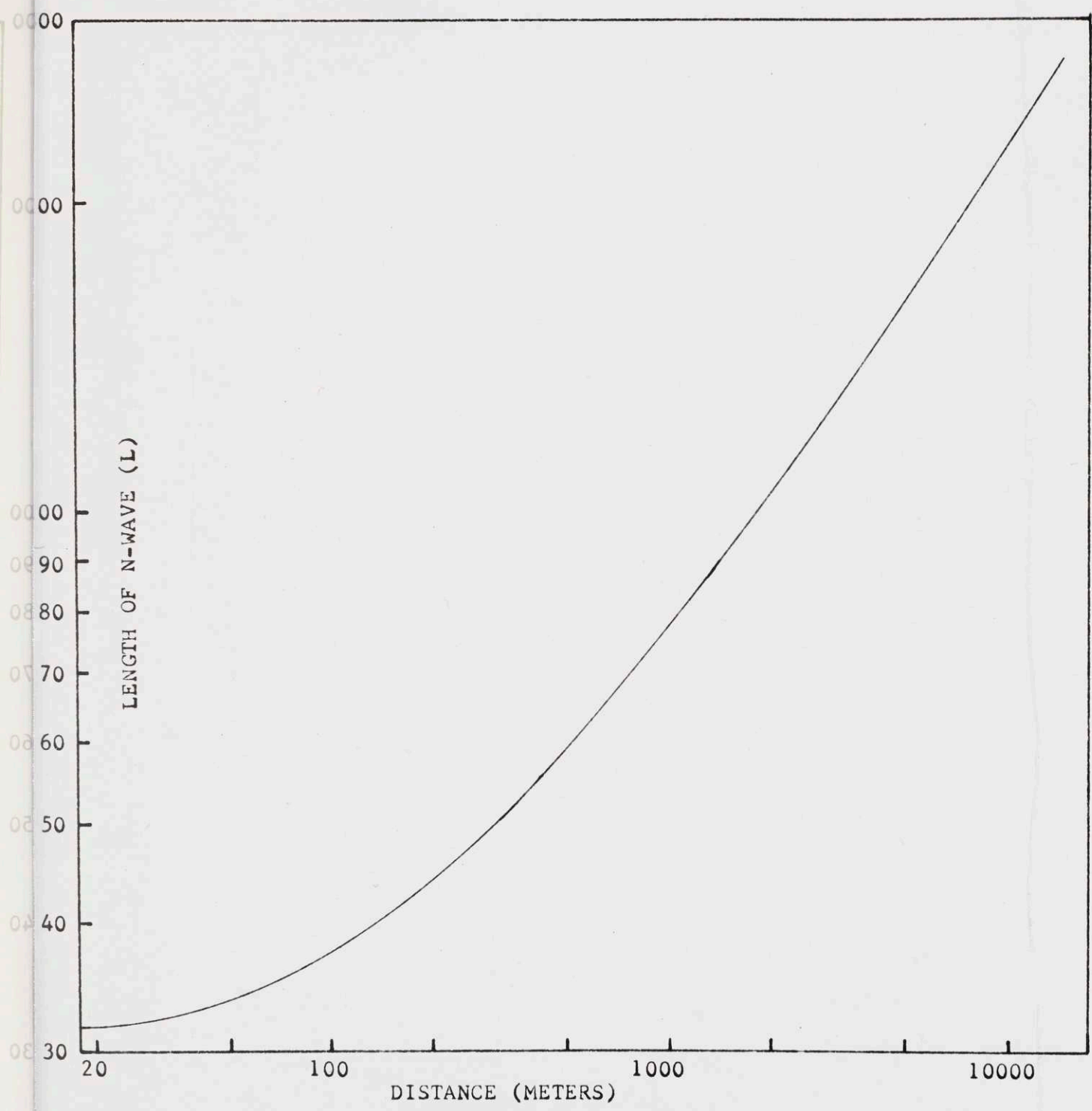
FIGURE 3-4
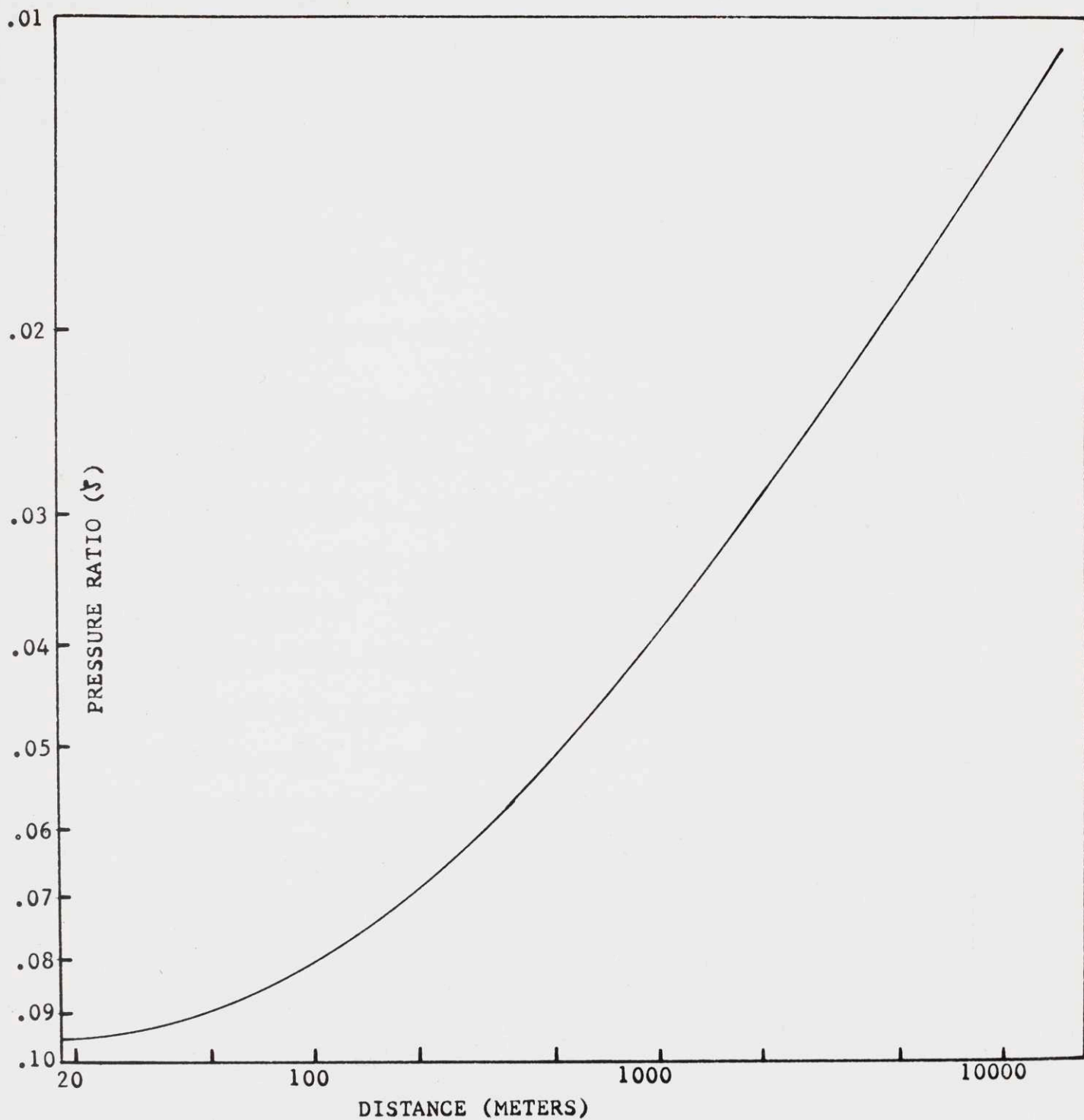
FIGURE 3-5

taken as a function of x because of the difference between the shock speed and the small-signal speed of sound. If we were to assume that $L = L_o = $ const., integration of Eq. (3-38a) immediately yields

$$\frac{1}{\zeta} = \frac{1}{\zeta_o} + \frac{\gamma + 1}{2\gamma L_o} x \qquad (3\text{-}43)$$

which shows that it is the neglect of the changing wave-length that produces a difference at large distances.

7. Application to N-Waves in an Inhomogeneous Medium

Having seen in section 6 how the equation derived in section 5 is to be applied, we next turn to the problem of the determination of the motion of an N-wave in an inhomogeneous medium. It should be recalled that the main distinguishing feature of the motion is that is is not isentropic in the Eulerian description that we have chosen, even when the loss-free equations of motion are used. We shall adopt the N-wave model used in the last section and again assume that the wave is weak. We will need $(dx/dt)_{p_d} = $ const. which in turn will require a knowledge of $\rho c (\partial u / \partial p)_s$. We first separate Eq. (3-17) for p into a time-dependent and time-independent part by using Eqs. (3-33a, b, c):

$$c(1 + \epsilon)\frac{\partial p_e}{\partial x} = c(1 + \epsilon)F_o \qquad (3\text{-}44)$$

$$\frac{\partial p_d}{\partial t} + (u + c(1 + \epsilon))\frac{\partial p_d}{\partial x} = c(1 + \epsilon)F_1 - u\frac{\partial p_e}{\partial x} \qquad (3\text{-}45)$$

where ϵ is defined by $1/(1 + \epsilon) = \rho c(\partial u/\partial p)_s$. We shall find ϵ later. Equation (3-44) is, of course, the equilibrium condition. We shall assume that the fluid is an isothermal ideal gas under the influence of a gravitational force $F = + \rho g$, and therefore it can be seen that

$$F = F_o + F_1 = \rho_e g + \delta g \qquad (3\text{-}46a)$$

$$\frac{1}{\rho_e} \frac{\partial \rho_e}{\partial x} = \frac{1}{p_e} \frac{\partial p_e}{\partial x} = \frac{\gamma g}{c_e^2} \qquad (3\text{-}46b)$$

$$\frac{\partial s_e}{\partial x} = \frac{c_p(1 - \gamma)g}{c_e^2} \qquad (3\text{-}46c)$$

The constant entropy gradient assumed here may be compared with the entropy gradient for the actual earth's atmosphere as calculated from pressure, density and temperature measurements given in the U.S. Air Force Handbook of Geophysics (1959). The comparison is illustrated in Figure 3-6.

Now, since $(dx/dt)_{p_d} = \text{const.} = - (\partial p_d/\partial t)/(\partial p_d/\partial x)$ we have, from Eq. (3-45).

$$\left(\frac{dx}{dt}\right)_{p_d = \text{const.}} = u + c(1 + \epsilon) - \frac{c(1 + \epsilon)\delta g - u \dfrac{\partial p_e}{\partial x}}{\dfrac{\partial p_d}{\partial x}} \qquad (3\text{-}47)$$

We will show later that $\epsilon = 0(\gamma g L/c_e^2)$ which is assumed to be small and therefore will adopt the following approximations throughout the analysis to follow. Neglect terms of

isothermal atmosphere

actual atmosphere

HEIGHT ABOVE EARTH'S SURFACE (KM.)
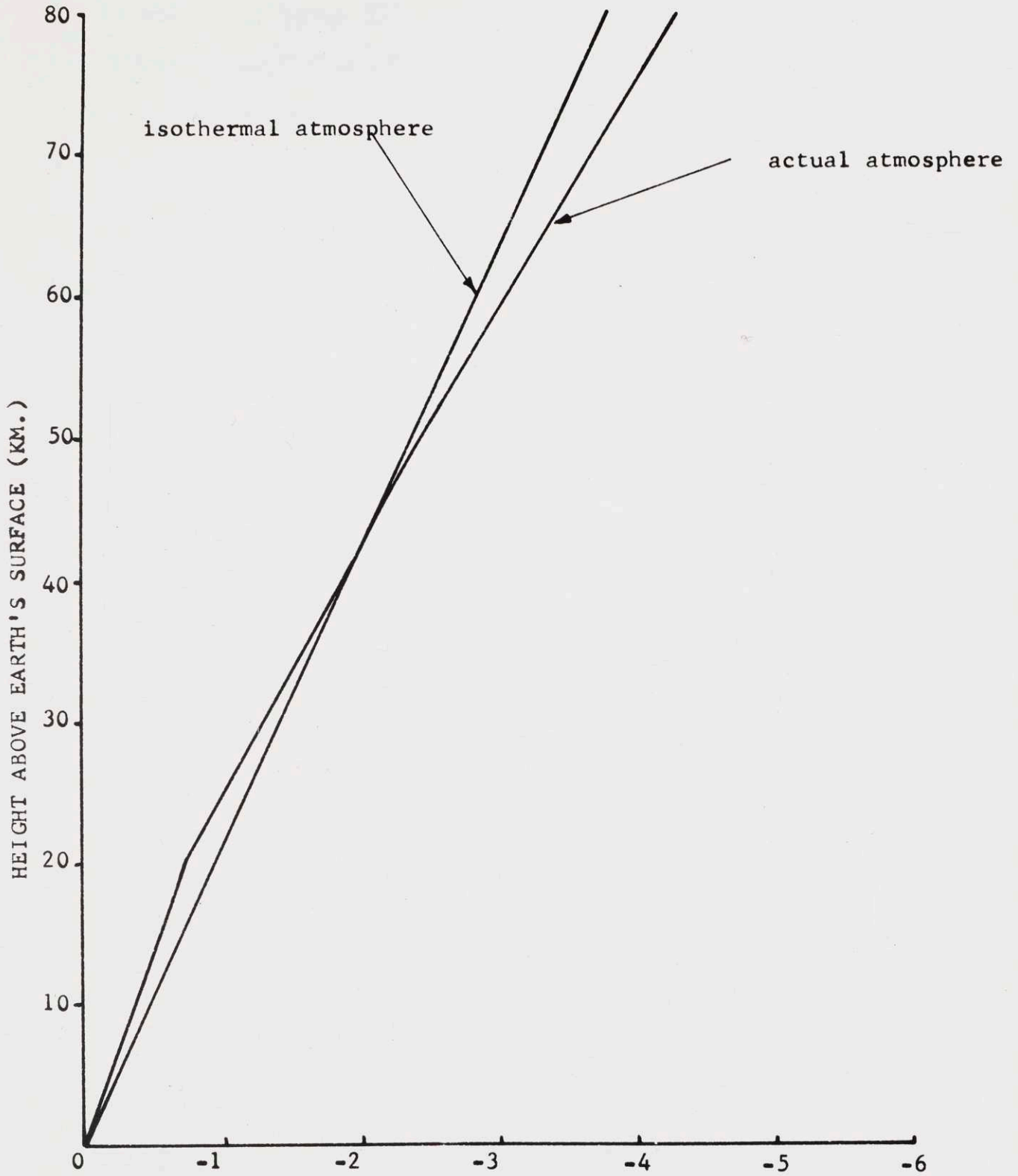
s/c_v

FIGURE 3-6

$O(\epsilon\Delta^2)$ and terms of $O(\epsilon^2\Delta)$. Thus, we will keep only terms of $O(\epsilon\Delta)$ or $O(\Delta^2)$. When Eq. (3-47) is evaluated directly behind the shock, we find that Eq. (3-35) may be written

$$\frac{d\zeta}{dx} = -\frac{2\zeta}{L}\left(\frac{\frac{4\Delta}{\gamma+1} + (1 + 2\frac{\gamma-1}{\gamma+1}\Delta)(1+\epsilon) - \frac{QL}{2\zeta}}{1+\Delta} - 1\right) - \frac{\gamma g}{c_e^2}\zeta$$

(3-48)

where

$$Q \quad (1 + 2\frac{\gamma-1}{\gamma+1}\Delta)(1+\epsilon)\frac{4\Delta}{\gamma+1}\rho_e g - \frac{\gamma g}{c_e^2}\frac{4\Delta}{\gamma+1}$$

When QL is simplified, it can be seen that it is of $O(\gamma g L \Delta^2/c_e^2)$ and can therefore be neglected. Thus, after further simplification we may write $d\zeta/dx$ as

$$\frac{d\zeta}{dx} = -\left(\frac{2\zeta\Delta}{L} + \left(\frac{2\epsilon}{L} + \frac{\gamma g}{c_e^2}\right)\zeta\right)$$

(3-49)

to the order of approximation outlined above. It can be seen that   is needed only to $O(\gamma g L/c_e^2)$. To find ϵ we use Eq. (3-14b) repeated below:

$$1 - \rho^2 c^2\left(\frac{\partial u}{\partial p}\right)_s^2 = \frac{F - \left(\frac{\partial p}{\partial s}\right)_u \frac{\partial s}{\partial x}}{\frac{\partial p}{\partial x} - \left(\frac{\partial p}{\partial s}\right)_u \frac{\partial s}{\partial x}}$$

(3-14b)

We will want to separate the right-hand side into equilibrium and motion-dependent parts. To do this, we write

$(\partial p/\partial s)_u = (\partial p/\partial s)_u^{(0)} + (\partial p/\partial s)_u^{(1)}$ and note that (from the part of the relation

$$\frac{\partial p}{\partial x} = \left(\frac{\partial p}{\partial u}\right)_s \frac{\partial u}{\partial x} + \left(\frac{\partial p}{\partial s}\right)_u \frac{\partial s}{\partial x} \tag{3-50}$$

that holds for the equilibrium quantities) we must have

$$\left(\frac{\partial p}{\partial s}\right)_u^{(0)} = \frac{\dfrac{\partial p_e}{\partial x}}{\dfrac{\partial s_e}{\partial x}} = \frac{p_e}{c_v(1 - \gamma)} \tag{3-51}$$

We shall next assume that $(\partial p/\partial s)_u = p/(c_v(1 - \gamma))$ and therefore that during the motion

$$\left(\frac{\partial p}{\partial s}\right)_u^{(1)} = \frac{p_e \zeta}{c_v(1 - \gamma)} \tag{3-52}$$

Equation (3-14b) then becomes

$$1 - \rho^2 c^2 \left(\frac{\partial u}{\partial p}\right)_s^2 = \frac{p_e g \dfrac{p_e}{c_v(1-\gamma)} \dfrac{\partial s_e}{\partial x} + \delta g - \left(\dfrac{p_e}{c_v(1-\gamma)} \dfrac{4}{\gamma+1} + \dfrac{p_e \zeta}{c_v(1-\gamma)}\right)\dfrac{\partial s_e}{\partial x}}{\dfrac{2\zeta p_e}{L} - \dfrac{p_e(1 + \zeta)}{1 - \gamma} \dfrac{\partial s_e}{\partial x}}$$

$$\tag{3-53}$$

where we have used $\partial s/\partial x = \partial s_e/\partial x + \partial\sigma/\partial x \doteq (\partial s_e/\partial x)(1 + u/c_e)$. Since $\gamma g L/c_e^2 \ll 1$, the second term in the denominator may be neglected and we have

$$1 - \rho^2 c^2 \left(\frac{\partial u}{\partial p}\right)_s^2 = \frac{\dfrac{\rho_e \varsigma g}{\gamma} - \dfrac{p_e \varsigma}{c_p(1-\gamma)} \dfrac{c_p(1-\gamma)g}{c_e^2} - \dfrac{p_e \varsigma}{c_v(1-\gamma)} \dfrac{c_p(1-\gamma)g}{c_e^2}}{\dfrac{2\varsigma p_e}{L}}$$

<div align="right">(3-54)</div>

$$= \frac{L}{2} \frac{\gamma g}{c_e^2}\left(\frac{1}{\gamma} - \frac{1}{\gamma} - 1\right)$$

$$= -\frac{L}{2} \frac{\gamma g}{c_e^2}$$

where the weak shock relations (Eqs. (3-27a, b, c)) and the entropy gradient in Eq. (3-46c) have been used. Since ϵ was defined by

$$\frac{1}{1+\epsilon} = \rho c \left(\frac{\partial u}{\partial p}\right)_s$$

<div align="right">(3-55)</div>

Eq. (3-54) becomes

$$1 - \frac{1}{(1+\epsilon)^2} \doteq 2\epsilon = -\frac{L}{2}\frac{\gamma g}{c_e^2}$$

or

$$\frac{2\epsilon}{L} = -\frac{\gamma g}{2c_e^2}$$

<div align="right">(3-56)</div>

This supplies the missing factor needed in the equation for $d\varsigma/dx$. Equation (3-49) may now be written

$$\frac{d\varsigma}{dx} = -\left(\frac{\gamma+1}{2\gamma L}\varsigma^2 + \frac{\gamma g}{2c_e^2}\varsigma\right)$$

<div align="right">(3-57)</div>

which together with the stretching equation

$$\frac{dL}{dx} = 2\Delta = \frac{\gamma + 1}{2\gamma}\varsigma \qquad (3\text{-}58)$$

determines the motion of the shock front. We see that for large values of ς the nonlinear term in Eq. (3-57) predominates whereas for ς small the linear term predominates. Thus, for

$$\varsigma \gg \frac{\gamma g}{c_e^2} \frac{\gamma}{\gamma + 1} L \qquad (3\text{-}59)$$

the solution is identical to that obtained in the previous section whereas for

$$\varsigma \ll \frac{\gamma g}{c_e^2} \frac{\gamma}{\gamma + 1} L \qquad (3\text{-}60)$$

the solution is simply $\varsigma = \text{const} \cdot \exp(-\gamma gx/2c_e^2) = \text{const} \cdot p_e^{-0.5}$. This result is identical to that obtained using Whitham's method[11] for weak shock waves as outlined in section 4 of this chapter. Note that Eq. (3-59) can be satisfied for weak waves because the right-hand side is usually very small. For $g = 9.8$ m/sec^2, $c_e = 344$ m/sec, $\gamma = 1.4$ and $L = 30$ meters, for example, the right-hand side of Eq. (3-59) is equal to 2×10^{-3}.

In order to see more clearly the relative importance of the linear and nonlinear terms in Eqs. (3-57) and (3-58) it is convenient to normalize the equations by defining $\varsigma_n = \varsigma/\varsigma_o$, $L_n = L/L_o$ and $\mathfrak{z} = \varsigma_o(\gamma + 1)x/(\gamma L_o)$. ς_o and L_o are the pressure ratio and length respectively at $x = 0$.

In terms of these variables Eqs. (3-57) and (3-58) may be written

$$\frac{d\zeta_n}{d\xi} + \frac{1}{2L_n}\zeta_n^2 + \beta\zeta_n = 0 \tag{3-61}$$

$$\frac{dL_n}{d\xi} = \frac{1}{2}\zeta_n \tag{3-62}$$

where $\beta = (L_0/\zeta_0)(\gamma g/2c_e^2)$. For $\beta = 0$, the solutions are simply $\zeta_n = (1 + \xi)^{-1/2}$ and $L_n = (1 + \xi)^{1/2}$. These functions have been plotted in Figures 3-7 and 3-8. For $\beta \neq 0$, a solution to the set may be obtained by means of the proper transformation. We first eliminate ζ_n from Eq. (3-61) and obtain the following equation for L alone:

$$\frac{d^2L_n}{d\xi^2} + \frac{1}{L_n}\left(\frac{dL_n}{d\xi}\right)^2 + \beta\frac{dL_n}{d\xi} = 0 \tag{3-63}$$

If we now define a new variable by $L_n = \exp(\int(1/y)dx)$, the equation for y is simply $dy/dx - \beta y = 1$. The solution, $y = (\text{const.})\exp(\beta x) - 1/\beta$ can be used to find L_n with the constant obtained by using the requirement that $L_n \longrightarrow 1$ as $\beta \longrightarrow 0$. When this is done, we obtain the following solutions for ζ_n and L_n:

$$L_n = (1 + \frac{1}{\beta}(1 - e^{-\beta\xi}))^{1/2} \tag{3-64}$$

$$\zeta_n = \frac{1}{L}e^{-\beta\xi} \tag{3-65}$$

NORMALIZED PRESSURE RATIO ($\mathcal{Y}_n$)
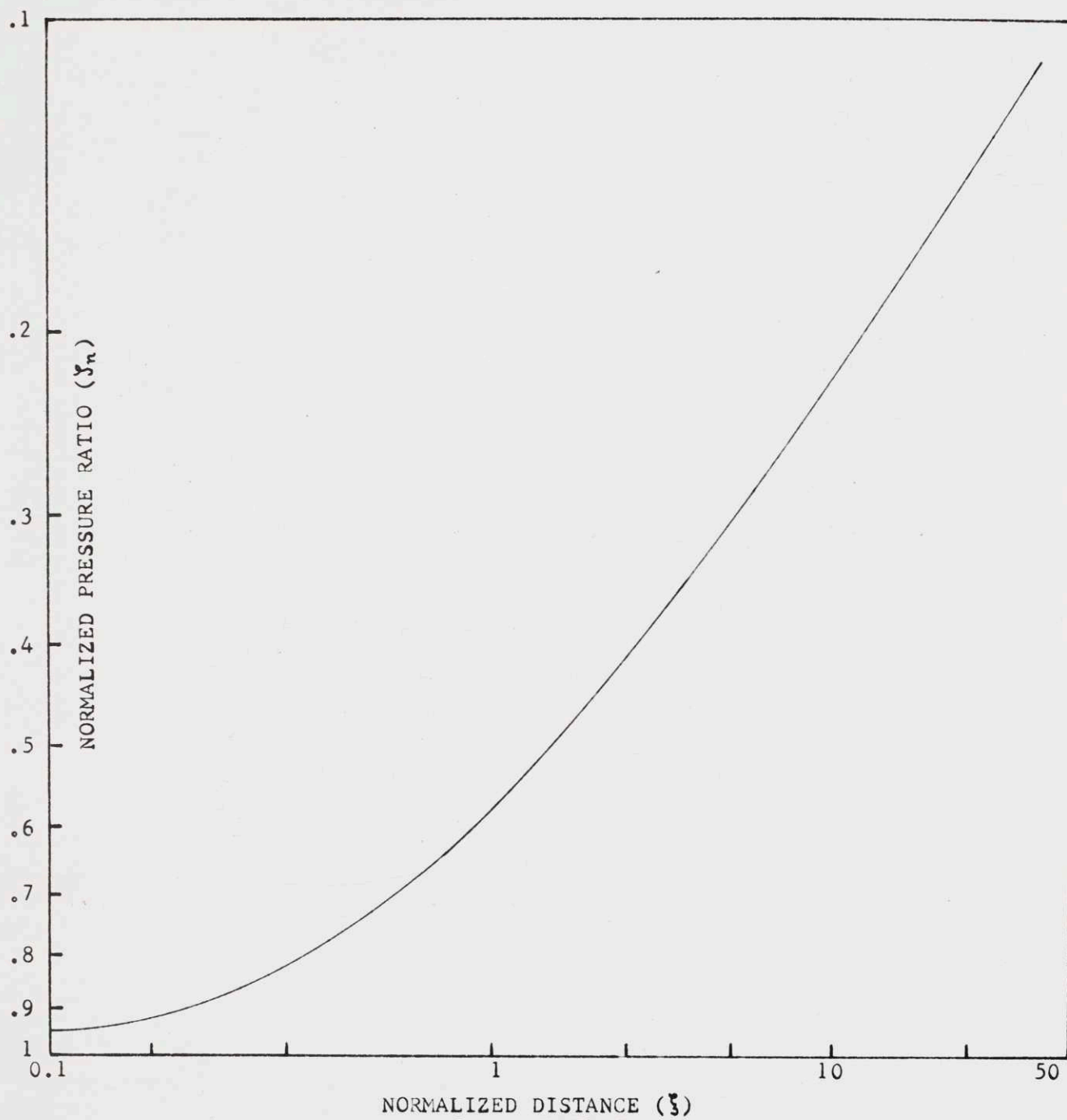
NORMALIZED DISTANCE ($\mathcal{Z}$)
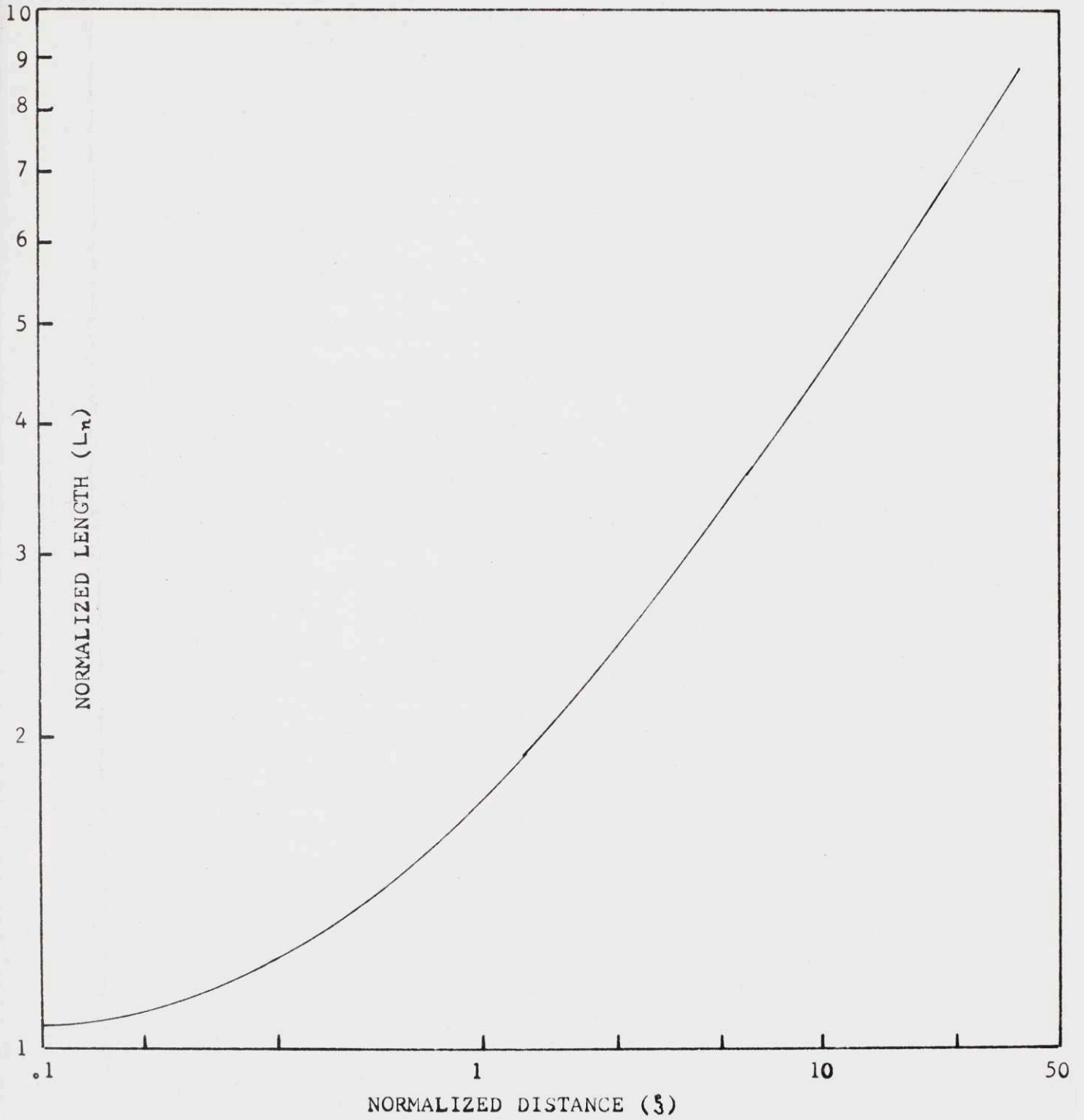
FIGURE 3-7

FIGURE 3-8

Equation (3-65) was obtained by using Eq. (3-62). These
results can also be obtained by another method. The rate
of energy lost at the shock front is set equal to the
negative of the rate of energy decay in the wave which is
proportional to $p_o \zeta^2 L$. Using the equation derived from
this requirement and the stretching equation one can obtain
similar results as shown by Reed[16],[17] in a note on shock wave
propagation. The method proposed here can, however, be used
to derive many results that cannot be obtained by energy
considerations. For example, if the wave has a very long
period, a cutoff wavelength similar to that obtained for
an acoustic wave in Chapter 1 can be obtained by this
method. In order to see this, it is necessary to keep
both terms in the denominator of Eq. (3-53). When the
second term is nearly equal to the first (L large),
$\rho c (\partial u / \partial p)_s$ is large and therefore according to Eq. (3-17)
a point of constant pressure is propagated with a velocity
less than c.

Note that when the wave propagates in the same direc-
tion as the gravitational force ($\beta > 0$) that the length
reaches a terminal length equal to $1/\sqrt{\beta}$ for $\beta << 1$ and that
the pressure ratio decreases as $\exp(- |\beta| \zeta)$. For propagation
in the opposite direction ($\beta < 0$) the length and pressure
ratio vary as $\exp(|\beta| \zeta /2)$. The anisotropic nature of the
wave propagation is thus clearly shown. It must be noted,
however, that for typical values of the constants ($L_o = 30$ m,

$\zeta_0 = 0.1$, $g = 9.8$ m/s^2, $c_e = 344$ m/s, and $\gamma = 1.4$) $\beta = 10^{-5}$ and therefore the exponential growth is not attained until x is extremely large. This can be seen from the examples plotted in Figures 3-9 and 3-10. The exponential growth would not be observed, for example, in the earth's atmosphere if the wave were to have the initial pressure ratio and length given above.

Finally, we note that Whitham's method predicts the correct asymptotic limit for $\beta > 0$, that $\zeta \sim p_0^{0.5}$. For $\beta < 0$ it can easily be shown that ζ is proportional to $p_0^{-0.25}$.
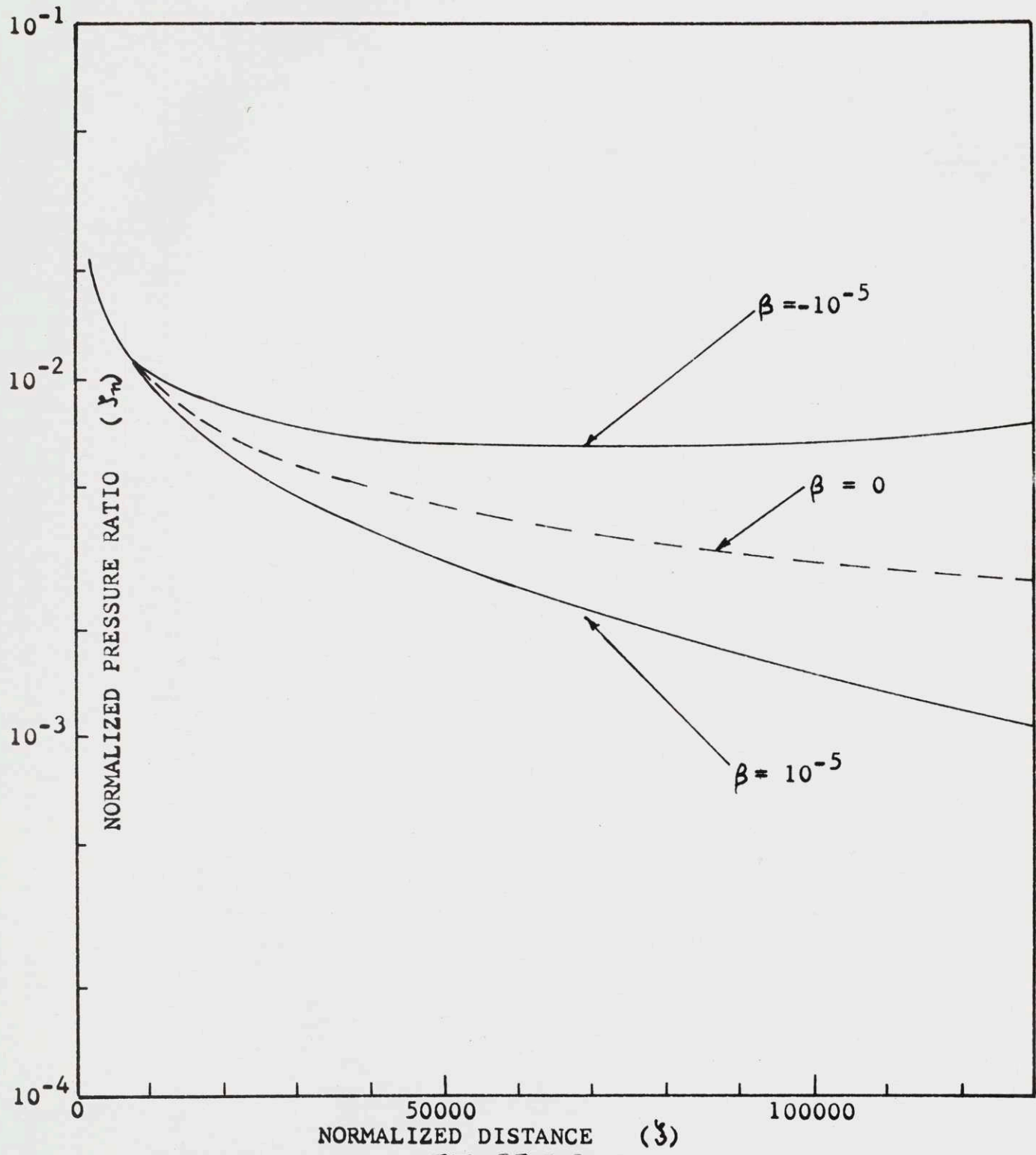
FIGURE 3-9
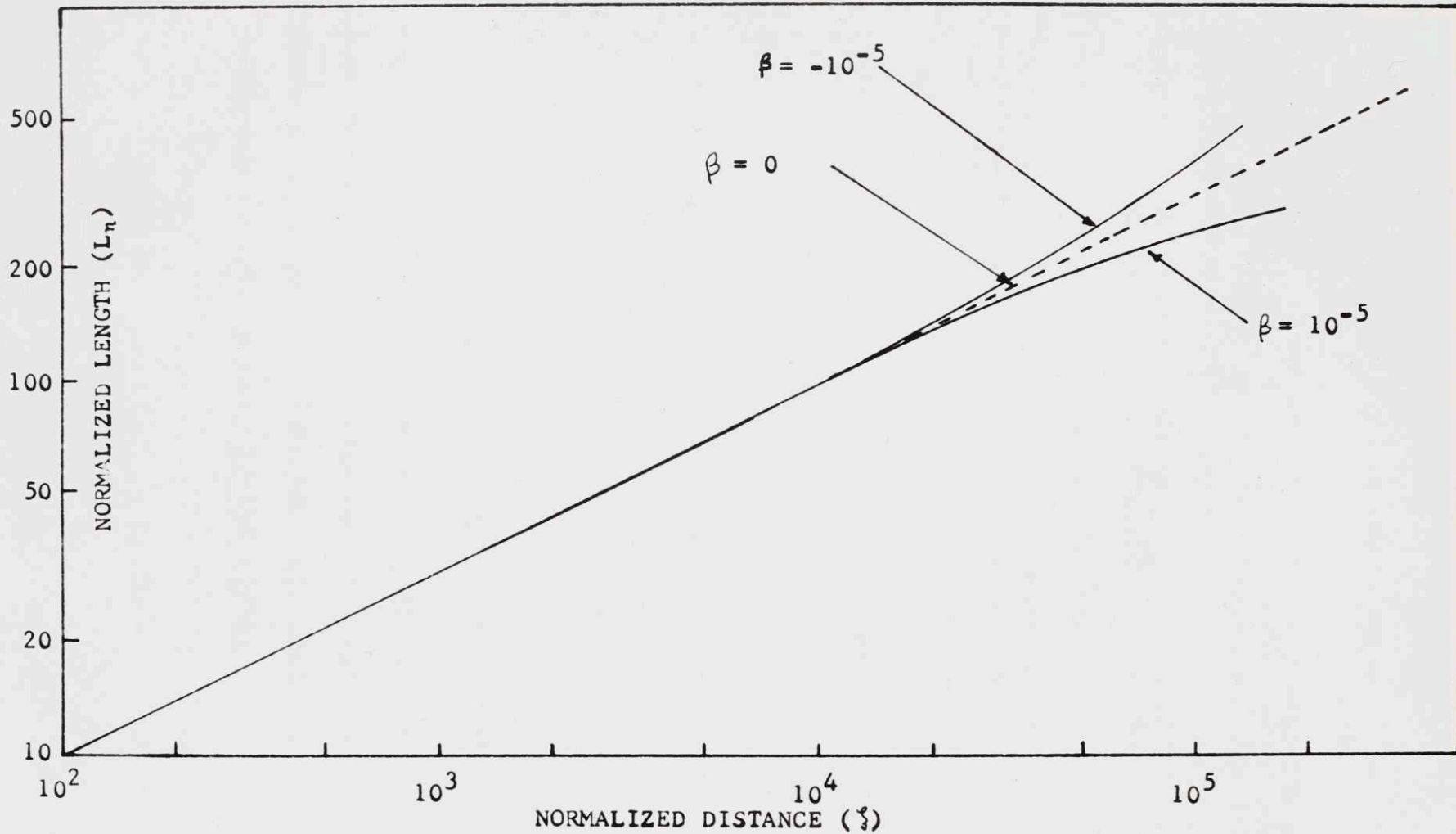
FIGURE 3-10

REFERENCES FOR CHAPTER THREE

1. Lighthill, M.J., Viscosity in Waves of Finite Amplitude, Surveys in Mechanics, (G.I. Taylor 70th Anniversary Volume), G.K. Batchelor and R.M. Davies Ed., Cambridge University Press (1956)

2. Fay, R.D., J. Acoust. Soc. Am., 3, 222 (1931), J. Acoust. Soc. Am., 28, 910 (1956)

3. Fubini, E., Alta Frequenza, 4, 530 (1935)

4. Blackstock, D.T., ONR Technical Memorandum No. 43, Acoustics Research Laboratory, Harvard University, (June 1960)

5. Rankine, W., Phil. Trans. Roy. Soc., 160, 277 (1870)

6. Hugoniot, A., J. Éc. Polyt. (Paris), 58, 1 (1889)

7. Riemann, B., Göttingen Abh., 8, 43 (1859)

8. Stokes, G.G., Phil. Mag., 33, 349 (1848)

9. Whitham, G.B., J. Fluid Mech., 4, 337 (1958)

10. Poisson, S.D., J. Éc. Polyt., 14, 319 (1808)

11. Whitham, G.B., J. Fluid Mech., 4, 337 (1958)

12. See Reference 1, Page 290.

13. Dumond, J.M., Cohen, E.R., Panofsky, W.H., and Deeds, E., J. Acoust. Soc. Am., 18, 97 (1946)

14. Fay, R.D., J. Acoust. Soc. Am., 34, 1269 (1962)

15. Rudnick, I., J. Acoust. Soc. Am., 25, 1012 (1953)

16. Reed, S.G., J. Acoust. Soc. Am., 31, 1265 (1959)

17. Reed, S.G., Phys. Fluids, 3, 134 (1960)

Chapter 4. Analysis of an Acoustic Instability Produced
by a Heat Source

1. Introduction

One of the simplest examples of an instability that
can arise because of the scattering of sound by a heat
source is the well-known Rijke phenomenon first discov-
ered by Rijke[1] in 1859. If a heated gauze or wire
heater is placed in the lower half of a vertical tube,
the tube is, under certain conditions, observed to pro-
duce a tone whose wavelength is approximately equal to
twice the length of the tube. Rijke was not able to give
any satisfactory explanation for this phenomenon but
Raleigh[2],[3] was able to give a qualitative explanation
of the effect by applying what has now come to be called
the Raleigh Criterion, that heat added to a fluid in
phase with the pressure perturbation tends to reinforce
the oscillations whereas heat added out of phase tends to
damp the oscillations. The first attempt to formulate
this criterion mathematically for application to the
Rijke tube was made by Lehman,[4] who assumed that the
mean flow through the tube (either forced convection or
free convection caused by the heat source) was small
compared to the particle velocity in the acoustic wave.

While such an analysis is important in determination of
the mechanism limiting the eventual amplitude of the
oscillation, one should be able to use a small-signal
theory to predict the onset of oscillations, and at least
approximately the dependence of the driving or damping on
heater position. A number of investigators[5],[6],[7]
have made analyses of the problem, and have presented
surveys of some of the unsatisfactory attempts to solve
the problem. Although some of the main features of the
oscillation are understood, it has not been possible to
calculate all of the results found experimentally. For
example, Kerwin[5] was only able to determine the magni-
tude of the real part of the complex eigenvalue for the
tube within a factor of approximately 10, whereas the
results obtained by Merk[7] using a heat transfer func-
tion derived by Carrier[6] predict that the tube should
oscillate over a much wider range of mean flow speeds than
is observed experimentally. All of these authors analyzed
the problem essentially by requiring that the acoustic
variables satisfy the appropriate boundary condition at
both ends of the tube, and that fluid mass, momentum and
energy be conserved at the heater. The energy conserva-
tion must of course include the heat added by the heater.
Such an approach, although undoubtedly correct, leads to
rather involved expressions that make it very difficult
to see the basic nature of the phenomenon. We shall adopt

a somewhat different approach that contains many of the
important features of the above methods. In the next
section a general criterion is formulated for the deter-
mination of the onset of the oscillations, and then this
result is first applied to a tube that is assumed to be
loss-free. Even this approximation leads to the experi-
mentally observed dependence of the oscillation strength
on heater position.

2.   A Stability Criterion

The well-known[8] wave equation for a medium that
contains a heat source is:

$$\frac{\partial^2 p}{\partial x^2} - \frac{1}{c^2}\frac{\partial^2 p}{\partial t^2} = -\frac{\gamma-1}{c^2}\rho\frac{\partial q}{\partial t} \qquad (4\text{-}1)$$

where q is the rate at which heat is added per unit mass
to the medium, and the other symbols have their customary
meaning. This equation is to be solved for a tube con-
taining a heater as illustrated in Figure 4-1. We will
be interested in the case when the mean flow through the
tube is very small compared with the speed of sound, and
will neglect the influence of the flow except when the
rate of heat release to the fluid is being calculated.
It will be found that the rate of heat release per unit
mass is very much dependent on the flow speed. Since we
assume that the total heat released to the medium per
unit mass is a function of flow speed, the fluctuating
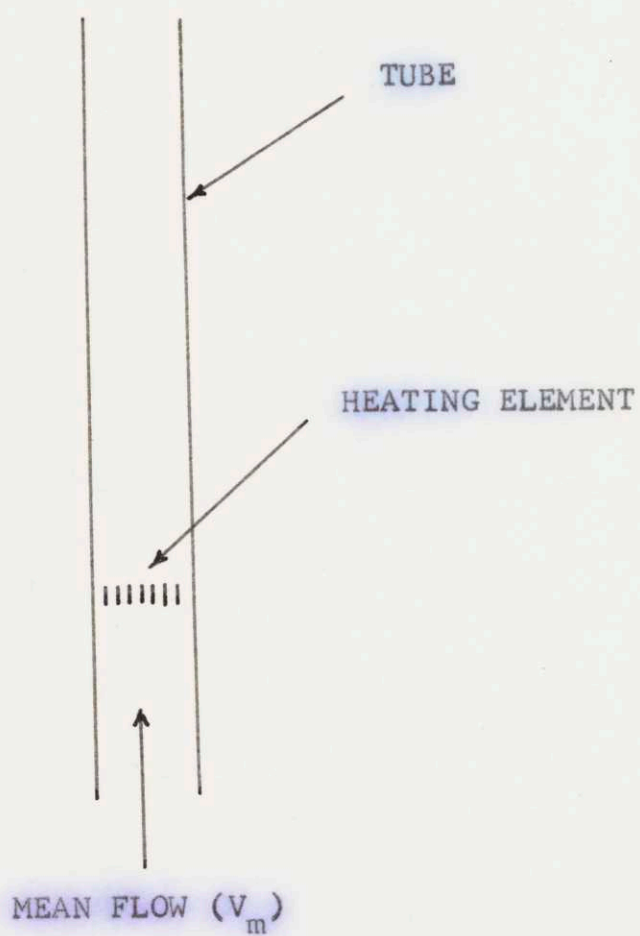
Figure 4-1.

part may be obtained by expansion in a Taylor series.
When we compare our results with experiment, specific
forms for the function will be considered, but in this
section we set $q = F'(V_m)u$ where u is the acoustic parti-
cle velocity. We shall allow for the fact that the heat
added can be out of phase with the particle velocity, and
will therefore take $F'(V_m) = F'_r(V_m) + iF'_i(V_m)$. Since the
rate at which heat is added is proportional to an acoustic
variable, the possibility arises that the acoustic vari-
ables may grow with time, and in order to investigate the
conditions under which such growth occurs we set $p(x,t) =$
$p(x)\exp(\kappa ct)$ and $u(x,t) = u(x)\exp(\kappa ct)$, where $\kappa = \sigma - ik$.
Thus, the oscillations grow for $\sigma > 0$ and decay for $\sigma < 0$.
We shall further assume that the heat transferred to the
gas depends on the particle velocity of the (cool) gas
directly before the heater, i.e., for $x = x_h - \epsilon$, and
that the spacial extent of the heater is small enough so
that it can be represented as a δ-function at $x = x_h$.
With these alterations, Eq. (4-1) may be written:

$$\frac{d^2 p}{dx^2} - \kappa^2 p = - \frac{\gamma - 1}{c} \rho F'(V_m)u(x_h - \epsilon)\delta(x - x_h) \quad (4-2)$$

The problem is therefore to find a Green's function when
the back-reaction of the sound field on the source is
represented by requiring that the source strength be pro-
portional to the value of an acoustic variable at the
source. The simplest way to find p appears to be to

expand it into an infinite series of orthonormal functions
that satisfy

$$\frac{d^2\phi_n}{dx^2} - \gamma_n^2\phi_n = 0 \qquad (4\text{-}3)$$

and the appropriate boundary conditions at the end of the
tube. The expansion can be performed using well-known[9]
techniques, and the result is

$$p = \sum_n \frac{\frac{\gamma-1}{c}\, \rho F'(V_m)u(x_h - \epsilon)\phi_n^*(x_h)\phi_n(x)}{\kappa^2 - \gamma_n^2} \qquad (4\text{-}4)$$

It is now necessary to apply a self-consistent requirement
to p, namely that

$$-\left(\frac{\partial p}{\partial x}\right)_{x=x_h-\epsilon} = \rho c\kappa u(x_h - \epsilon) \qquad (4\text{-}5)$$

We therefore obtain a relation that does not include any
of the acoustic variables. Thus in principle the stability
boundaries (defined by $\sigma = 0$) can be found as a function of
the other known variables. Since the tube tends to oscil-
late at a single frequency corresponding to one mode, we
may choose a particular ϕ_n and γ_n, ϕ_1 and γ_1, such that
$\kappa \doteq \gamma_1$, then only one term in the sum in Eq. (4-4) will be
important, and the self-consistent requirement can be
applied to the single term. We therefore let $n = 1$ in
Eq. (4-4) and set $\partial p/\partial x = \rho c\kappa u(x_h - \epsilon)$ as required by
Eq. (4-5). The result is:

$$\kappa^2 - \gamma_1^2 = -\frac{\gamma - 1}{c^2} F'(V_m)\phi_1^*(x_h)\frac{\partial \phi_1}{\partial x}\bigg|_{x=x_h} \tag{4-6}$$

This is a stability criterion for the system since κ can be found once the appropriate eigenfunctions are used, and the appropriate form is assumed for the heat transfer function. The above method is obviously not limited to the stability analysis of the Rijke tube, but with minor modifications can be applied to any system that contains a source whose strength depends on the field variable at some point, and that tends to oscillate at a single frequency. This latter requirement is clearly fulfilled for many unstable systems.

3. Analysis for No Radiation Loss

As an example we shall apply Eq. (4-6) to the simplest possible problem, namely the case when radiation losses at the end of the tube can be neglected. As a first approximation we shall also neglect the fact that the sound speed is increased in the upper half of the tube because of the heat added to the gas at the heater. Under these conditions, the appropriate eigenfunction for excitation of the half-wavelength mode of the tube is simply $\phi_1 = 2/L \sin \pi x/L$, and the eigenvalue is $\gamma_1 = -i\pi/L$. Substitution into Eq. (4-6) yields:

$$\left(\frac{\pi}{L}\right)^2 - k^2 - 2ik\sigma = -\frac{\gamma - 1}{c^2} F'(V_m)\left(\frac{2\pi}{L^2}\right)\sin\frac{\pi x_h}{L}\cos\frac{\pi x_h}{L} \tag{4-7}$$

where we have assumed that $\sigma \ll k$. Separation of Eq. (4-7) into real and imaginary parts yields

$$\left(\frac{\pi}{L}\right)^2 - k^2 = -\frac{\pi}{L^2}\frac{\gamma-1}{c^2}F'_r(V_m)\sin\frac{2\pi x_h}{L} \qquad (4-8)$$

and

$$\sigma = \frac{\pi}{2kL^2}\frac{\gamma-1}{c^2}F'_i(V_m)\sin\frac{2\pi x_h}{L} \qquad (4-9)$$

We have written $F'(V_m) = F'_r(V_m) + iF'_i(V_m)$. The stability of the system is determined by Eq. (4-9) whereas the wave number is determined by Eq. (4-8). We shall see in a later section that both σ and the change in wave number are small. The importance of phase lag at the heater is also directly shown by the fact that no oscillations can grow unless there is a lag of q behind u. Since p and u are 90° out of phase, the requirement that the tube oscillate is that the heat release must have a component in phase with the pressure. This condition is in agreement with the Raleigh Criterion. As will be shown in a later section, q does tend to lag behind u and so the tube tends to oscillate when the heater is in the lower half of the tube and the oscillations are damped when the heater is in the upper half of the tube. This dependence is in agreement with experimental observations.[10] If the grid is cooled instead of being heated, q changes sign and the dependence of the driving or damping on grid position is reversed.

These results are also in agreement with experimental observations.[11]

Finally, it should be noted that the tube has been observed to oscillate in higher modes as well as the half-wavelength mode assumed here. In practice, it is more difficult to excite these modes because the losses to be overcome are greater at the higher frequencies, but the dependence of σ on driving position can easily be found by taking $\phi_2 = \sqrt{2/L} \sin 2\pi x/L$. σ will then be found to be proportional to $\sin 4\pi x_h/L$ when Eq. (4-9) is used, and therefore the tube will tend to oscillate when $0 < x_h < L/4$ and $L/2 < x_h < 3L/4$. These results are also in agreement with experimental observations.[7]

4. Analysis Including Radiation Losses

Since the Rijke tube is open at both ends, it is to be expected that the radiation of sound from both ends of the tube is an important energy loss that must be overcome by the heat source if oscillations are to occur. In this section we work out the expressions for σ and k when radiation losses are included in the analysis. We shall, however, still assume that the increase in sound speed in the upper half of the tube can be neglected, and when we compare our results with experiment, a mean sound speed will be used. Under these conditions, the appropriate eigenfunction is $\phi_1 = A \sinh(\gamma_1 x + \zeta)$ where $\gamma_1 = -2\zeta/L - i\pi/L$. ζ is the real part of the radiation impedance, and is small compared

with unity. The value of A is determined by the require-
ment that ϕ_1 be normalized, and it can easily be shown by
integration that $A = \sqrt{2/L(2\mathcal{S}/\sinh 2\mathcal{S})}$. Since we wish to
include only terms linear in $\mathcal{S}$ ($\mathcal{S} \ll 1$) we may take
$A = \sqrt{2/L}$. Separation of the stability equation into real
and imaginary parts is straightforward but tedious. We
shall present only the results here:

$$\sigma = \frac{2\pi}{kL^2} \left[-\mathcal{S} + \frac{\gamma-1}{4c^2} F_i'(V_m)\sin\frac{2\pi x_h}{L} - F_r'(V_m)(\frac{2\mathcal{S}}{\pi}\sin\frac{2\pi x_h}{L} + 2\mathcal{S}(1 - \frac{2x_h}{L})) \right]$$

$$(4-10)$$

$$\left(\frac{\pi}{L}\right)^2 - k^2 = - \left[\frac{\gamma-1}{c^2} \frac{\pi}{L^2} F_r'(V_m)\sin\frac{2\pi x_h}{L} + F_i'(V_m)(\frac{2\mathcal{S}}{\pi}\sin\frac{2\pi x_h}{L} + 2\mathcal{S}(1 - \frac{2x_h}{L})) \right]$$

$$(4-11)$$

The competition between the generation of sound at the heat
source and the losses due to radiation is now directly
shown in Eq. (4-10). In the absence of a heat source
$(F'(V_m) = 0)$ the tube will have a value of σ equal to
$-2\pi\mathcal{S}/kL^2 = -2\mathcal{S}/L$ and is therefore damped. The term in
square brackets represents the contribution of the heat
source to σ and therefore the tube will start to oscillate
when this term is greater than $\mathcal{S}$. It can also be seen that
in this analysis even in the presence of radiation losses
there must be a phase lag between q and u, that is,
$F_i'(V_m) > 0$. For $\mathcal{S} = 0$ Eqs. (4-10) and (4-11) clearly
reduce to those presented in the previous section.

This ends the theoretical treatment of the Rijke phenomenon. In the next section we shall present some data on the magnitude of the heat released to the medium as a function of flow velocity and frequency, and in the following section we will compare the calculated results with some experimental data obtained by the author.

5.   Heat Released to the Gas

In this section we shall find an explicit form for the function $F'(V_m)$ by using a boundary layer theory due to Carrier[13] to find the fluctuating component of the heat transferred to the medium by conduction. Not all of the heat supplied to the heater is given up to the gas by conduction; we shall present some measurements in the next section that indicate that an important source of energy loss is thermal radiation from the heater, and therefore the mean heat per second given up to the fluid by convection is

$$Q_m = W(1 - C_2 T_h^4) \qquad (4\text{-}12)$$

W is the power supplied to the heater, C_2 is a constant to be determined, and T_h is the surface temperature of the heater. If q' is the fluctuating component of the heat added per second, then Carrier has shown[13] that for a heated ribbon oriented parallel to a mean flow (V_m) the ratio q'/Q_m may be expressed as:

$$\frac{q'}{Q_m} = \left[-\frac{1}{2} \frac{V_m}{\omega d} \left[\left(\pi a_2 d\right)^{1/2} erf\left(a_2 d\right)^{1/2} - \left(e^{-a_2 d} - 1\right) \frac{u}{V_m} \right] \right] \equiv T \frac{u}{V_m}$$

(4-13)

where ω is the frequency of the velocity fluctuations, d is the length of the ribbon in the direction of the flow, and u is the perturbation in the stream velocity. a_2 is given by:

$$a_2 = \frac{1}{2} \left\{ \sqrt{1 + \frac{4ik\omega}{\rho c_p V_m^2}} - 1 \right\} \frac{\rho c_p V_m}{k}$$

(4-14)

where k is the thermal conductivity of the gas, and the other symbols have their usual meaning. We shall denote the function in square brackets in Eq. (4-13) by $T = E + iF$. The argument of the error function is in general complex, but for $4k\omega/\rho c_p V_m^2 \ll 1$, a_2 is almost imaginary, and Merk[7] has pointed out that Eq. (4-13) can be expressed in terms of Fresnel integrals.[14] For the values of d, ω, and so on that were used in the experiments to be described in the next section, a_2 is either very nearly imaginary, or complex and large. In the latter case, an asymptotic series representation may be used for the error function[14] and the real and imaginary parts of T found as a function of V_m. If we take $\omega = 2\pi(200)$ radians per second, $d = .632 \times 10^{-2}$ meters, $k = .0239$ Joules/second-meter-$^{\circ}$K, $c_p = 10^3$ Joules/kilogram-$^{\circ}$K and $\rho = 1.18$ kilogram/meter^3, the above approximations may be used to obtain the curves

illustrated in Figure 4-2. If Eqs. (4-13) and (4-14) are expanded for small values of ω, it will be found that $T \longrightarrow .5$ as $\omega \longrightarrow 0$. This implies that the mean heat transferred to the gas per second is proportional to $(V_m)^{1/2}$ as can be seen by putting the heat transfer relation into a form due to Merk:[7]

$$Q_m = (T_h - T_g)A_d\alpha(Re,Pr) \qquad (4\text{-}15)$$

$(T_h - T_g)$ is the temperature difference between the gas and the heater, A_d is the surface area of the heater and α is a function of the Reynolds number ($Re = V_m d/\mu$) and the Prandtl number ($Pr = c_v \rho\mu/k$). Then, as $\omega \longrightarrow 0$ this relation can be expanded for a perturbation (u) in V_m, and the ratio of the fluctuating part of the heat transferred may be expressed in terms of u/V_m:

$$\frac{q}{Q_m} = \frac{\partial(\ln \alpha)}{\partial(\ln Re)} \frac{u}{V_m} \qquad (4\text{-}16)$$

Since $\partial(\ln \alpha)/\partial(\ln Re) = T = .5$ at $\omega = 0$, we must have $Q_m \sim V_m^{1/2}$. This result will be useful when we compare the results of our analysis with the experiments described in the next section. Since the function $F'(V_m)$ was defined by

$$q = F'(V_m)u \qquad (4\text{-}17)$$

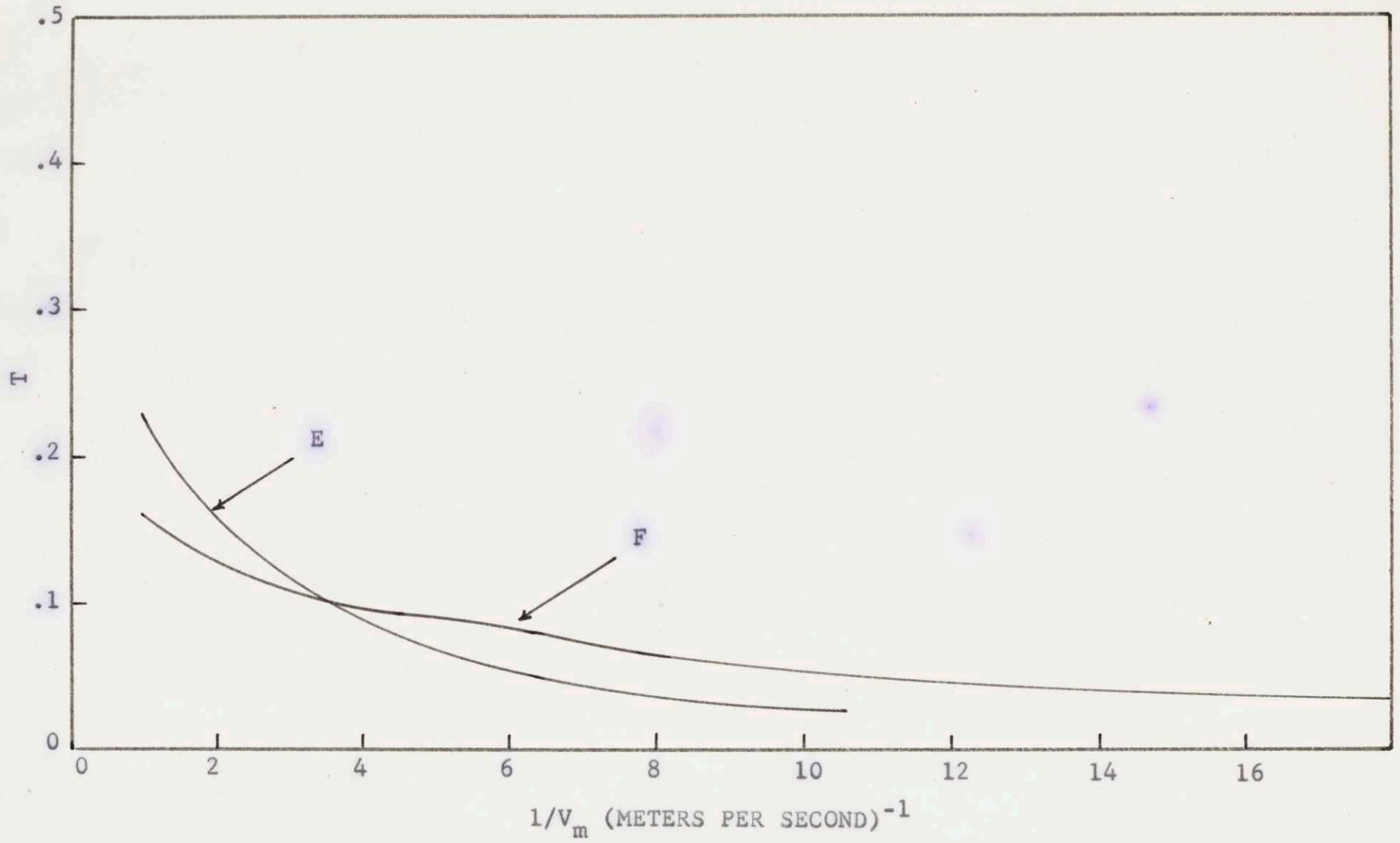we may use Eqs. (4-12), (4-13) and (4-17) to express $F'(V_m)$ in the following convenient form:

Figure 4-2.

$$F'(V_m) = \frac{Q_m}{V_m} \frac{T}{\rho_o V_m A_t} \qquad (4\text{-}18)$$

$$= \frac{W(1 - C_2 T^4)}{\rho_o V_m^2 A_t} T \qquad (4\text{-}19)$$

All of the symbols except the cross-sectional area of the tube (A_t) have been defined previously. The factor $\rho_o V_m A_t$ in the denominator of Eq. (4-16) occurs because the source term in the wave equation is the rate at which heat is added per unit mass to the fluid. At very low flow speeds, this result should be corrected to account for the finite size of the heater, but we shall be dealing with flow speeds high enough so that that correction may be neglected.

Equation (4-19) and Figure 4-2 therefore give us sufficient information about the fluctuating heat released to the fluid to be able to determine whether or not the tube will oscillate. Since such a determination requires a knowledge of the surface temperature at the heater as well as a constant (C_2) that can best be determined by experiment, it is desirable to present some experimental results before presenting the comparison between theory and experiment.

6. Experimental Apparatus and Results

The experimental configuration used to obtain the data presented in this section was very simple. A brass tube 32 in. long and 3.5 in. in diameter was mounted over a hole near the edge of a plywood board that was arranged to be

5 ft above the laboratory floor. A 125 ft^3 box was constructed from thin plastic film and placed underneath the plywood board, shown in Figure 4-3. The rate of air flow through the tube could be controlled by means of a small centrifugal blower placed in a lower corner of the plenum chamber. The plastic film was used for the plenum chamber so that the radiation impedance on each end of the tube would be approximately the same. The heater used in these experiments was constructed by cutting a ring (3 1/4 in. o.d., 2 3/4 in. i.d.) from 1/2 in. thick asbestos board. Machine screws mounted around the ring then served as supports for a nicrome ribbon 1/4 in. in width and 0.0063 in. thick. The spacing between the ribbons which were run back and forth across the asbestos ring was approximately 0.2 in. For all of the experiments to be described in this section, the heater was placed a distance L/4 from the bottom end of the tube.

Sound pressure level measurements were made with a condenser microphone system and Ballantine voltmeter. Other quantities measured were: (1) the air temperature at the top of the tube by means of a high-temperature mercury thermometer, (2) the air flow through the tube using a Hastings Corp. air flow meter, and (3) the surface temperature of the heater ribbon. The latter quantity was obtained by removing the heater from the tube and recording the surface temperature (measured using Tempil-sticks,
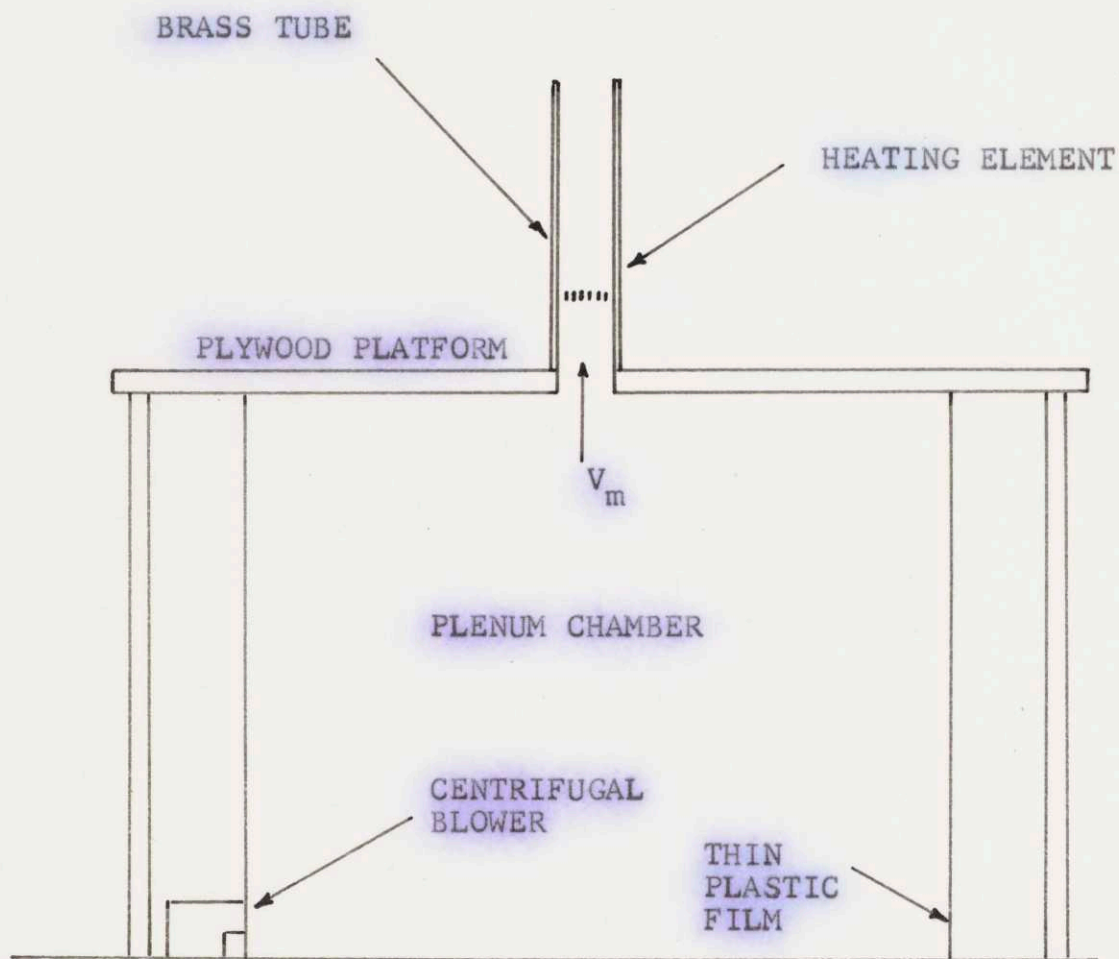
Figure 4-3.

commercially available pencils containing a material with
a known melting point) as a function of the observed color
of the heating element. When the heating element was
replaced in the tube, the color could be observed by means
of a mirror mounted below the tube and thus the surface
temperature estimated. The Q of the tube at a wavelength
equal to twice the length of the tube was measured by
exciting the tube from the outside with a loudspeaker and
measuring frequency of the half-power points with a con-
denser microphone placed at the center of the tube. If ω
is the bandwidth between the half-power points, then the Q
is, of course, defined by $\omega/\Delta\omega$. The Q of the tube was
varied by varying the position of a fine-mesh screen in
the tube.

Since the theory presented in the earlier sections
was a small-signal theory, one cannot predict the final
intensity of the oscillation, and so we shall limit our-
selves in this section to a determination of the onset of
the oscillations. The first observation that can be made
is the dependence of the temperature in the upper half of
the tube (T_B) on the mean flow velocity in the lower half
of the tube. The measured data are presented in Figure 4-4
for three different values of power supplied to the heater
together with some calculated curves. The calculated
curves were obtained by assuming that the gas takes up all
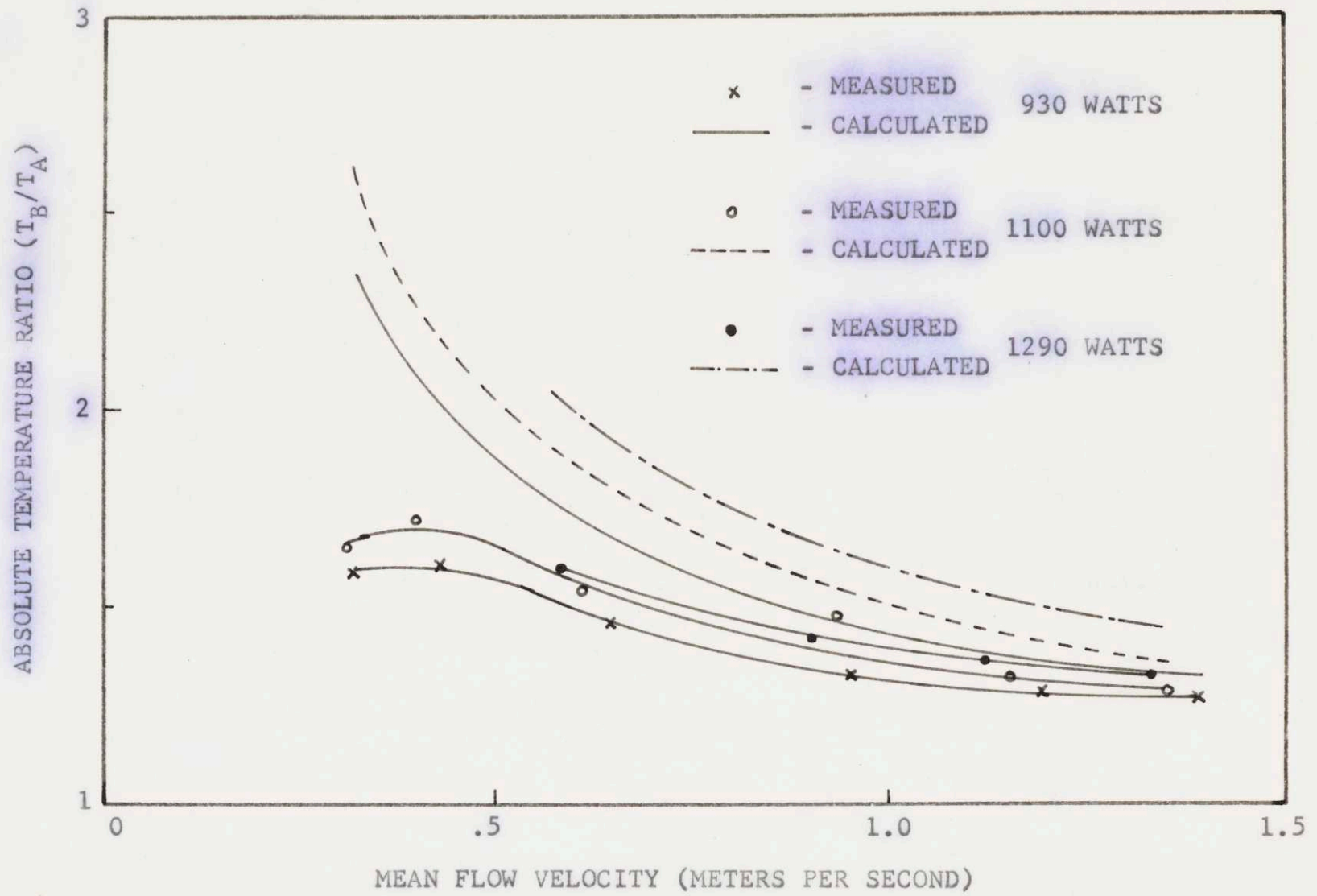of the energy supplied to the heater, and it can be seen

Figure 4-4.

that although the two are in good agreement for high flow speeds, there is a great deal of energy unaccounted for at low flow speeds. In Figure 4-5 we have plotted $(1 - W_g/W)$ as a function of measured absolute temperature of the heater. W_g is the power delivered to the gas. The unaccounted-for energy is seen to be proportional to T_h^4 and therefore radiation from the heater appears to be an important source of energy loss at low flow speeds. From the slope of line in Figure 4-5, it can be determined that the power per second delivered to the gas by convection is $Q_m = W(1 - C_2 T_h^4)$ where $C_2 = .346 \times 10^{-12} \, {}^{\circ}K^{-4}$.

The gas temperature T_B and the heater temperature T_h have been measured as a function of V_m for three different values of heater power. We may compare these results with values calculated by taking

$$W(1 - C_2 T_h^4) = C_1(T_h - T_B)V_m^{1/2} \tag{4-19}$$

and

$$\frac{W(1 - C_2 T_h^4)}{\rho c_p V_m A_t} = T_B - T_A \tag{4-20}$$

where C_1 is a constant that is determined to give the best fit with the experimental data, $C_1 = 1.45 \, \text{Joule/sec}^{1/2}\text{-meter}^{1/2} \, {}^{\circ}K$. Using the two constants, C_1 and C_2, the heater temperature and T_B may be calculated as functions of V_m using Eqs. (4-19) and (4-20). The results of these
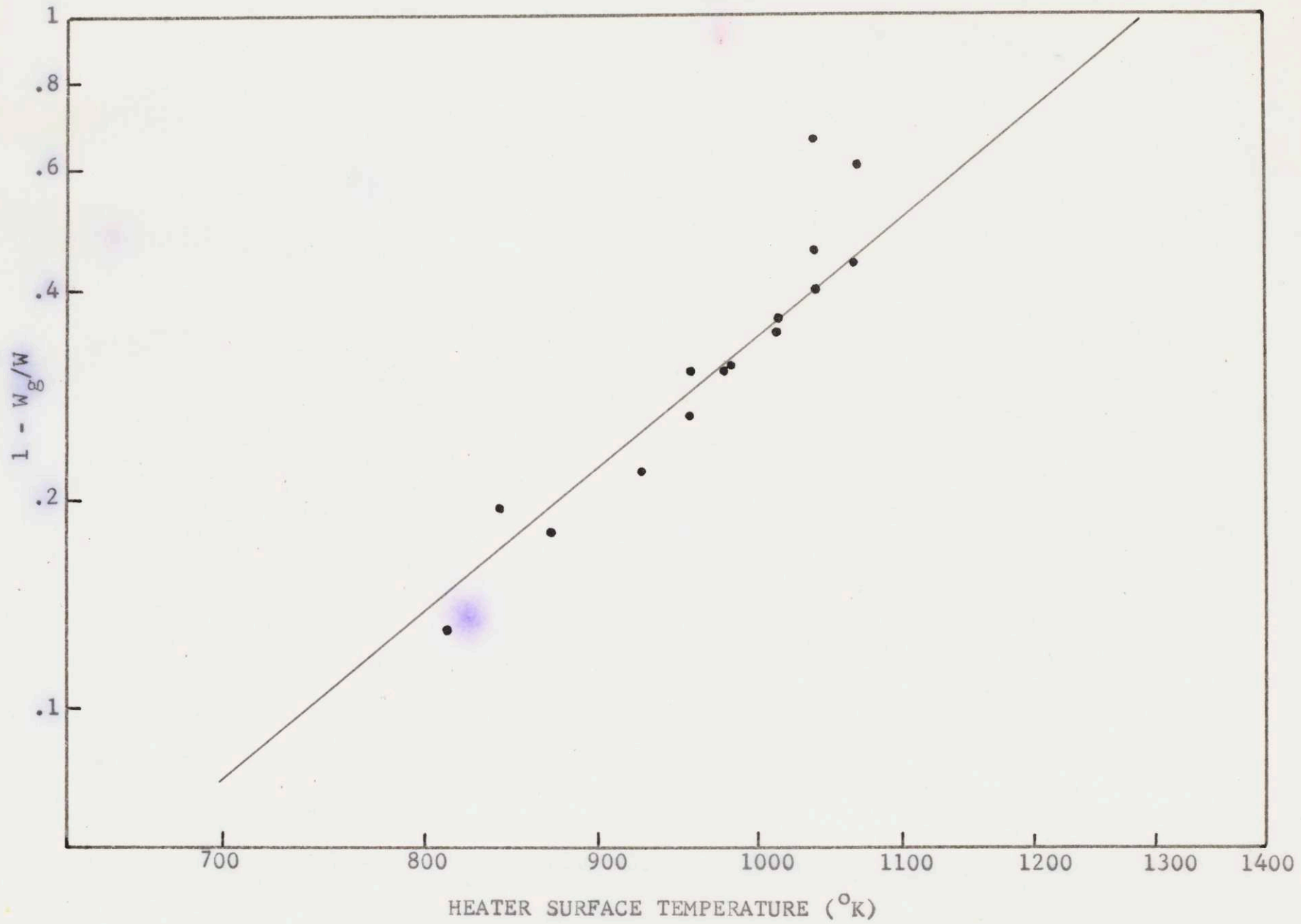
Figure 4-5.

calculations and the experimental points are shown in Figures 4-6 and 4-7.

The Q of the tube as a function of the position of a fine-mesh screen in the upper half of the tube was also measured for the first mode of the tube, and the results are presented in Figure 4-8.

The dependence of the onset of oscillation on screen position was measured for three mean flow speeds and three values of the heater power. The data are presented in Table I below.

Heater Power (Watts)	Screen Position (in. from upper end of the tube)	Q from Figure 4-8	Mean Flow Speed m/sec
930	11 3/4	43	.64
1100	7	41.5	.61
1290	6 3/4	41.5	.57
930	6	41.5	.43
1100	4	40.8	.40

Table I. Values of heater power, Q, and mean flow at which the onset of oscillation occurs.

At the lowest flow speed, the heater was too hot to use an input power of 1290 watts.

The dependence of the onset of oscillation on flow speed was measured when the screen was removed. The highest flow speeds at which the tube will oscillate are .84, .87, and .91 meters per second for heater powers of
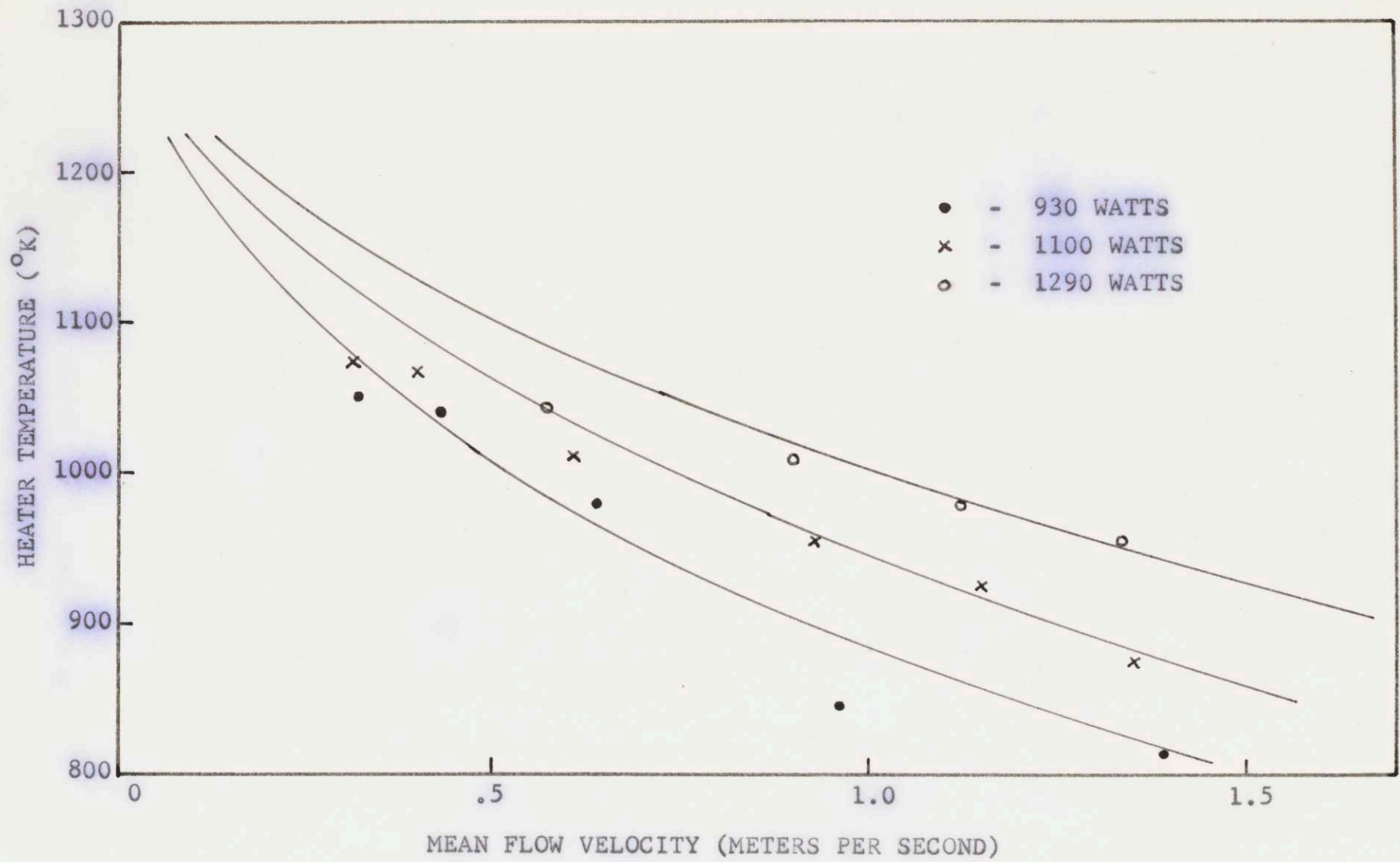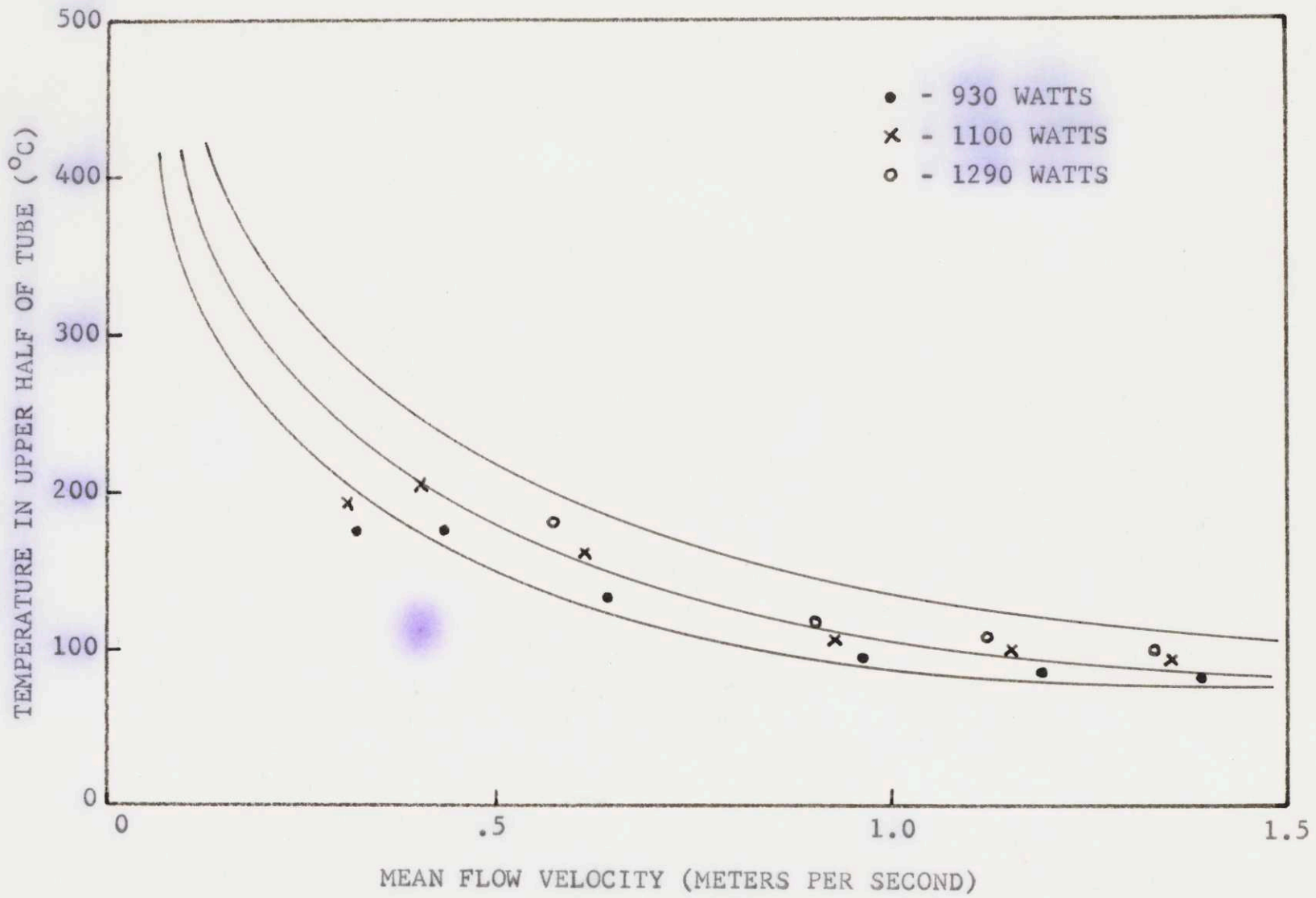
MEAN FLOW VELOCITY (METERS PER SECOND)

Figure 4-6.
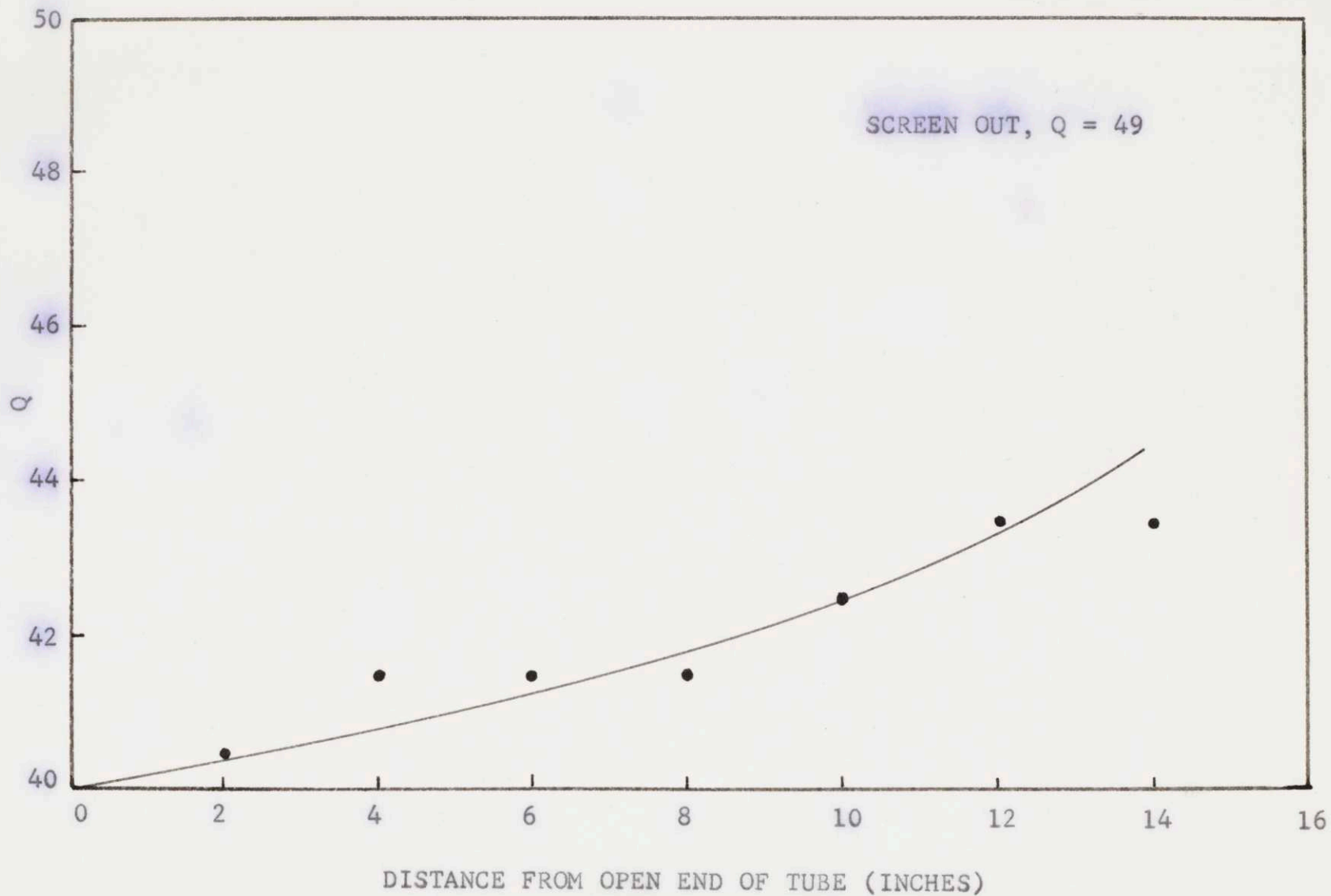
Figure 4-7.

DISTANCE FROM OPEN END OF TUBE (INCHES)

Figure 4-8.

930, 1100 and 1290 watts respectively. The lowest flow speeds are more difficult to determine because the heater becomes very hot, and care must be taken to prevent it from burning up. The best observation that can be made is that the tube stops oscillating when the speed is in range 0.2-0.25 m/sec for heater powers between 930 and 1290 watts. As we shall see in the next section, the theoretical calculations are in good agreement with experiment at high flow velocities, but it does not seem to be possible to get agreement with theory at the low velocity cutoff, and therefore these data will be sufficiently accurate for our purposes.

7. Comparison between Theory and Experiment

Before presenting a detailed comparison between the analysis presented in sections 1-5 and our experiments, we present some experimental data obtained by Lehman,[4] who measured the high and low velocity cutoffs as a function of heater power using a somewhat different experimental arrangement. It is not possible to use the data at the low velocity cutoff because thermal radiation from the heater was presumably an important source of energy loss in those experiments and no detailed measurements of heater temperatures were reported. At the high-velocity cutoff, thermal radiation can be neglected, and from Eqs. (4-10) and (4-18) we see that under these conditions the quantity W/V_m^2 should be constant at the onset of

oscillations provided that the radiation impedance is unchanged. The quantity T can be taken to be approximately constant over the small range of flow speeds used. The experimental data are shown in Figure 4-9, and it is seen that W/V_m^2 is indeed reasonably constant. For comparison, W/V_m has also been plotted, and it can be seen that it changes drastically. These measurements are therefore in good agreement with theory.

The author has also tried to compare some of the experimental results obtained by Kerwin[5] with the analysis presented here. Data on heater surface temperature, gas temperature, mean flow speeds and power input were used to calculate the amount of energy given up to the gas by convection. It was found that 59% - 86% of the input power was unaccounted for, depending on the heater power and flow speed, and in addition that the unaccounted-for energy did not depend on surface temperature as T_h^4, but rather as some much weaker function of T. In that study the complex eigenvalue for the tube was measured by introducing known losses until the tube just stopped oscillating, and so one can see if the measured eigenvalue is proportional to W/V_m^2 as required by Eq. (4-18). Unfortunately these attempts were unsuccessful even when the energy loss described above was accounted for, but one can see from the data that σ increases as W is increased, and also increases as V_m is decreased. The
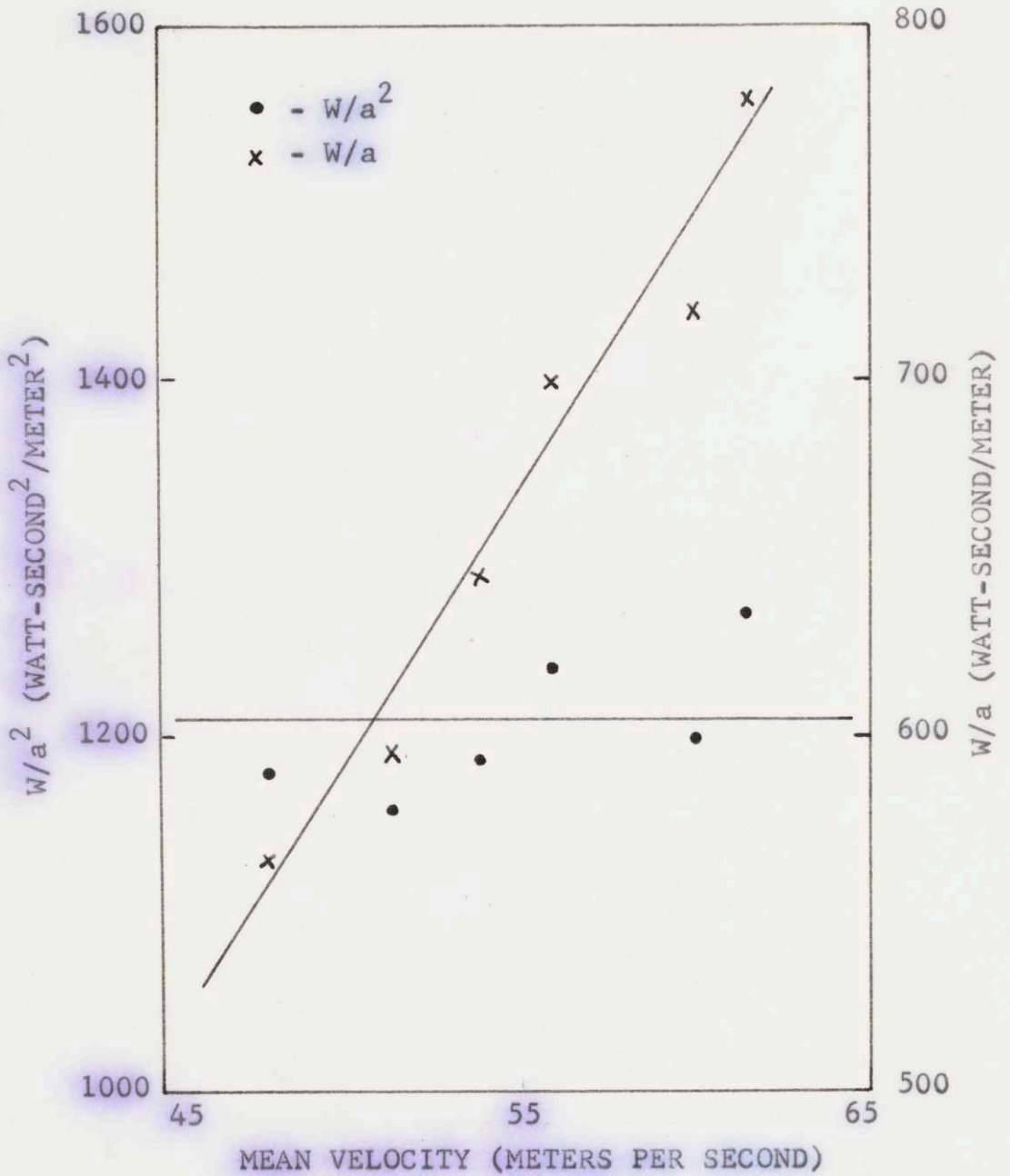
Figure 4-9.

results are therefore in qualitative agreement with this theory. No explanation of the failure to get quantitative agreement with the theory presented has been found, and so we proceed to a comparison of the analysis with the experiments described in the previous section.

The first comparison to be made is between the Q of the tube measured with a cold heater in place and the Q calculated using Eq. (4-10) and the relation $Q = k/2\sigma$. Using these we have

$$Q = \frac{k}{2\sigma} = \frac{k^2 L^2}{4\pi \mathcal{S}} = \frac{\pi}{4\mathcal{S}}$$

for $F'(V_m) = 0$ and $kL = \pi$. If we use a value of $\mathcal{S}$ for an opening at the end of a long tube,[15] $\mathcal{S} = (ka)^2/4$ where a is the radius of the tube, we find that for the dimensions of the tube used in this experiment Q = 106. The measured Q was 49 and since the theoretical calculation does not include losses introduced by the heater, or losses due to viscosity and heat conduction at the tube walls, we shall use the experimentally determined value. Since $\mathcal{S}$ is small, the term that contains $F'_r(V_m)$ in Eq. (4-10) can be neglected, and therefore we use as a condition for the onset of oscillations

$$\frac{\pi}{(kL)^2} \frac{\gamma - 1}{c^2} F'_i(V_m) > \frac{1}{Q} \tag{4-21}$$

for $x_h = L/4$. If we use an average speed of sound equal to 400 meters per second which corresponds to room

temperature in the lower quarter of the tube and a
temperature ratio of 1.5 in the upper three-quarters of
the tube, take $\gamma = 1.4$, $kL = \pi$, and $Q = 49$, then the
stability relation is simply

$$F'(V_m) > 2.56 \times 10^4 \qquad (4\text{-}22)$$

Using Eq. (4-19) and the plot of T vs V_m presented in
Figure 4-2, we may plot $F_i'(V_m)$ for the three different
values of heater power used in these experiments. The
points A, B, and C in Figure 4-10 are the cutoff points
according to Eq. (4-22). The calculated values of the
cutoff velocity, .71, .81, and .90 meters per second are
in very good agreement with the measured values, .84, .87,
and .91 meters per second. The analysis therefore compares
very well with experiment at the high velocity cutoff.

At low flow velocities, the situation is consid-
erably more complicated. According to the calculations
presented in Figure 4-10, the source strength, $F'(V_m)$,
continues to rise as V_m approaches zero, and no cutoff
is obtained for small values of V_m. It can be seen
qualitatively from the data presented in Table I that as
the flow speed is decreased, the onset of oscillations
occurs for a lower value of Q, and so the measurements
are at least in qualitative agreement with the calcula-
tions. Kerwin[5] also found that the strength of the
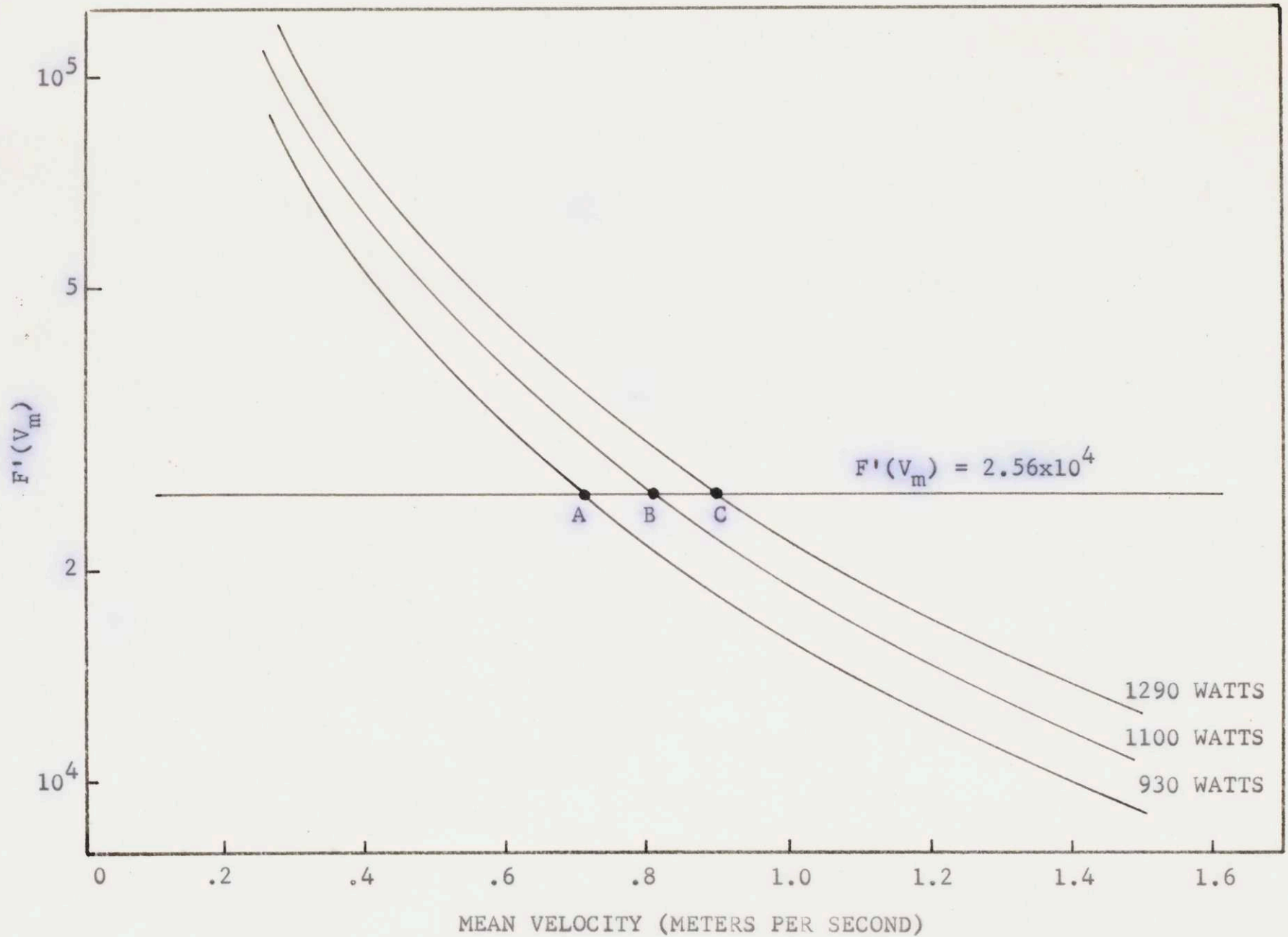source term increased with decreasing flow velocity, and

Figure 4-10.

obtained an oscillation at zero flow velocity for which
no quantitative explanation could be given. The source
strength rises first, because we have taken $Q_m \sim V_m^{1/2}$ and
therefore a perturbation in Q_m resulting from a perturba-
tion u in V_m becomes large as V_m approaches zero, and
second, because the source strength is proportional to the
heat added per unit mass of the fluid, and this introduces
a factor of $1/V_m$ in the denominator of Eq. (4-18). Both of
these effects are modified, however, in the limit of zero
flow velocity. The first, because for $V_m = 0$ the heat
added to the gas is independent of the sign of u and
therefore the period of the heat addition is $T/2$ if u has
a period T. Thus, the source strength is zero at the
fundamental frequency, $\omega = 2\pi/T$. The second effect is
modified because of the finite size of the heater. At
zero mean flow velocity, the heat is given up to the mass
of gas in contact with the heater. Thermal radiation from
the heater is also an important factor in the decrease of
the source strength, but this factor has already been
included in the calculated curves presented in Figure 4-10.
According to Figure 4-5, all of the energy put into the
heater should be radiated at a surface temperature of
approximately 1300°K as can be seen if the straight line
is extrapolated. This limit is reached, however, only
when the flow velocity approaches zero as can be seen from
the calculated curves presented in Figure 4-5. It has

been found by Kerwin that an instability in the mean flow
through the heater occurs for very low values of the
Reynolds number, and although the cutoff point in these
experiments occurred at a higher Reynolds number, it
appears that one would have to study such instabilities
in more detail in order to obtain a quantitative theory
to explain the low-velocity cutoff. In these experiments,
the plenum chamber was not completely air-tight, and there-
fore it was necessary to reverse the direction of the
centrifugal blower to obtain mean flow speeds very much
below the mean flow speed corresponding to free convec-
tion. As the suction was increased to decrease the mean
flow speed, the oscillation stopped very suddenly, and
was accompanied by a sudden decrease in the flow speed
and a sudden rise in the heater temperature, almost to
the point of burnout.

Finally, we note that the quantity $F'(V_m)/QV_m^2 =$
constant, or $W(1 - C_2 T_h^4)/QV_m^2 =$ constant for intermediate
values of the flow speed. We may use the values of W, V_m,
and Q presented in Table I, the values of T_h for each mean
flow presented in Figure 4-6, and the previously determined
value of C_2, $C_2 = .346 \times 10^{-12}\ ^\circ K^{-4}$ to test the above rela-
tion. If this is done, it will be found that the "constant"
varies by a factor of approximately 2 and so in this respect
the experimental data are not found to be in particularly
good agreement with the analysis. Although the source

strength has been found to increase with decreasing flow velocity, it would be desirable to find a method of introducing losses into the tube in a symmetric fashion before making a detailed comparison between the analysis and experiments. It would also be desirable to control the mean flow velocity by a different method, and in this way the low-velocity cutoff could be studied in more detail.

REFERENCES FOR CHAPTER FOUR

1. Rijke, P.L., Phil. Mag., _17_ 419 (1859)

2. Raleigh, Lord J.W.S., Nature, _18_ 319 (1878)

3. Raleigh, Lord J.W.S., The Theory of Sound, Dover
    Publications, (1945)

4. Lehman, K.O., Ann. Physik, _29_, 527 (1937)

5. Kerwin, E.M. Jr., Sc.D. Thesis (VI), Mass. Institute
    of Technology, (1954)

6. Carrier, G.F., Quart. Appl. Math., _12_, 383 (1955)

7. Merk, H.J., Appl. Sci. Res. A, _6_, 402 (1957)

8. Handbook of Physics, Condon, E.V. and Odishaw, H.,
    McGraw Hill, (1958). (See 3-112, Acoustics by
    K.U. Ingard)

9. Morse, P.M. and Feshback, H., Methods of Theoretical
    Physics, McGraw Hill, (1953)

10. Merk, H.J., Appl. Sci. Res. A, _6_, 402 (1957)

11. Bosscha, Pogg. Ann., _17_, 342 (1859)

12. Carrier, G.F., Quart. Appl. Math., _12_, 383 (1955)

13. Formulas and Theorems for the Functions of Mathematical
    Physics, W. Magnus and F. Oberhettinger, Chelsea
    Publishing Company (1949)

BIBLIOGRAPHY

1.   Batchelor, G.K., Homogeneous Turbulence, Cambridge
      University Press (1953)

2.   Blackstock, D.T., ONR Technical Memorandum No. 43,
      Acoustics Research Laboratory, Harvard University,
      (June 1960)

3.   Bosscha, Pogg. Ann., 17, 342 (1859)

4.   Carrier, G.F., Quart. Appl. Math., 12, 383 (1955)

5.   Chernov, L.A., Dokl. Akad. Nauk., USSR, 98, 953 (1954)

6.   Chernov, L.A., Wave Propagation in a Random Medium,
      McGraw-Hill (1960)

7.   Condon, E.V. and Odishaw, H., Handbook of Physics,
      McGraw-Hill (1958). (See 3-112, Acoustics by
      K.U. Ingard)

8.   Dumond, J.M., Cohen, E.R., Panofsky, W.H., and Deeds, E.,
      J. Acoust. Soc. Am., 18, 97 (1946)

9.   Fay, R.D., J. Acoust. Soc. Am., 3, 222 (1931)

10.   Fay, R.D., J. Acoust. Soc. Am., 28, 910 (1956)

11.   Fay, R.D., J. Acoust. Soc. Am., 34, 1269 (1962)

12.   Fubini, E., Alta Frequenza, 4, 530 (1935)

13.   Hugoniot, A., J. Éc. Polyt. (Paris), 58, 1 (1889)

14.   Ingard, K.U., Notes for Physics 8.461, Massachusetts
      Institute of Technology, Fall 1962.

15.   Ingard, K.U., Field Studies of Sound Propagation over
      Ground, M.I.T. Acoustics Laboratory (1954)

16.   Kerwin, E.M. Jr., Sc.D. Thesis (VI), Massachusetts
      Institute of Technology (1954)

17. Kraichman, R.H., J. Acoust. Soc. Am., 29, 65 (1957)

18. Krasilnikov, V.A., Dokl. Akad. Nauk., USSR, 58, 1353 (1957)

19. Lehman, K.O., Ann. Physik, 29, 527 (1937)

20. Lighthill, M.J., Proc. Cambridge Phil. Soc., 49, 531 (1952)

21. Lighthill, M.J., Proc. Roy. Soc. (London) A, 211, 564 (1952)

22. Lighthill, M.J., Proc. Roy. Soc. (London) A, 222, 1 (1954)

23. Lighthill, M.J., Viscosity in Waves of Finite Amplitude, Surveys in Mechanics, (G.I. Taylor 70th Anniversary Volume), G.K. Batchelor and R.M. Davies Ed., Cambridge University Press (1956)

24. Magnus, W. and Oberhettinger, F., Formulas and Theorems for the Functions of Mathematical Physics, Chelsea Publishing Company (1949)

25. Merk, H.J., Appl. Sci. Res. A, 6, 402 (1957)

26. Minzer, D., J. Acoust. Soc. Am., 25, 922 (1953)

27. Minzer, D., J. Acoust. Soc. Am., 25, 1107 (1953)

28. Morse, P.M. and Ingard, K.U., Linear Acoustic Theory, Handbuch der Physik, XI/1 Springer-Verlag (1961)

29. Morse, P.M. and Feshback, H., Methods of Theoretical Physics, McGraw-Hill (1953)

30. Obukhov, A.M., Dokl. Acad. Nauk., USSR, 30, 611 (1941)

31. Poisson, S.D., J. Éc. Polyt., 14, 319 (1808)

32. Raleigh, Lord J.W.S., The Theory of Sound, Dover Publications (1945)

33. Raleigh, Lord J.W.S., Nature, 18 319 (1878)

33. Rankine, W., Phil. Trans. Roy. Soc., 160, 277 (1870)

34. Reed, S.G., J. Acoust. Soc. Am., 31, 1265 (1959)

35. Reed, S.G., Phys. Fluids, 3, 134 (1960)

36. Riemann, B., Göttingen Abh., 8, 43 (1859)

37. Rijke, P.L., Phil. Mag., 17, 419 (1859)

38. Rudnick, I., J. Acoust. Soc. Am., 25, 1012 (1953)

39. Stokes, G.G., Phil. Mag., 33, 349 (1848)

40. Tatarski, V.I., Wave Propagation in a Turbulent Medium, McGraw-Hill (1961)

41. Whitham, G.B., J. Fluid Mech., 4, 337 (1958)

BIOGRAPHY

George C. Maling, Jr. was born on February 24, 1931
in Boston, Massachusetts. He was educated in the public
schools and graduated from Glen-Nor High School, Glenolden,
Pennsylvania in 1948. He entered Bowdoin College in 1948,
the Massachusetts Institute of Technology in 1951, and
received the A.B. degree Cum Laude from Bowdoin (Physics)
and S.B., S.M. from M.I.T. (Electrical Engineering) in 1954.

During the three years at M.I.T., he was a student in
Course VI-A and a Philco Corp. Co-op. He returned to
Philco in 1954 as a research engineer in acoustics, and
in 1955 was "asked" to join the armed forces for a two
year tour. During that time he was an Electrical Engineering
Assistant engaged in classified work on radar systems.

In 1957 he returned to M.I.T. and received the degree
Electrical Engineer in 1958. Since that time he has been
working towards a doctorate in Physics at M.I.T.

In December, 1960 he married Norah Horsfield, and
became the father of Ellen Patricia in April, 1962. He is
a member of Eta Kappa Nu, Tau Beta Pi and Sigma Xi.